Science
AAAS

Supplementary Materials for

Directed evolution of enzymatic silicon-carbon bond cleavage in siloxanes

Nicholas S. Sarai *et al*.

Corresponding authors: Dimitris E. Katsoulis, dimi.katsoulis@dow.com; Frances H. Arnold, frances@cheme.caltech.edu

Science **383**, 438 (2024)
DOI: 10.1126/science.adi5554

The PDF file includes:

Materials and Methods
Supplementary Text
Figs. S1 to S46
Tables S1 to S50
References

Other Supplementary Material for this manuscript includes the following:

MDAR Reproducibility Checklist

Table of Contents

List of Figures 4
List of Tables 6
1. Materials and Methods 8
1.1 Abbreviations 8
1.2 General 8
1.3 Cloning, Mutagenesis, and Plasmid Isolation 9
1.3.1 Site-Saturation Mutagenesis 9
1.3.2 Random Mutagenesis 11
1.3.3 Recombination via Staggered Extension Process 15
1.3.4 Transformation of T7 Express Chemically Competent E. coli Cells and Isolation of Plasmids/Gibson Products 18
1.4 Small-Scale Protein Expression for Mutant Library Evaluation 18
1.5 Large-Scale Protein Expression for Validation and Mechanistic Experiments 19
1.6 Determination of Hemeprotein Concentration 19
1.7 Protein Purification 20
1.8 Screening of Enzyme Mutant Libraries 20
1.8 Enzymatic Reactions for Validation of Enzymatic Activity 21
1.9 Enzymatic Reactions for Mechanistic Studies 22
2. Discovery of Initial Activity 23
3. GC/MS Analytical Methods 28
3.1 GC/MS Analysis of Hexamethyldisiloxane (**1**) Biocatalytic Reactions 28
3.2 GC/MS Analysis of Octamethyltrisiloxane (**2**) Biocatalytic Reactions 36
3.2 GC/MS Analysis of Octamethyltrisiloxane (**2**) Biocatalytic Reactions 52
4. Experimental Data Relevant to Figure 2A 60
5. Experimental Data Relevant to Figure 2B 64
6. Experimental Data Relevant to Figure 2C 68
7. Experimental Data Relevant to Figure 3A 72
8. Experimental Data Relevant to Figure 3B 74
9. Experimental Data Relevant to Figure 3C 77
9.1 Enzymatic ABTS Assay for Methanol 77
9.2 Purpald Assay for Formaldehyde 83
10. Experimental Data Relevant to Figure 3D 87
11. Hydrolysis in the Siloxane **1** Reaction Manifold 89
12. pH-Dependent Hydrolysis of Carbinol **4** 94
13. Protein-Concentration Dependence 97
14. Oxygen-Dependence Studies 100
14.1 Aerobic 100
14.2 Aerobic with catalase/GOX 101
14.3 35 ppm O_2 Atmosphere 101
13.4 35 ppm O_2 with catalase/GOX 101
14.5 35 ppm O_2, then recovery after 1 h 102
14.6 Buffer with catalase/GOX 102
15. Experimental Data Relevant to Figure 4 107
15.1 Observation of Formylsiloxane **10** in GC/MS Traces 107
15.2 High-Resolution Mass Spectrometry of Carbinol **4** Enzymatic Reactions 111
15.2 Studies of Formylsiloxane **10** Prepared *in situ* via Swern Oxidation of Carbinol **4** 111

17. Comparison of Tris and KPi Buffers 117
18. Enzymatic Reaction Time-Course with Siloxane **2** 119
19. Enzymatic Reaction Time-Course with Siloxane **3** 122
20. DNA Sequences of Engineered Enzymes 125
14.1 DNA Sequence of *L*SilOx1 125
14.2 DNA Sequence of *L*SilOx2 125
14.3 DNA Sequence of *L*SilOx3 126
14.4 DNA Sequence of *L*SilOx4 126
14.5 DNA Sequence of *L*SilOx5 127
14.6 DNA Sequence of *L*SilOx6 127
14.7 DNA Sequence of *L*SilOx7 128
14.8 DNA Sequence of *C*SilOx1 129
14.9 DNA Sequence of *C*SilOx2 129
14.10 DNA Sequence of *C*SilOx3 130
20. Materials and Methods for the Preparation of Analytical Standards 131
21. NMR Spectra 142

List of Figures

Figure S1. Representative gas chromatogram and EI mass spectrum of a 0.482 mM sample of carbinol **4** (4.00 min) with 5 mM 1,3,5-trimethoxybenzene (5.94 min). Note: the peak present at 2.491 min corresponds to ethyl propionate, an impurity present in EtOAc. 32
Figure S2. Calibration curve for carbinol **4**. 33
Figure S3. Representative gas chromatogram and EI mass spectrum of a 0.341 mM sample of silanol **5** (3.11 min) with 5 mM 1,3,5-trimethoxybenzene (5.90 min). Note: the peak present at 2.51 min corresponds to ethyl propionate, an impurity present in EtOAc. 34
Figure S4. Calibration curve for silanol **5** in reactions with siloxane 1 or carbinol **4**. 35
Figure S5. Representative gas chromatogram and EI mass spectrum of a 0.341 mM sample of silanol **5** (2.46 min) with 5 mM 1,3,5-trimethoxybenzene (5.45 min). 40
Figure S6. Calibration curve for silanol 5 in reactions with siloxane **2**. 41
Figure S7. Representative gas chromatogram and EI mass spectrum of a 0.482 mM sample of carbinol **4** (3.16 min) with 5 mM 1,3,5-trimethoxybenzene (5.45 min). 42
Figure S8. Calibration curve for carbinol 4 in reactions with siloxane **2**. 43
Figure S9. Representative gas chromatogram and EI mass spectrum of a 0.436 mM sample of silanol **7** (3.39 min) with 5 mM 1,3,5-trimethoxybenzene (5.44 min). 44
Figure S10. Calibration curve for silanol **7**. 45
Figure S11. Representative gas chromatogram and EI mass spectrum of a 0.394 mM sample of silanol **S2** (3.43 min) with 1,3,5-trimethoxybenzene (5.45 min). 46
Figure S12. Calibration curve for silanol **S2**. 47
Figure S13. Representative gas chromatogram and EI mass spectrum of a 0.222 mM sample of carbinol **S1** (4.04 min) with 1,3,5-trimethoxybenzene (5.44 min). 48
Figure S14. Calibration curve for carbinol **S1**. 49
Figure S15. Representative gas chromatogram and EI mass spectrum of a 0.328 mM sample of carbinol **6** with 5 mM 1,3,5-trimethoxybenzene. 50
Figure S16. Calibration curve for carbinol **6**. 51
Figure S17. Representative gas chromatogram and EI mass spectrum of a 0.320 mM sample of carbinol **8** (1.87 min) with 5 mM 1,3,5-trimethoxybenzene (2.39 min). 56
Figure S18. Calibration curve for carbinol **8**. 57
Figure S19. Representative gas chromatogram and EI mass spectrum of a 0.362 mM sample of silanol **9** (1.66 min) with 5 mM 1,3,5-trimethoxybenzene (2.37 min). 58
Figure S20. Calibration curve for silanol **9**. 59
Figure S21. Representative example of a reaction trace of siloxane 1 with *L*SilOx4 with progressive levels of zoom showing silanol **5** and trace levels of carbinol **4**. The peak present at 2.50 is ethyl propionoate, an impurity present in the ethyl acetate extraction solvent. 62
Figure S22. Stacked GC chromatograms of representative enzymatic reactions with siloxane **1** using wild-type $P450_{BM3}$ (red, top) and *L*SilOx7 (blue). The wild-type enzyme has no detectable activity whereas the engineered *L*SilOx4 enzyme generates silanol **5** and trace amounts of carbinol **6**. 63
Figure S23. Representative example of a reaction trace of siloxane **2** with *L*SilOx7 with progressive levels of zoom showing silanol **7**, silanol **5** (via hydrolysis), and trace levels of carbinol **6**. 66
Figure S24. Stacked GC chromatograms of representative enzymatic reactions with siloxane **2** using wild-type $P450_{BM3}$ (red, top) and *L*SilOx7 (blue). The wild-type enzyme has no detectable activity whereas the engineered *L*SilOx7 enzyme generates silanol **7**, silanol **5** (from hydrolysis), and trace amounts of carbinol **6**. 67

Figure S25. Representative example of a reaction trace of siloxane 3 with *C*SilOx2 with progressive levels of zoom showing silanol **9** and trace levels of carbinol 8. Although *C*SilOx3 has higher activity per unit of enzyme, the traces shown are an example of *C*SilOx2 because of the increased protein expression and higher overall product. 70
Figure S26. Stacked GC chromatograms of representative enzymatic reactions with siloxane **3** using wild-type $P450_{BM3}$ (red, top) and *C*SilOx2 (blue). The wild-type enzyme has no detectable activity whereas the engineered *C*SilOx2 enzyme generates silanol **9** and trace amounts of carbinol **8**. 71
Figure S27. ABTS calibration curve for detection of methanol. 80
Figure S28. ABTS assay calibration points (left) and reaction analysis with siloxane **1**, carbinol **4**, methanol, formaldehyde, and no substrate (right). 81
Figure S29. Calibration curve for formaldehyde detection using the Purpald reagent. 84
Figure S30. Purpald assay calibration points (left) and reaction analysis with siloxane **1**, carbinol **4**, methanol, formaldehyde, and no substrate (right). 85
Figure S31. Response of siloxane **1** vs. 1,3,5-trimethoxybenzene internal standard over time in *E. coli* lysate at pH 7.00. 91
Figure S32. Plot for the change in concentration of carbinol 4 and silanol 5 over time in *E. coli* lysate at pH 7.00. 93
Figure S33. Hydrolysis of carbinol **4** at varying pH in 100 mM Tris buffer. 95
Figure S34. Plot for protein concentration dependence data of reactions with carbinol **4** as substrate including imidazole, heat treatment, and buffer controls. 99
Figure S35. Bar graph of oxygen-dependence experiments with siloxane **1** as substrate. 104
Figure S36. Bar graph of oxygen-dependence experiments with carbinol **4** as substrate. 106
Figure S37. Appearance of a trace peak at 3.55 min in an enzymatic reaction time-course with carbinol **4** (Figure 3D) 108
Figure S38. Mass spectrum of the trace peak observed with 3.55 min retention time in a 5 min timepoint of an enzymatic reaction with carbinol **4** as substrate. 109
Figure S39. Decay of the 3.55 min peak over time is observed by analyzing an enzymatic reaction sample on GC/MS over time. 110
Figure S40. $^{1}H–^{29}Si$ HMBC at –40 ºC showing correlation of the formyl C–H δ 11.66 (s, 1H) to a Si center with methyl groups. 113
Figure S41. ^{1}H NMR (400 MHz, CD_2Cl_2, –40 ºC) of the Swern reaction mixture, showing the formylsiloxane **10** and trace amounts of formaldehyde as a byproduct. 114
Figure S42. ^{1}H NMR (400 MHz, CD_2Cl_2, 25 ºC) of the Swern reaction mixture, showing the formylsiloxane **10** and small amounts of formaldehyde as a byproduct. 115
Figure S43. A GC/MS trace and mass fragmentation pattern of the formylsiloxane (**10**) peak corresponding to the same peak in both retention time and mass fragmentation as observed in enzymatic reactions. The signal present at 3.09 corresponds to silanol **5**. 116
Figure S44. Comparion of Tris and KPi buffers and NADPH and NADPH cofactor regeneration for reactions with siloxane **1** and carbinol **4** as substrates. 119
Figure S45. Enzymatic reaction time-course for siloxane **2** at 3.7 µM *L*SilOx7. 121
Figure S46. Enzymatic reaction time-course for siloxane **2** at 0.19 µM *C*SilOx3. 124

List of Tables

Table S1. Thermocycler conditions for SSM PCR. 10
Table S2. Primers used for PCR mutagenesis and amplification. 12
Table S3.Thermocycler conditions for insert epPCR. 13
Table S4. Thermocycler conditions for BB1/BB2. 14
Table S5. Thermocycler conditions for recombination of PCR products. 16
Table S6. Thermocycler conditions for amplification of StEP insert 17
Table S7. GC/MS oven parameters for GC-FID analysis. 25
Table S8. Summary of analytes. 26
Table S9. Summary of initial activity screen with GC-FID for formation of silanol 5. 27
Table S10. GC/MS oven parameters. 29
Table S11. Mass spectrometer parameters (scan mode). 30
Table S12. Summary of analytes. 31
Table S13. GC/MS oven parameters. 37
Table S14. Mass spectrometer parameters (scan mode). 38
Table S15. Summary of analytes. 39
Table S16. GC/MS oven parameters. 53
Table S17. Mass spectrometer parameters (scan mode) 54
Table S18. Summary of analytes 55
Table S19. Summary of enzyme lineage for hexamethyldisiloxane (**1**). 60
Table S20. Experimental data relevant to Figure 2A. 61
Table S21. Summary of enzyme lineage for octamethyltrisiloxane (**2**). 64
Table S22. Experimental data relevant to Figure 2B. Carbinol **S1**, silanol **S2**, and carbinol **4** were not detected in any reactions and are therefore omitted from the table. 65
Table S23. Summary of enzyme lineage for octamethylcyclotetrasiloxane (**3**). 68
Table S24. Experimental data relevant to Figure 2C. Carbinol **S1**, silanol **S2**, and carbinol **4** were not detected in any reactions and are therefore omitted from the table. 69
Table S25. Experimental data relevant to Figure 3A with siloxane **1** as substrate. The concentration of *L*SilOx4 was 4.7 µM. 72
Table S26. Experimental data relevant to Figure 3A with carbinol **4** as substrate. The concentration of *L*SilOx4 was 4.7 µM. 73
Table S27. Primers used for truncation of *L*SilOx4 to prepare variant *L*SilOx4ΔFAD with the FAD domain removed. 74
Table S28. Experimental data relevant to Figure 3B with siloxane **1** as substrate. 75
Table S29. Experimental data relevant to Figure 3B with carbinol **4** as substrate. 76
Table S30. Preparation of ABTS methanol calibration points. 79
Table S31. Methanol detected by the ABTS assay and silanol **5** detected in parallel reactions analyzed by GC/MS. Note: Formaldehyde solution contains 10–15% methanol as stabilizer. While the ABTS assay is selective for methanol, it can detect other alcohols and may detect carbinol **4** with low activity. 82
Table S32. Formaldehyde detected by the Purpald reagent assay and silanol **5** detected in parallel reactions analyzed by GC/MS. 86
Table S33. Experimental data relevant to Figure 3D with siloxane **1** as substrate. The concentration of *L*SilOx4 was 9.35 µM. 87
Table S34. Experimental data relevant to Figure 3D with carbinol **4** as substrate. The concentration of LSilOx4 was 9.35 µM. 88

Table S35. Experimental data for siloxane **1** response relative to internal standard 1,3,5-trimethoxybenzene over time in *E. coli* lysate. 90
Table S36. Experimental data for carbinol **4** and silanol **5** concentration over time in *E. coli* lysate at pH 7.00. 92
Table S37. pH-dependent hydrolysis of carbinol **4** data. Formation of silanol **5** is not observed at any pH. 96
Table S38. Protein concentration dependence data with carbinol **4** as substrate including imidazole, heat treatment, and buffer only controls. 98
Table S39. Oxygen dependence data for reactions with siloxane **1** as a substrate with 5 μM *L*SilOx4. ... 103
Table S40. Oxygen dependence data for reactions with carbinol **4** as a substrate with 5.0 μM *L*SilOx4. 105
Table S41. High-resolution mass spectrometry data for enzymatic reaction analytes. [a]Siloxane **S4** is a trace impurity in carbinol **4** which is a constitutional isomer of formylsiloxane **10**. 111
Table S47. Comparison of Tris and KPi buffers and NADPH cofactor and cofactor regeneration with siloxane **1** as a substrate. *L*SilOx4 was 3.1 μM in Tris buffer and 4.2 μM in KPi buffer. 117
Table S48. Comparison of Tris and KPi buffers and NADPH cofactor and cofactor regeneration with carbinol **4** as a substrate. *L*SilOx4 was 3.1 μM in Tris buffer and 4.2 μM in KPi buffer. 118
Table S49. Experimental data relevant to Figure S44 with siloxane **2** as substrate. *L*SilOx7 was measured at 3.7 μM. 120
Table S50. Experimental data relevant to Figure S44 with siloxane **3** as substrate. *C*SilOx3 was measured at 0.19 μM. 123

1. Materials and Methods

1.1 Abbreviations

1,3,5-TMB	1,3,5-trimethoxybenzene
ALA	5-aminolevulinic acid
ABTS	2,2′-azino-bis(3-ethylbenzothiazoline-6-sulfonic acid) diammonium salt
Bz	benzoyl
DNA	deoxyribonucleic acid
dSSM	double site-saturation mutagenesis
epPCR	error-prone PCR
equiv	equivalents
FI	field ionization
G6P	D-glucose-6-phosphate
G6PDH	D-glucose-6-phosphate dehydrogenase
GC	gas chromatography
GC/MS	gas chromatography/mass spectrometry
HMBC	hetereonuclear multiple bond correlation
IPTG	isopropyl β- D -1-thiogalactopyranoside
KPi	potassium phosphate buffer
LB_{amp}	Luria–Bertani medium with 100 μg/mL ampicillin
LB_{carb}	Luria–Bertani medium with 100 μg/mL carbenicillin
MeCN	acetonitrile
$NADP^+$/NADPH	nicotinamide adenine dinucleotide phophate
NEB	New-England Biolabs
NMR	nuclear magnetic resonance
PCR	polymerase chain reaction
SOC	super optimal broth with catabolite repression
SSM	site-saturation mutagenesis
StEP	staggered extension process *in vitro* recombination
TB_{amp}	terrific broth medium with 100 μg/mL ampicillin
TB_{carb}	terrific broth medium with 100 μg/mL carbenicillin
THF	tetrahydrofuran
TLC	thin-layer chromatography
Tris	tris(hydroxymethyl)aminomethane buffer
UV	ultraviolet

1.2 General

Expression vector pET22(b)+ was used, and cloning was performed using Gibson assembly (*42*). *Escherichia coli* cells were grown using Luria-Bertani medium or Terrific Broth with 100 μg/mL carbenicillin (LB_{carb} or TB_{carb}) or 100 μg/mL ampicillin (LB_{amp} or TB_{amp}). T7 Express competent *E. coli* cells were purchased from New England Biolabs Inc (NEB, Ipswich, MA). T5 exonuclease, Phusion polymerase, and Taq ligase were purchased from NEB. Standard Taq buffer (6x concentrate) and Phusion GC buffer (6x concentrate) were purchased from NEB and diluted to 1x final concentration in PCRs. Tris(hydroxymethyl)aminomethane buffer (abbreviated as Tris, pH 7.00) was used as a buffering system for

cell lysates and purified proteins, unless otherwise specified. The following proteins were all purchased from Sigma-Aldrich: bovine serum albumin (BSA), glucose oxidase (from *Aspergillus niger*), alcohol oxidase (from *Pichia pastoris*), peroxidase (from horseradish), catalase (from *C. glutamicum*), and glucose-6-phosphate dehydrogenase (from *S. cerevisiae*).

Biocatalytic reaction analysis was performed with an Agilent 8890 gas chromatograph equipped with a 5977B mass spectrometer detector and a DB-5MS capillary column (30 m length, 0.250 mm diameter, 0.25 μm film thickness using split-mode capillary injection and electron-impact ionization) or with an Agilent 7820A gas chromatograph equipped with a flame ionization detector (FID). Calibration curves were generated using serial dilutions of the appropriate material with 5 mM 1,3,5-trimethoxybenzene as an internal standard. Yields were determined by adjusting the calculated concentration of product relative to internal standard, accounting for the dilution factor of enzymatic reaction extraction.

1.3 Cloning, Mutagenesis, and Plasmid Isolation

1.3.1 Site-Saturation Mutagenesis

Site-saturation mutagenesis (SSM) experiments were performed using primers bearing degenerate codons (NDT, VHG, TGG) as per the "22-codon trick" using a modified QuikChange protocol (*43*). A break in the ampicillin cassette was introduced, resulting in two fragments. The degenerate primer targeting the site of interest (forward) and the Amp_int_reverse (reverse) primer were used to yield one fragment. The primer targeting the site of interest (reverse) and the Amp_int_forward (forward) primer were used to yield the other fragment. The PCR conditions were as follows (final concentrations): 1x Phusion GC Buffer, 200 μM dNTPs, 0.5 μM of forward primer, 0.5 μM reverse primer, and 0.02 U/μL of Phusion polymerase. Thermocycling conditions are outlined below (Table S1). Upon completion of PCRs, the remaining template DNA was digested with *Dpn*I (1 μL). Gel purification was performed using gel electrophoresis (1% agarose gel containing a SYBR Gold nucleic acid gel stain), and DNA was visualized on a blue transilluminator. DNA was isolated using a Zymoclean DNA gel recovery kit. The purified PCR product was then assembled using the Gibson assembly protocol (*42*).

Step	Temperature (ºC)	Time (min:s)	Number of Cycles
Initial Denaturation	98	00:30	1
Denaturation	98	00:10	5
Annealing	98 to 55 at 1 ºC/s	00:15	
Extension	72	2:06	
Denaturation	98	0:10	25
Annealing	55	0:15	
Extension	72	2:06	
Extension	72	5:00	1
Hold	10	–	

Table S1. Thermocycler conditions for SSM PCR.

1.3.2 Random Mutagenesis

Random mutations were introduced during error-prone PCR via the addition of varying $MnCl_2$ concentrations (200–500 μM) to *Taq* PCRs using the primers described below (**Table S2**). A break in the ampicillin cassette was introduced in error-prone PCRs, resulting in two backbone fragments (BB1/BB2), while a third fragment (insert) was amplified that encodes the heme domain of the enzyme. Mutations within this third fragment were introduced by varying the concentration of $MnCl_2$ in the PCRs. The insert PCR thermocycler conditions are outlined below (**Table S3**). Final concentrations for the insert PCR are as follows: 1x standard Taq buffer, 200 μM dNTPs, 0.5 μM forward primer, 0.5 μM reverse primer, 0.08 U/μL of *Taq* polymerase, and 200–400 μM $MnCl_2$. The two backbone PCR conditions were as follows: 1x Phusion GC buffer, 5% DMSO, 200 μM dNTPs, 0.5 μM forward primer, 0.5 μM reverse primer, and 0.02 U/μL of Phusion polymerase. Primers NSS005 (forward) with HR1-v2 (reverse) or RLO005 (forward) with HR1-v4 (reverse) were used to amplify the region encoding the enzyme (insert). Two primer pairs (Amp_int_forward (forward) with NSS007 (reverse) or RLO007 (reverse)) and (HF1-v2 (forward) or HF1-v4 (forward) and Amp_int_reverse (reverse)) were used to amplify the backbone fragments (BB1/BB2) using Phusion polymerase and the parent DNA template. Thermocycler conditions for the insert and BB1/BB2 are outlined below (**Tables S3 and S4**). Upon completion of the PCRs, remaining template DNA was digested using *Dpn*I (1 μL). The amplified fragments were purified by gel electrophoresis (1% agarose gel containing a SYBR Gold nucleic acid gel stain), and DNA was visualized on a blue transilluminator. The three amplified fragments were then assembled into a circular plasmid using a Gibson assembly protocol (*42*).

Primer	Amplicon	Sequence (5’ to 3’)
RLO005	Insert forward (use with v4)	GGATAACAATTCCCCTCTAGAAATAATTTTG TTTAACTTTAAGAAGGAGATATACATATG
RLO007	BB1 reverse (use with v4)	CATATGTATATCTCCTTCTTAAAGTTAAACA AAATTATTTCTAGAGGGGAATTGTTATCC
NSS005	Insert forward (use with v2)	AACTTTAAGAAGGAGATATACATATGACAA TTAAAGAAATGCCTCAGCCA
NSS007	BB1 reverse (use with v2)	TGGCTGAGGCATTTCTTTAATTGTCATATGT ATATCTCCTTCTTAAAGTT
HR1-v2	insert reverse (use with NSS)	CTTTTTTAGCAGACTGTTCAGTGCTAGGTGA AGGAATACC
HR1-v4	insert reverse (use with RLO)	CGTATTATGAGCGTTTTCTGCCTTTTTGCG
HF1-v2	BB2 forward (use with NSS)	GGTATTCCTTCACCTAGCACTGAACAGTCTG CTAAAAAAG
HF1-v4	BB2 forward (use with RLO)	CGCAAAAAGGCAGAAAACGCTCATAATACG
Amp_int_forward	BB1 forward	GCTAACCGCTTTTTTGCACAACATG
Amp_int_reverse	BB2 reverse	TTGTGCAAAAAAGCGGTTAGCTCC

Table S2. Primers used for PCR mutagenesis and amplification.

Step	Temperature (ºC)	Time (min:s)	Number of Cycles
Initial Denaturation	98	5:00	1
Denaturation	98	00:30	30
Annealing	64	00:30	
Extension	72	1:30	
Extension	72	5:00	1
Hold	10	–	

Table S3. Thermocycler conditions for insert epPCR.

Step	Temperature (ºC)	Time (min:s)	Number of Cycles
Initial Denaturation	98	00:30	1
Denaturation	98	00:10	5
Annealing	98 to 64 at 1 ºC/sec	00:15	
Extension	72	2:06	
Denaturation	98	0:10	25
Annealing	64	0:15	
Extension	72	2:06	
Extension	72	5:00	1
Hold	10	–	

Table S4. Thermocycler conditions for BB1/BB2.

1.3.3 Recombination via Staggered Extension Process

Staggered extension process (StEP) PCR was performed using a mixture of plasmids of the variants to be recombined in equimolar fashion, using this mixture as the template DNA. The StEP PCR was then conducted by varying the annealing temperature and by using a shorter extension time following a standard protocol (*44*, *45*). The PCR conditions were as follows (final concentrations): 1x standard *Taq* buffer, 200 µM dNTPs, 0.5 µM of primer NSS005 and 0.5 µM of primer HR1-v2 or µM of primer RLO005 and 0.5 µM of primer HR1-v4, and 0.08 U/µL of *Taq* polymerase. Amplification of the recombined fragment was conducted using a Phusion PCR protocol. Thermocycling conditions are outlined below (**Tables S5** and **S6**). Upon completion of PCRs, the remaining template DNA was digested with *Dpn*I (1 µL). The PCR product was purified by gel electrophoresis (1% agarose gel containing a SYBR Gold nucleic acid gel stain), and DNA was visualized on a blue light transilluminator. The insert library was inserted into the pET22(b)+ vector using Gibson assembly (*42*) with BB1/BB2 fragments as outlined in section 1.3.2 Random Mutagenesis.

Step	Temperature (ºC)	Time (min:s)	Number of Cycles
Initial Denaturation	95	5:00	1
Denaturation	95	0:10	120
Annealing	55	0:05	
Extension	Gradient (50 → 72)	0:05	
Hold	10	–	

Table S5. Thermocycler conditions for recombination of PCR products.

Step	Temperature (ºC)	Time (min:s)	Number of Cycles
Initial Denaturation	98	5:00	1
Denaturation	98	00:30	30
Annealing	64	00:30	
Extension	72	1:30	
Extension	72	5:00	1
Hold	10	–	

Table S6. Thermocycler conditions for amplification of StEP insert.

1.3.4 Transformation of T7 Express Chemically Competent E. coli Cells and Isolation of Plasmids/Gibson Products

T7 Express Competent *E. coli* cells were utilized for all experiments. Plasmids were mixed with competent cells on ice in PCR tubes. The mixture was kept on ice for 30 min, after which time transformation was accomplished by heat shocking the mixture in a 42 ºC water bath for exactly 10 seconds. After a 5-min recovery on ice, the cells were diluted with SOC medium and plated on LB_{carb} agar plates. Plasmids were isolated from stationary-phase cultures by miniprep (Qiagen), and sequencing was performed by Laragen, Inc. (Culver City, CA) using T7 promoter and HR1-V2 terminator primers.

1.4 Small-Scale Protein Expression for Mutant Library Evaluation

After a site-saturation mutagenesis (SSM), error-prone PCR (epPCR), or staggered extension process (StEP) library was generated, 84 single colonies were randomly picked and cultured in 400 μL of LB medium with 100 μg/mL carbenicillin (LB_{carb}) or 100 μg/mL ampicillin (LB_{amp}) in a sterilized 96-well culture plate (2-mL well volume). The plate typically contained eight wells inoculated with single colonies expressing the parent enzyme, two sterile wells, and two wells inoculated with single colonies expressing tryptophan synthase variant Tm9D8* as a non-hemoprotein control (*46*). The cultures were covered with EasyApp microporous film and grown at 37 ºC, 220 rpm, and 80% relative humidity for 12–16 h. A separate, sterilized 96-well culture plate was filled with 930 μL of Terrific Broth medium containing 100 μg/mL carbenicillin (TB_{carb}) or 100 μg/mL ampicillin (TB_{amp}). The plate with TB_{carb} or TB_{amp} was inoculated with the LB_{carb} or LB_{amp} preculture (20 μL/well) and incubated at 37 ºC, 220 rpm, and 80% relative humidity for 3 h. The plate was then cooled on ice for 30 min, induced with 0.5 mM IPTG, 1 mM ALA, 3.5 μM $FeCl_3$, and 1:1000 trace metals master mix (as described in (*47*)) (final concentrations), and then incubated at 22 ºC and 220 rpm for 16–22 h. After expression, the cells were pelleted (4,500 *g*, 15 min, 4 ºC) via centrifugation and the supernatant was discarded. The pelleted cells were sealed with a TempPlate sealing foil and stored in a –20 ºC freezer for at least 16 h prior to lysis.

1.5 Large-Scale Protein Expression for Validation and Mechanistic Experiments

Culture volumes of 50-mL, 250-mL, and 1-L validation of enzymatic activity and mechanistic experiments were grown as follows. *E. coli* transformed with pET22b(+) constructs encoding P450 variants were grown in a 15-mL culture tube at 37 ºC and 220 rpm in 5–11-mL LB_{carb} or LB_{amp} medium for 16–20 h. Subsequently, 0.01 mL preculture/1 mL expression culture was used to inoculate TB_{carb} or TB_{amp} media in a sterile Erlenmeyer flask covered with sterilized aluminum foil. The culture was incubated at 37 ºC and shaken at 220 rpm for approximately 2–4 h until the optical cell density at 600 nm (OD_{600}) was 0.7–0.9. Then, the culture was cooled in an ice bath for 30 min, induced with 0.5 mM IPTG, 1 mM ALA, 3.5 µM $FeCl_3$, and 1:1000 trace metals master mix (as described in (47)) (final concentrations), and then incubated at 22 ºC and 220 rpm for 16–22 h for protein expression. After expression, the cultures were transferred to 50-mL Falcon tubes or screw-cap bottles and pelleted via centrifugation (4,500 g, 15 min, 4 ºC). The Falcon tube supernatants were discarded, and the cell pellets were stored in a freezer at –20 ºC for at least 16 h prior to lysis. Cultures pelleted in bottles were transferred to tared 50-mL Falcon tubes by resuspension in a small volume of culture and pelleted via centrifugation (4,500 g, 15 min, 4 ºC). After the supernatant was discarded, the cell pellets were stored in a freezer at –20 ºC for at least 16 h prior to lysis.

1.6 Determination of Hemeprotein Concentration

Hemeprotein concentration was determined for purified protein and cell lysate by performing a CO-binding assay (*48, 49*). Hemeprotein solution was added to Greiner Bio-One clear plastic flat-bottomed 96-well plates (180 µL/well) in 3–6 technical replicates per protein. To the wells was then added a solution of 300 mM sodium dithionite in 1 M pH 8.00 potassium phosphate buffer (KPi) (20 µL/well). Absorbance was measured at 450 nm and 490 nm using a Tecan Spark multimode microplate reader. The 96-well plate was then placed in a CO-chamber. The atmosphere in the chamber was evacuated with a vacuum pump to approximately 20 mmHg, and the chamber was refilled to atmospheric pressure with CO. The 96-well plate was incubated in the CO atmosphere for 30 min, then measured again using the microplate reader at 450 nm and 490 nm. Beer's law was used to determine the hemeprotein concentration of the solution using the $\Delta A_{450–490}$ between the CO-bound and dithionite reduced samples, the $\varepsilon_{450–490}$ value of 0.091, dilution factor of 1.1, and the pathlength of 0.74 cm. In some samples with higher expression the sample was further diluted for CO-binding measurements.

1.7 Protein Purification

For purification, cell pellets were frozen at −20 °C for at least 24 hours. Cells were thawed and resuspended in binding buffer (20 mM Tris, 100 mM NaCl, 20 mM imidazole, pH 7.00 (at 23 ºC)), approx. 5 mL/g wet cell pellet) and lysed by sonication (QSonica Q500 sonicator, 25% amplitude, 33% duty cycle, 2 minutes, 1 s on, 2 s off) or in 100 mM pH 7.00 Tris buffer containing 1 mg/mL lysozyme, 0.5 mg/mL DNAse, and 2 mM $MgCl_2$ and lysed by incubation at 37 ºC and 180 rpm for 1 h. The lysate was clarified by centrifugation (20,817 g, 15 min, 4 °C) followed by filtration (0.22-μm syringe filter). The protein was purified using a 1-mL HisTrap HP column (GE Healthcare) or a column packed with 5–10 g Ni-NTA agarose (Qiagen), washing with 2–3 column volumes of binding buffer and eluting with elution buffer (25 mM Tris, 100 mM NaCl, 300 mM imidazole, pH 7.00 (at 23 ºC)). Fractions containing purified enzyme were pooled and concentrated with repeated centrifugation and dilution in 100 mM pH 7.00 Tris buffer or 100 mM pH 7.00 KP*i* in an Amicon ultra-centrifugal filter (30 kDa molecular weight cutoff). The concentrated protein was divided into aliquots (100 μL) in PCR tubes and flash frozen on powdered dry ice or in liquid nitrogen. The frozen aliquots were stored at −80 °C. Protein concentration of the protein aliquots was determined after a freeze/thaw cycle via the CO-binding assay with appropriate dilutions of the protein solutions (0 to 20-fold).

1.8 Screening of Enzyme Mutant Libraries

Enzyme mutant libraries were evaluated on a 350-μL scale using crude cell lysate in individual snap-cap 2.0-mL microtubes for siloxane **1** or 96-well plates constructed from individual 1.0-mL autosampler neckless shell vials for siloxanes **2** and **3**. The 96-well plates of individual shell vials were constructed by inserting 1.0-mL autosampler neckless shell vials into a 96-well microtiter plate using a USA Scientific 1000-μL pipette tip rack as an alignment guide. The snap-cap vials were sealed by individual capping after the addition of all biocatalytic reaction components. The 96-well shell vial plates were sealed by capping with an additional 96-well microtiter plate and centrifugation (3,000 g, 1 min, 25 ºC).

The 96-well plates containing frozen cell cultures were thawed for 10 min at 25 ºC, and the pelleted cells were then resuspended in lysis buffer (400 μL/well) containing 1 mg/mL lysozyme, 0.07 mg/mL DNAse, and 2 mM $MgCl_2$. The cells were then lysed at 37 ºC and 160 rpm for 1 h. Cell debris was then pelleted by centrifugation (4,500 g, 15 min, 4 ºC). The biocatalytic reaction vessels were then charged with the NADPH cofactor regeneration system (12.5 μL/vessel) for final reaction concentrations of 0.5 mM $NADP^+$, 40 mM glucose-6-phosphate, and 2 U/mL of glucose-6-phosphate dehydrogenase. A 140 mM

substrate stock was prepared by dissolving the appropriate substrate in the specified cosolvent (MeCN for silxoane **2**, EtOH for siloxanes **1** and **3**). The cell lysate was then added (325 μL/reaction) to the reaction vessel, followed by the substrate (12.5 μL/reaction) to give a final concentration of 5 mM substrate. The reaction vessels were sealed immediately after the addition of substrate and shaken at 800 rpm for 4 h at 25 ºC. After the 4 h reaction, the reaction vessels were unsealed and 5 mM 1,3,5-trimethoxybenzene in ethyl acetate were added (450 μL/well) quickly. The organic and aqueous phases were mixed by using a vortex mixer (microtubes) or by pipetting the mixture up and down with a multi-channel pipette (glass shells). Phase separation in microtubes was facilitated by centrifugation at 20,817 g and 4 ºC for 15 min. The 96-well shell vial plates were sealed with TempPlate sealing foil and centrifuged at 4,000 g and 4 ºC for 15 min. Aliquots of the organic phase (300 μL/reaction) were then transferred to individual 400-μL flat bottom glass inserts in 2-mL screw-cap vials which were sealed with septum screw caps. Analysis was performed using GC/MS with product concentrations and yield determined by response relative to the 5 mM 1,3,5-trimethoxybenzene internal standard using a calibration curve.

1.8 Enzymatic Reactions for Validation of Enzymatic Activity

Validation of enzymatic activity was performed with 50-mL expression cultures (1.5 Large-Scale Protein Expression for Validation and Mechanistic Experiments). The Falcon tubes containing frozen cell cultures were thawed for 30 min at 25 ºC, and the pelleted cells were resuspended in lysis buffer (4 mL/1 g of pellet) containing 1 mg/mL lysozyme, 0.07 mg/mL DNAse, 2 mM $MgCl_2$. The Falcon tubes were then incubated at 37 ºC with shaking at 180 rpm for 1 h. The lysed cultures were then transferred to 2.0-mL microtubes and centrifuged at 20,817 *g* and 4 ºC for 15 min. The supernatants for each variant were combined in 15-mL Falcon tubes. The NADPH cofactor regeneration system (12.5 μL/vessel) was then added to 2.0-mL microtubes to give final reaction concentrations of 0.5 mM NADP+, 40 mM glucose-6-phosphate, and 2 U/mL of glucose-6-phosphate dehydrogenase. A 140 mM substrate stock was prepared by dissolving the appropriate substrate in the specified cosolvent (MeCN for siloxane **2**, EtOH for siloxanes **1** and **3**). The cell lysate was then added (325 μL/reaction) to the reaction vessel, followed by the substrate (12.5 μL/well) to give a final concentration of 5 mM substrate. The microtubes were sealed immediately after the addition of substrate and shaken at 800 rpm for 4 h at 23 ºC. The hemeprotein concentration was measured for each variant (see 1.6 Determination of Hemeprotein Concentration). After the 4 h reaction, the reaction vessels were unsealed and 5 mM 1,3,5-trimethoxybenzene in ethyl acetate were added (450 μL/reaction). The organic and aqueous phases were mixed by using a vortex mixer for 10 s. Phase

separation was facilitated by centrifugation at 20,817 *g* and 4 ºC for 15 min. Aliquots of the organic phase (200–300 μL/reaction) were then transferred to individual 400-μL flat bottom glass inserts in 2-mL screw-cap vials which were sealed with septum screw caps. Analysis was performed using GC/MS with product concentrations and yield determined by response relative to the 5 mM 1,3,5-trimethoxybenzene internal standard using a calibration curve. Superior variants were selected for subsequent rounds of evolution by comparing product concentration relative to the measured protein concentration.

1.9 Enzymatic Reactions for Mechanistic Studies

All mechanistic experiments were performed on a 350-μL reaction volume scale in 2.0-mL microtubes or 2.0-mL crimp-cap glass vials using 325 μL *E. coli* lysate, purified protein solution (at the specified concentration), or buffer (without protein) as specified in individual experimental protocols. For reactions in lysate, Falcon tubes containing cell pellets from 50-mL, 250-mL, or 1-L expression cultures were used for reactions with *E. coli* lysate (see 1.5 Large-Scale Protein Expression for Validation and Mechanistic Experiments). The Falcon tubes containing frozen cell cultures were thawed for 30 min at 25 ºC, and the pelleted cells were resuspended in lysis buffer (4 mL/1 g of pellet) containing 1 mg/mL lysozyme, 0.07 mg/mL DNAse, 2 mM $MgCl_2$. The Falcon tubes were then incubated at 37 ºC with shaking at 180 rpm for 1 h. The lysed cultures were then transferred to 2.0-mL microtubes and centrifuged at 20,817 *g* and 4 ºC for 15 min. The supernatants for each variant were combined in 15- or 50-mL Falcon tubes, and protein concentration was measured by the CO-binding assay. For reactions with purified protein, frozen aliquots were thawed on ice prior to dilution in buffer as specified. Protein concentration for purified protein was determined either for the frozen aliquots or for the diluted protein stock as noted.

For all mechanistic experiments, enzymatic reactions were performed with the NADPH cofactor regeneration system (12.5 μL/vessel, final reaction concentrations of 0.5 mM NADP+, 40 mM glucose-6-phosphate, and 2 U/mL of glucose-6-phosphate dehydrogenase), NADPH (12.5 μL/vessel, final reaction concentrations as specified), or no cofactor (12.5 μL buffer/vessel added). Substrates were prepared as 140 mM substrate solutions in the specified organic cosolvent (5 mM final reaction concentration). The order of addition for all reactions was cofactor, followed by enzyme solution or buffer, then substrate. After the addition of all components, reactions were sealed and shaken at 800 rpm for the specified time. After the reaction was complete, the vessels were unsealed and 5 mM 1,3,5-trimethoxybenzene in ethyl acetate were added (450 μL/reaction). The organic and aqueous phases were mixed by using a vortex mixer for 10 s. Phase separation was facilitated by centrifugation at 20,817 *g* and 4 ºC for 15 min. Aliquots of the organic

phase (200–300 μL/reaction) were then transferred to individual 400-μL flat bottom glass inserts in 2-mL screw-cap vials which were sealed with septum screw caps. Analysis was performed using GC/MS with product concentrations and yield determined by response relative to the 5 mM 1,3,5-trimethoxybenzene internal standard using a calibration curve. Superior variants were selected for subsequent rounds of evolution by comparing product concentration relative to the measured protein concentration.

2. Discovery of Initial Activity

Cytochromes P450s from the Arnold Lab collection were tested in *E. coli* lysate in 96-well plate format (see section 1.8 Screening of Enzyme Mutant Libraries). The collection consisted of 60 distinct variants accumulated from prior directed evolution campaigns. Of these, eight variants were selected for larger scale validation as follows. Freshly transformed *E. coli* were grown on LB_{amp} agar plates, and single colonies were picked and used to inoculate 2 mL of LB_{amp} in 5-mL culture tubes. Three cultures were inoculated for each variant, and the tubes were placed in an incubator and shaken at 220 rpm at 37 ºC. After approximately 18 h, 160 μL of the LB_{amp} cultures were used to inoculate 7.5 mL of TB_{amp} in 15-mL culture tubes, each. The TB_{amp} cultures were then incubated at 37 ºC with shaking at 220 rpm for 3.5 h. After an OD_{600} of 0.80 was reached, the TB_{amp} cultures were cooled on ice for 30 min before being induced with 340 μL of 0.5 mM IPTG, 680 μL of 1 mM ALA, 3.5 μM of $FeCl_3$ with 1:1000 trace metals master mix (as described in (*47*)). The cultures were incubated at 22 ºC with shaking at 220 rpm for approximately 18 h. The cultures were then centrifuged at 4,500 *g* and 4 ºC for 15 min. The supernatant was removed, and the wet pellets were stored in a –20 ºC freezer for at least 16 h prior to lysis.

The frozen pellets were thawed on ice prior to lysis for enzymatic reactions. For each variant, one pellet was resuspended in 2-mL of lysis buffer prepared by adding 16 μL of 2 M $MgCl_2$ and approx. 2 mg of DNAse to 16 mL of 100 mM pH 8.00 KPi buffer. The pellet was then lysed using a beadbeater (30 s on, 30 s off) in a chilled block. Separately, the remaining two pellets for each variant were resuspended in 2 mL of lysis buffer prepared by adding 30 μL of 2 M $MgCl_2$, approx. 4 mg of DNAse, and 30 mg of lysozyme to 30 mL of 100 mM pH 8.00 KPi buffer. The resuspended pellets containing lysozyme lysis buffer were then incubated at 37 ºC with shaking at 220 rpm for 1 h. The lysed cultures were transferred to 2-mL Eppendorf tubes and centrifuged at 20,817 *g* for 10 min at 4 ºC. The supernatant was removed and used directly for enzymatic reactions as described below.

Enzymatic reactions were performed in 2-mL Eppendorf tubes as follows. To the Eppendorf tubes were added 25 μL of NADPH (78 mM in 100 mM pH 8.00 KPi buffer) followed by 975 μL of lysate and

2.1 μL of siloxane **1**. The reactions were then sealed and incubated at 23 ºC with shaking at 60 rpm. Final concentrations were 2 mM NADPH and 10 mM siloxane 1. After 4 h, the reaction tubes were opened and 500 μL of diethyl ether were added. The tubes were vortexed for 10 s and then centrifuged at 20,817 *g* for 10 min at 4 ºC. A 200-μL aliquot of the organic extract was then added to a GC vial insert followed by 8 μL of acetophenone (40 mM in cyclohexane) as an internal standard. The extracts were analyzed by GC-FID with a DB-WAXetr column (30 m × 0.32 mm, 0.25-μm film thickness) using the following parameters: helium carrier gas, column flow 2.5 mL/min, split ratio 20:1, injection temperature 250 °C, detector temperature 300 °C, using the temperature programs specified below. Variant gen1 (*L*SilOx1) was selected as the parent enzyme for evolution. Relative to the wild-type enzymes, *L*SilOx1 has 13 amino acid substitutions as follows: V78A, A82V, F87G, P142S, T175I, A184V, S226R, H236Q, E252G, A290V, L353V, I366V, E442K.

	Rate (ºC/min)	Value (ºC)	Hold Time (min)
Initial		50	1
Gradient 1	20	60	0
Gradient 2	70	260	0.7

Table S7. GC/MS oven parameters for GC-FID analysis.

Analyte	Retention Time (min)
Silanol **5**	2.37
acetophenone	3.66

Table S8. Summary of analytes.

Enzyme Variant (culture collection code)	Lysis Method	Silanol **5** (peak area)	Acetophenone (peak area)	Relative Peak Area
wild-type $P450_{BM3}$ (4862)	beadbeater	0.00	328.02	0.0000
	lysozyme	0.00	1248.85	0.0000
	lysozyme	0.00	1567.94	0.0000
4x (n/a)	beadbeater	1.16	1333.85	0.0009
	lysozyme	0.00	1263.96	0.0000
	lysozyme	0.00	1547.77	0.0000
B9 (1856)	beadbeater	2.28	1235.13	0.0018
	lysozyme	5.00	1473.07	0.0034
	lysozyme	4.26	1349.23	0.0032
gen1 (*L*SilOx1) (5199)	beadbeater	13.45	1115.65	0.0121
	lysozyme	6.90	1455.81	0.0047
	lysozyme	6.78	1476.02	0.0046
B1 C205F (n/a)	beadbeater	0.00	1481.11	0.0000
	lysozyme	0.00	1566.99	0.0000
	lysozyme	0.00	1226.75	0.0000
2C6dr (2558)	beadbeater	2.35	1179.84	0.0020
	lysozyme	3.11	1255.85	0.0025
	lysozyme	3.15	1333.17	0.0024
9C7 (2561)	beadbeater	4.49	1213.07	0.0037
	lysozyme	3.46	1259.75	0.0027
	lysozyme	5.58	1431.51	0.0039
B1SYN (2564)	beadbeater	5.21	1428.50	0.0036
	lysozyme	5.53	1464.26	0.0038
	lysozyme	4.77	1366.60	0.0035

Table S9. Summary of initial activity screen with GC-FID for formation of silanol **5**.

3. GC/MS Analytical Methods

GC/MS analysis was performed to analyze all biocatalytic reactions for directed evolution and mechanistic studies using a DB-5MS Ultra Inert, 30 m x 250 µm x 0.25 µm column and parameters as noted below. Calibration curves were generated using series dilutions of each analyte with 5 mM 1,3,5-trimethoxybenzene as an internal standard. All calibration standards were prepared for individual analytes to prevent speciation. Three replicate injections were acquired for each calibration point. The calibration curves plot analyte response relative to the 5 mM 1,3,5-trimethoxybenzene internal standard response (y-axis) against the ratio of the analyte concentration to the internal standard concentration (x-axis). GC/MS quantification was performed using the Agilent Masshunter Quantitative Analysis software using retention time and 2–4 mass qualifiers with 20% relative mass uncertainty to identify and quantify analytes. Integration was performed using Agile2 integration with peak filtering of 10,000 total ion count. Analytes identified below this peak integration threshold by retention time and mass fragmentation are reported as trace. Specific parameters for GC/MS and data analysis are outlined below for each analyte.

3.1 GC/MS Analysis of Hexamethyldisiloxane (**1**) Biocatalytic Reactions

The following tables outline GC/MS parameters relevant to the analysis of biocatalytic reactions involving siloxane substrate **1**, carbinol **4**, and silanol **5**.

	Rate (ºC/min)	Value (ºC)	Hold Time (min)
Initial		50	2
Gradient	50	300	1

Table S10. GC/MS oven parameters.

Solvent Delay (min)	Start Mass (*m*/*z*)	End Mass (*m*/*z*)	Scan Speed (u/s)
2.00	50	300	3.125

Table S11. Mass spectrometer parameters (scan mode).

Analyte	Retention Time (min)	Qualifier Ions (*m*/*z*) (Relative Abundance)
Siloxane **1**	2.20	147.2 (100), 73.1 (10.6)
Carbinol **4**	4.01	147.0 (100), 135.0 (23.4), 118.9 (18.1), 163.0 (15.7)
Silanol **5**	3.12	149.1 (100), 133.0 (84.7), 75.1 (10.0)

Table S12. Summary of analytes.

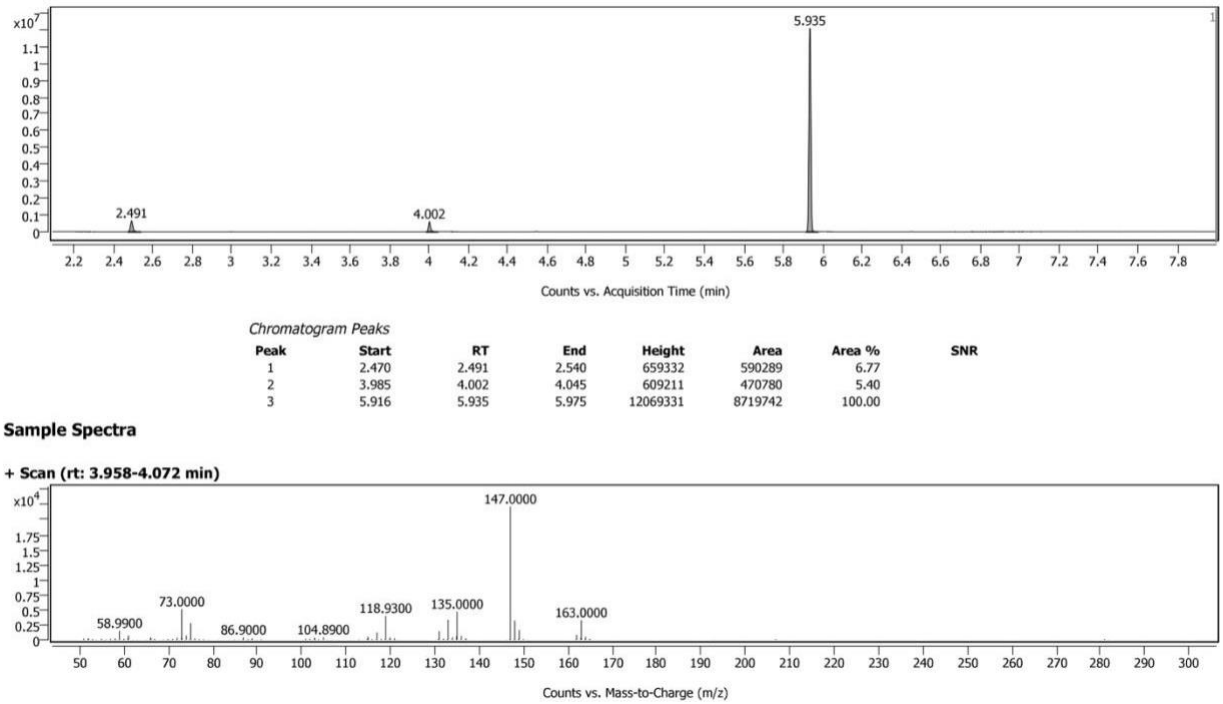

Figure S1. Representative gas chromatogram and EI mass spectrum of a 0.482 mM sample of carbinol **4** (4.00 min) with 5 mM 1,3,5-trimethoxybenzene (5.94 min). Note: the peak present at 2.491 min corresponds to ethyl propionate, an impurity present in EtOAc.

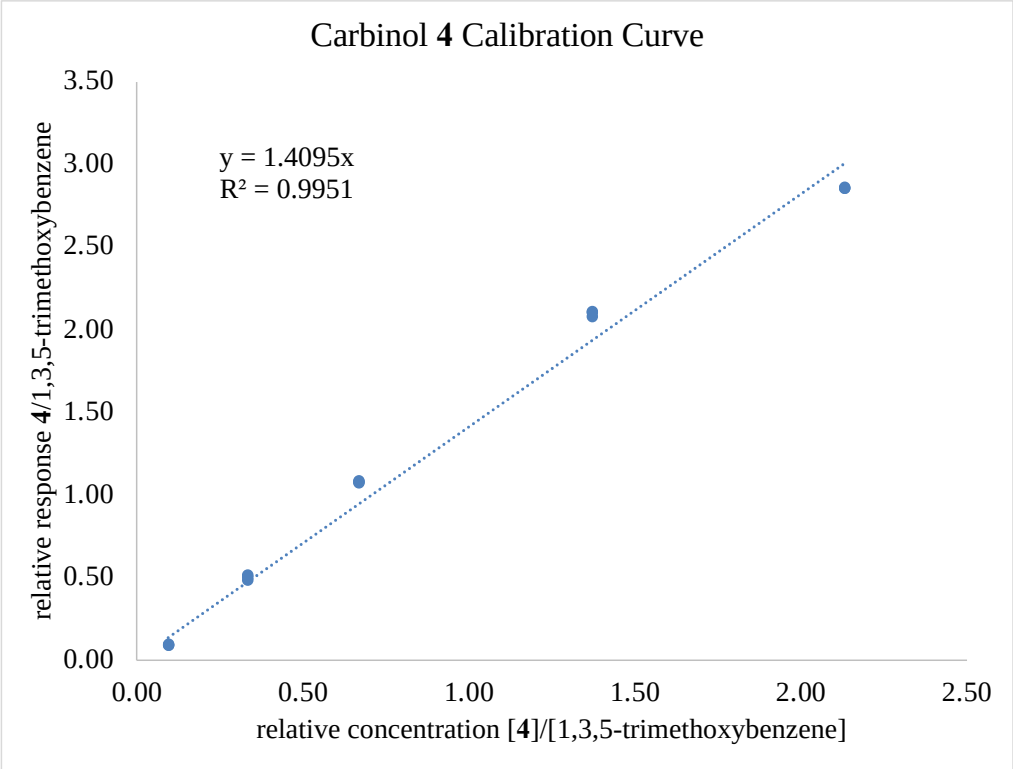

Figure S2. Calibration curve for carbinol **4**.

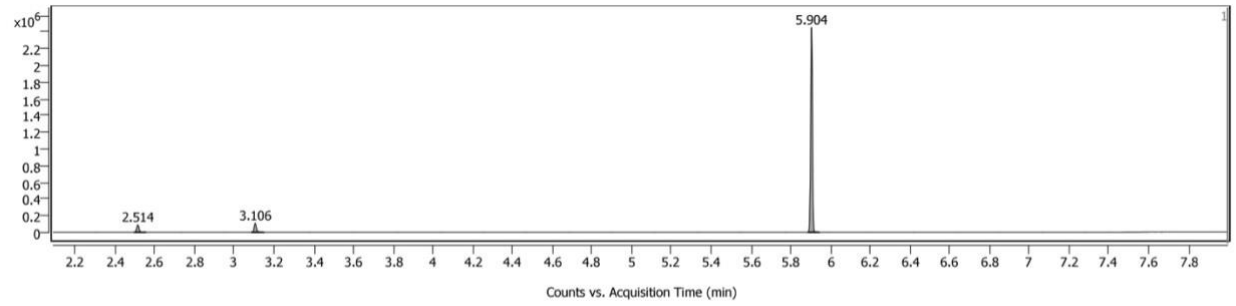

Chromatogram Peaks

Peak	Start	RT	End	Height	Area	Area %	SNR
1	2.494	2.514	2.557	90644	75401	4.76	
2	3.084	3.106	3.148	108972	91616	5.78	
3	5.887	5.904	5.943	2454124	1585143	100.00	

Sample Spectra

+ Scan (rt: 3.051-3.165 min)

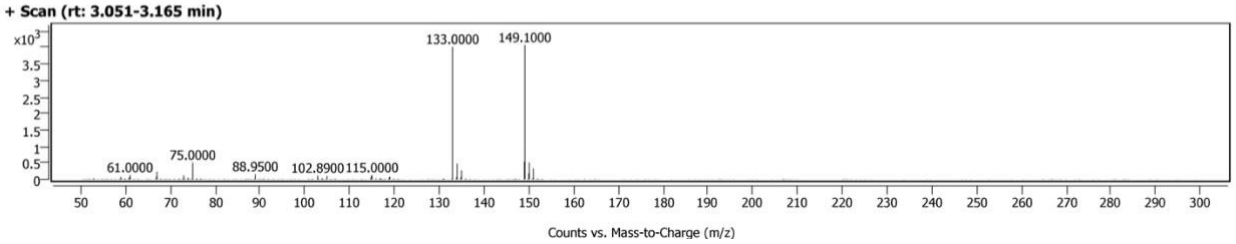

Figure S3. Representative gas chromatogram and EI mass spectrum of a 0.341 mM sample of silanol **5** (3.11 min) with 5 mM 1,3,5-trimethoxybenzene (5.90 min). Note: the peak present at 2.51 min corresponds to ethyl propionate, an impurity present in EtOAc.

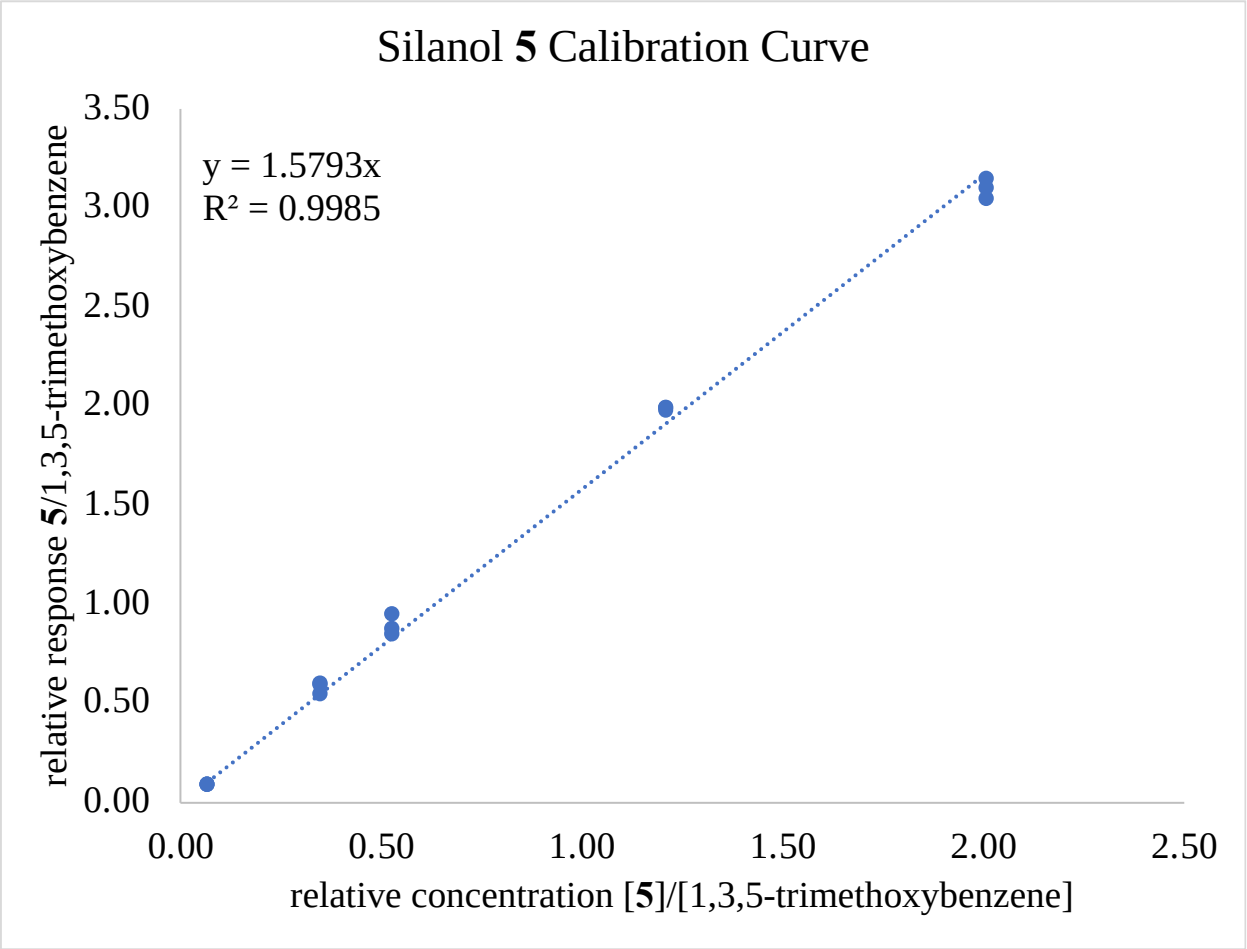

Figure S4. Calibration curve for silanol **5** in reactions with siloxane **1** or carbinol **4.**

3.2 GC/MS Analysis of Octamethyltrisiloxane (**2**) Biocatalytic Reactions

The following tables outline GC/MS parameters relevant to the analysis of biocatalytic reactions involving siloxane substrate **2**, carbinol **6**, silanol **7**, and silanol **5**. We do not detect the product of internal siloxane C–H bond oxidation (carbinol **S1**), internal Si–C bond cleavage (silanol **S2**), or carbinol **4** (via hydrolysis). The GC analysis for carbinol **S1**, silanol **S2,** and carbinol **4** are provided below for completeness. Note that the calibration curves for carbinol **4** and silanol **5** provided below are specific to the GC/MS method used for the analysis of reactions with siloxane **2** using the Agilent Masshunter Quantitative Analysis software.

	Rate (ºC/min)	Value (ºC)	Hold Time (min)
Initial		50	1
Gradient 1	60	120	1
Gradient 2	60	300	1

Table S13. GC/MS oven parameters.

Solvent Delay (min)	Start Mass (*m*/*z*)	End Mass (*m*/*z*)	Scan Speed (u/s)
2.2	50	350	3.125

Table S14. Mass spectrometer parameters (scan mode).

Analyte	Retention Time (min)	Qualifier Ions (*m*/*z*) (relative abundance)
Silanol **5**	2.45	149.1 (100), 133.0 (86.2), 75.1 (10.6)
Carbinol **4**	3.16	147.0 (100), 135.0 (24), 118.9 (18.2), 163.0 (16.8)
Silanol **7**	3.40	207.1 (100), 223.1 (23.1)
Silanol **S2**	3.42	207.1 (100), 223.1 (23.8)
Carbinol **S1**	4.04	193.0 (100), 221.0 (64.3), 237.0 (16.2)
Carbinol **6**	4.10	193.1 (100), 221.1 (64.7)

Table S15. Summary of analytes.

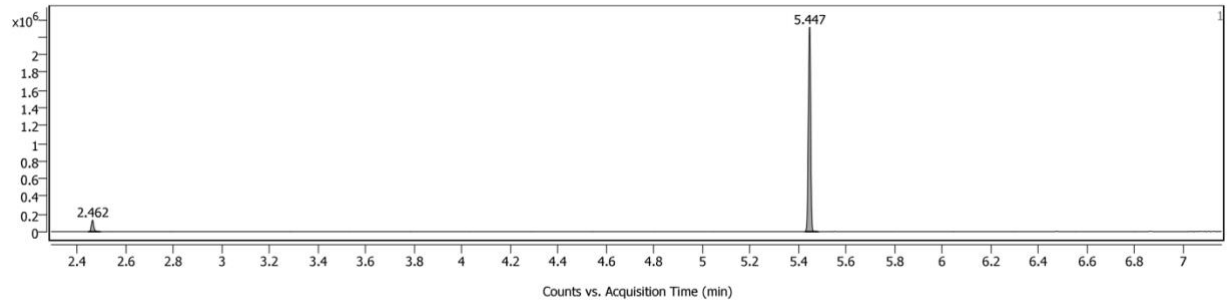

Chromatogram Peaks

Peak	Start	RT	End	Height	Area	Area %	SNR
1	2.442	2.462	2.493	129990	95624	5.99	
2	5.425	5.447	5.482	2309929	1597714	100.00	

Sample Spectra

+ Scan (rt: 2.438-2.481 min)

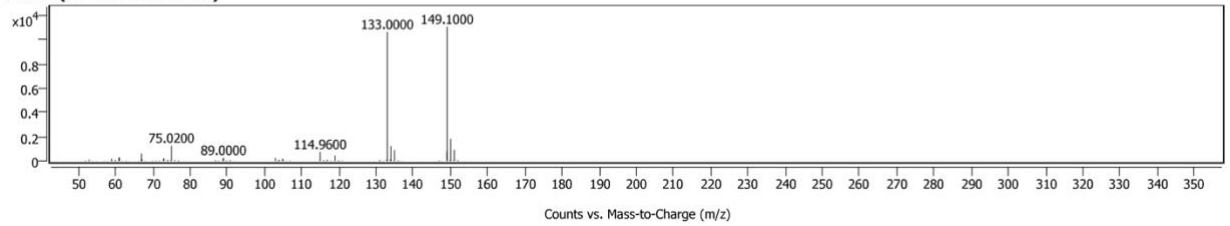

Figure S5. Representative gas chromatogram and EI mass spectrum of a 0.341 mM sample of silanol **5** (2.46 min) with 5 mM 1,3,5-trimethoxybenzene (5.45 min).

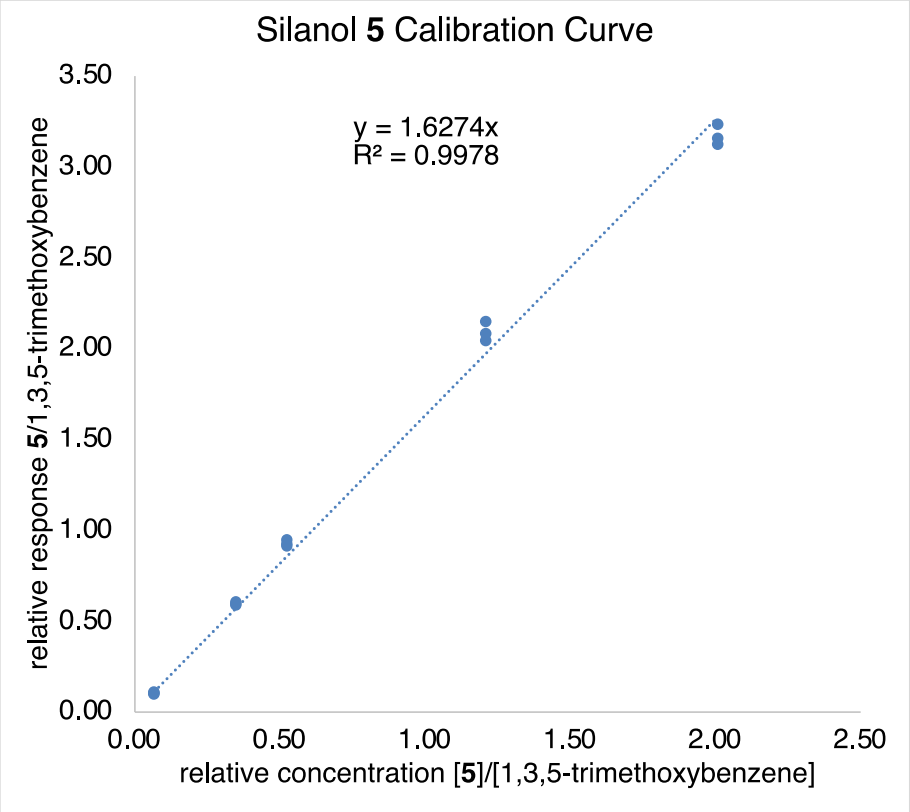

Figure S6. Calibration curve for silanol **5** in reactions with siloxane **2**.

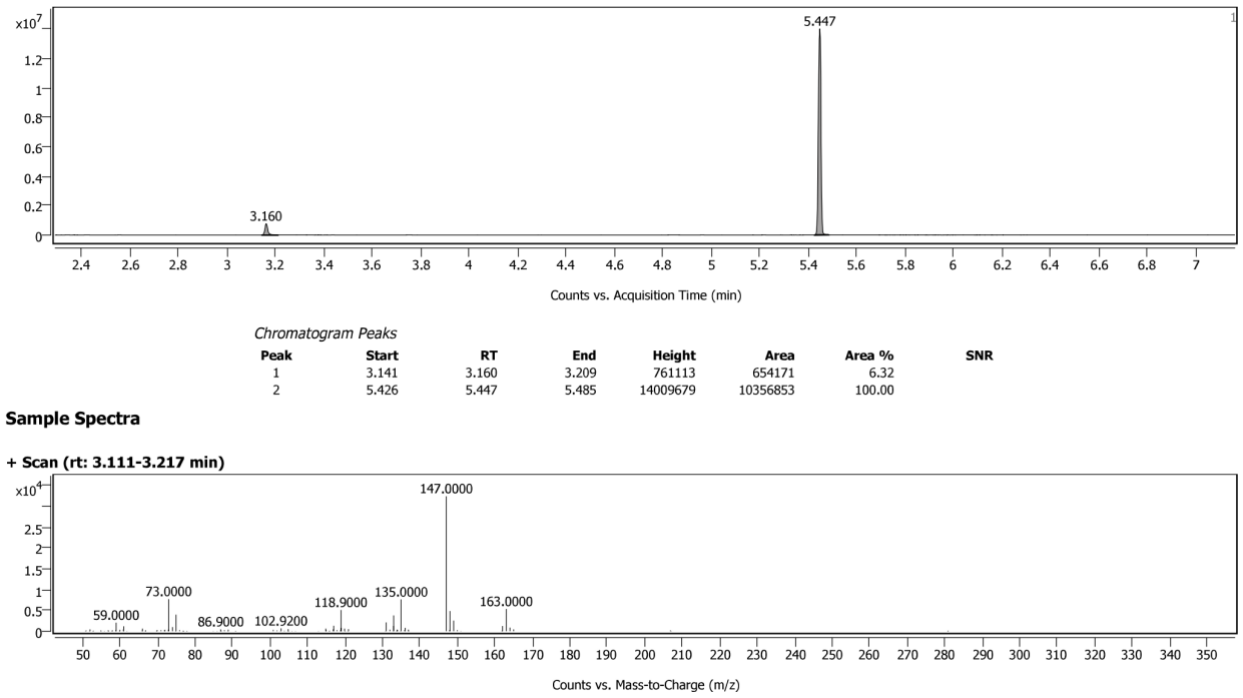

Chromatogram Peaks

Peak	Start	RT	End	Height	Area	Area %	SNR
1	3.141	3.160	3.209	761113	654171	6.32	
2	5.426	5.447	5.485	14009679	10356853	100.00	

Sample Spectra

+ Scan (rt: 3.111-3.217 min)

Figure S7. Representative gas chromatogram and EI mass spectrum of a 0.482 mM sample of carbinol **4** (3.16 min) with 5 mM 1,3,5-trimethoxybenzene (5.45 min).

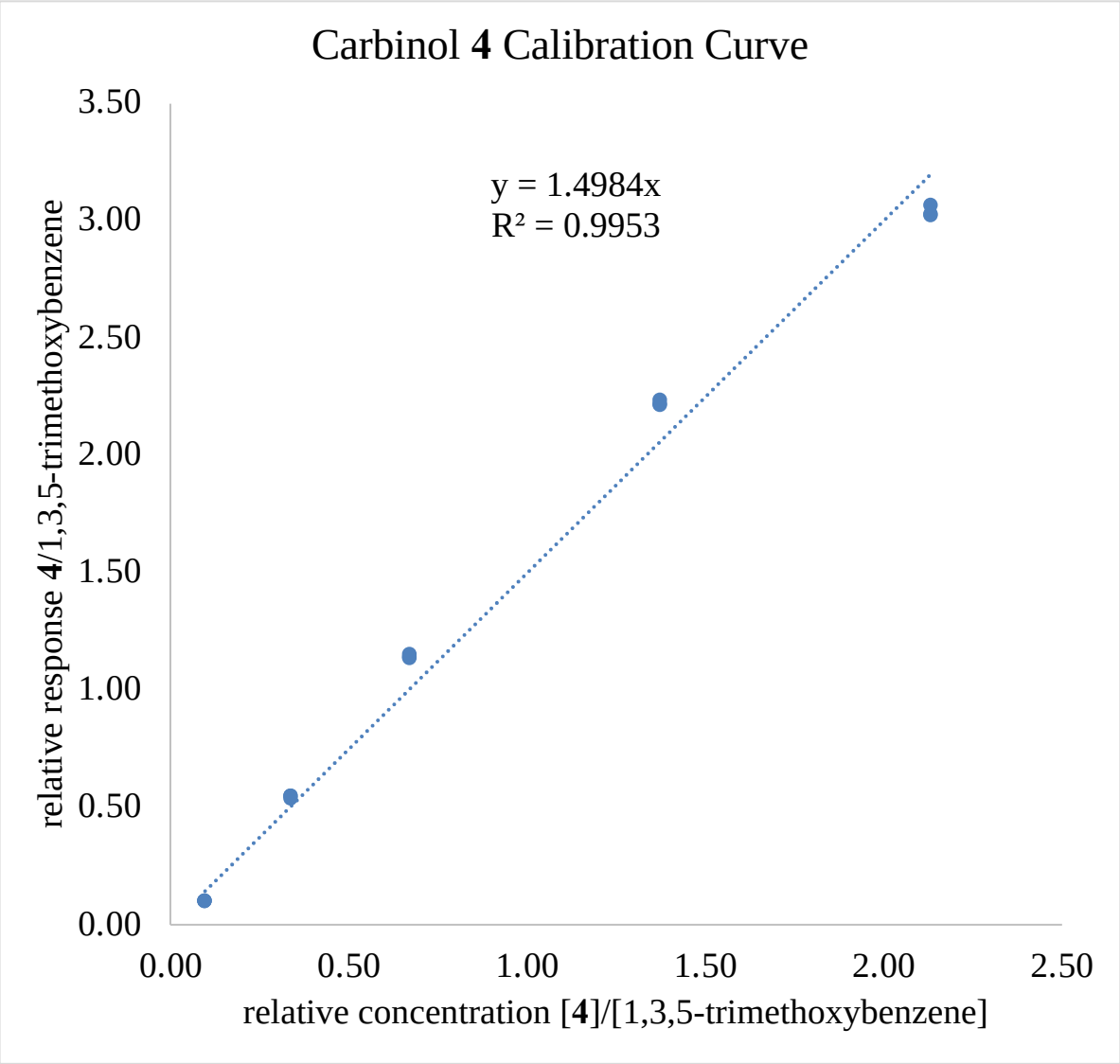

Figure S8. Calibration curve for carbinol **4** in reactions with siloxane **2**.

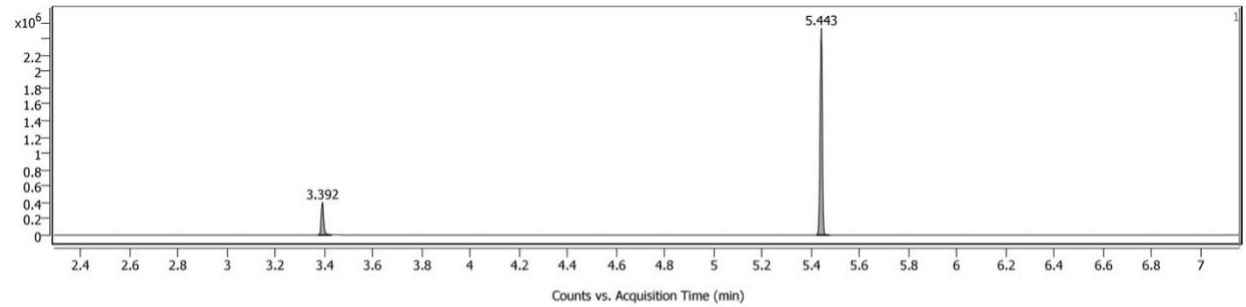

Chromatogram Peaks

Peak	Start	RT	End	Height	Area	Area %	SNR
1	3.372	3.392	3.427	402568	300856	17.83	
2	5.424	5.443	5.477	2530311	1687401	100.00	

Sample Spectra

+ Scan (rt: 3.339-3.445 min)

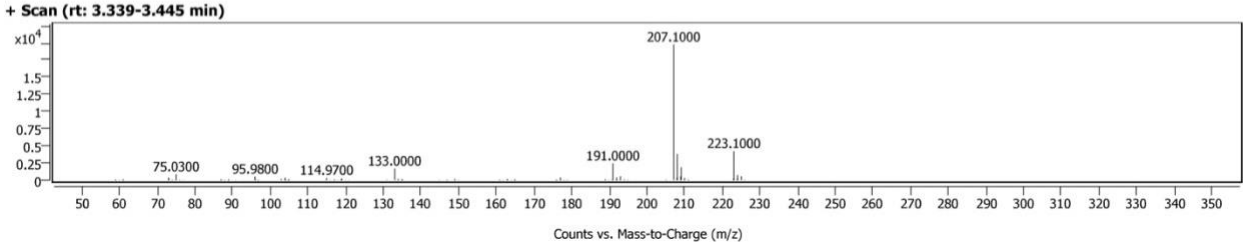

Figure S9. Representative gas chromatogram and EI mass spectrum of a 0.436 mM sample of silanol **7** (3.39 min) with 5 mM 1,3,5-trimethoxybenzene (5.44 min).

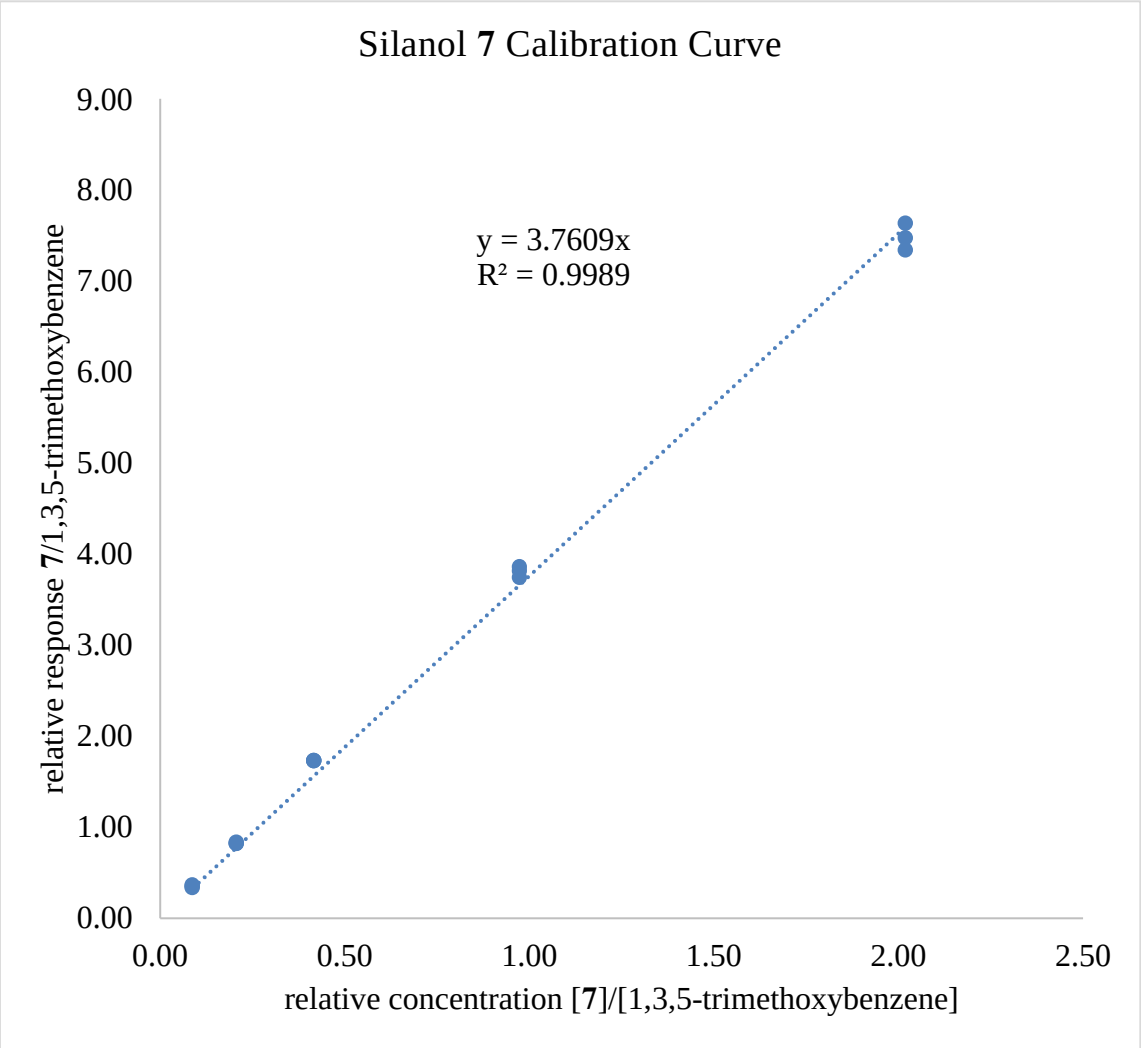

Figure S10. Calibration curve for silanol **7.**

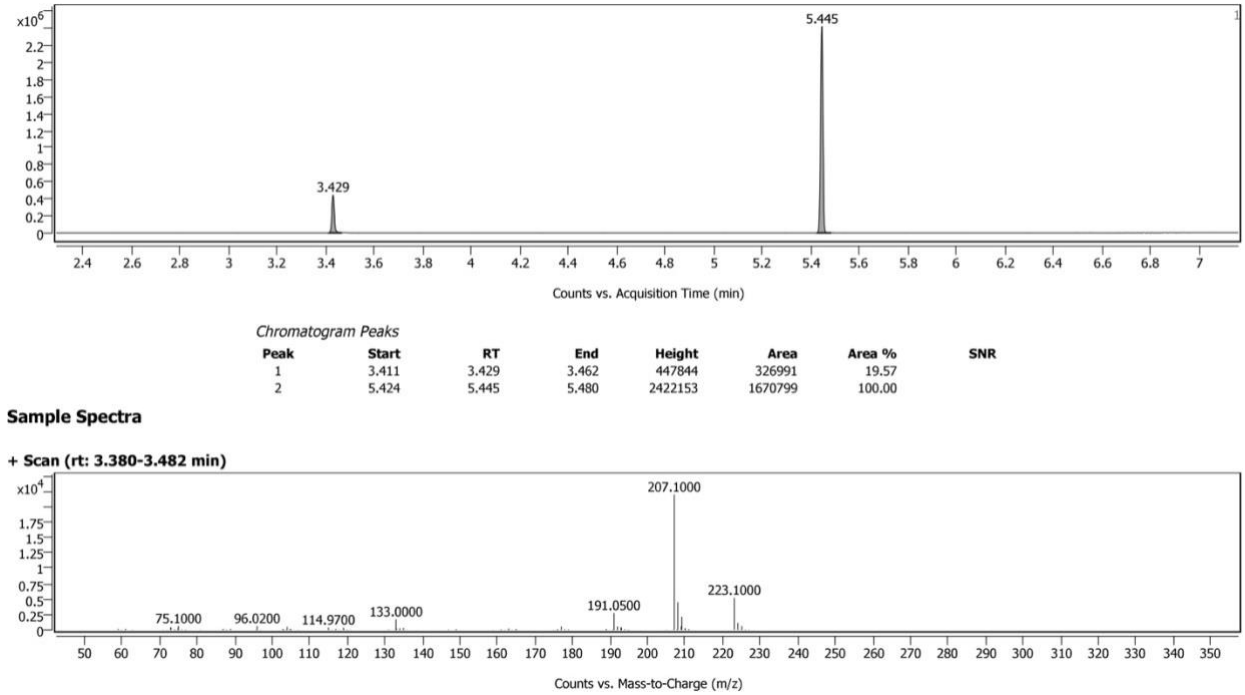

Figure S11. Representative gas chromatogram and EI mass spectrum of a 0.394 mM sample of silanol **S2** (3.43 min) with 1,3,5-trimethoxybenzene (5.45 min).

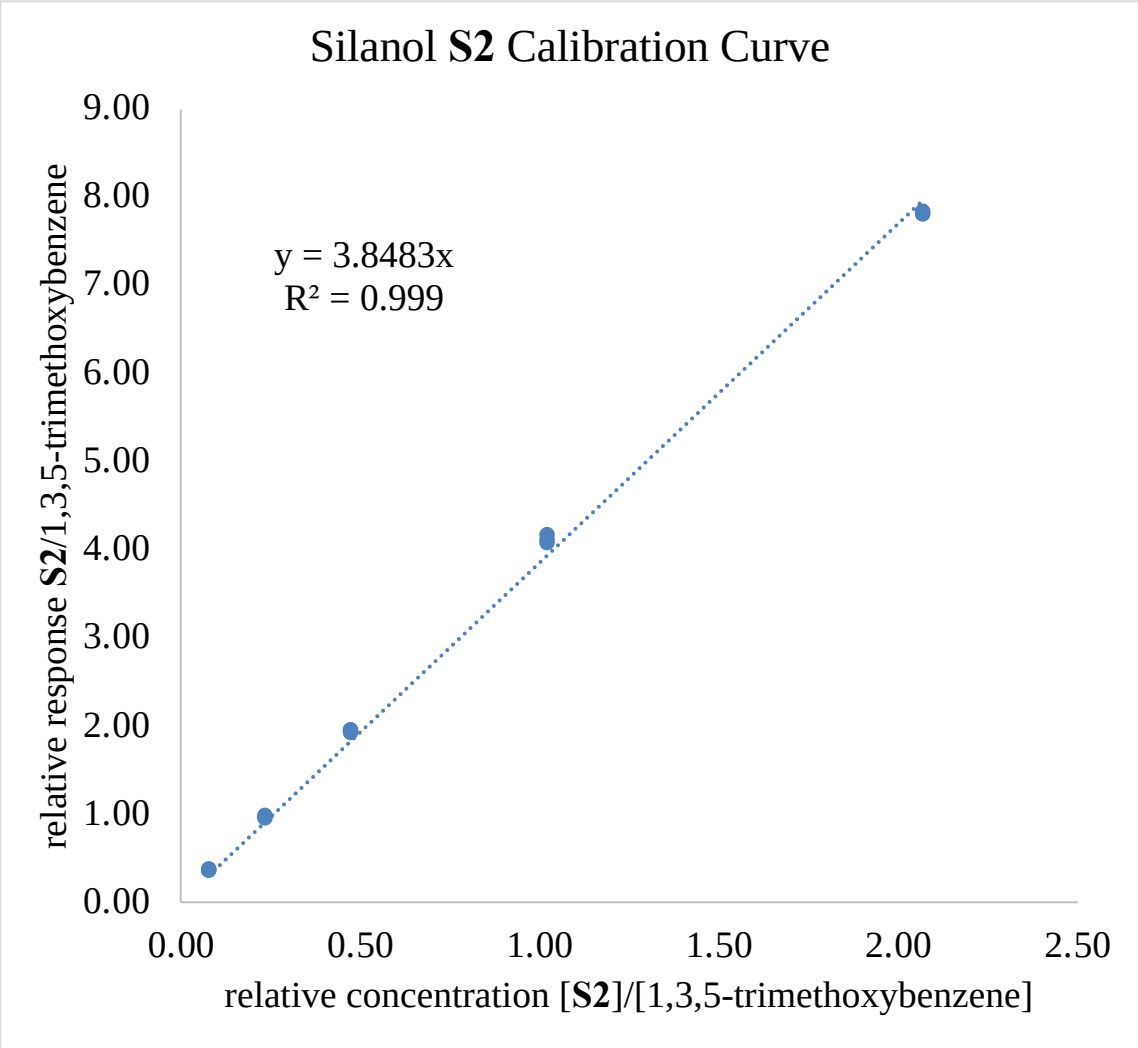

Figure S12. Calibration curve for silanol **S2**.

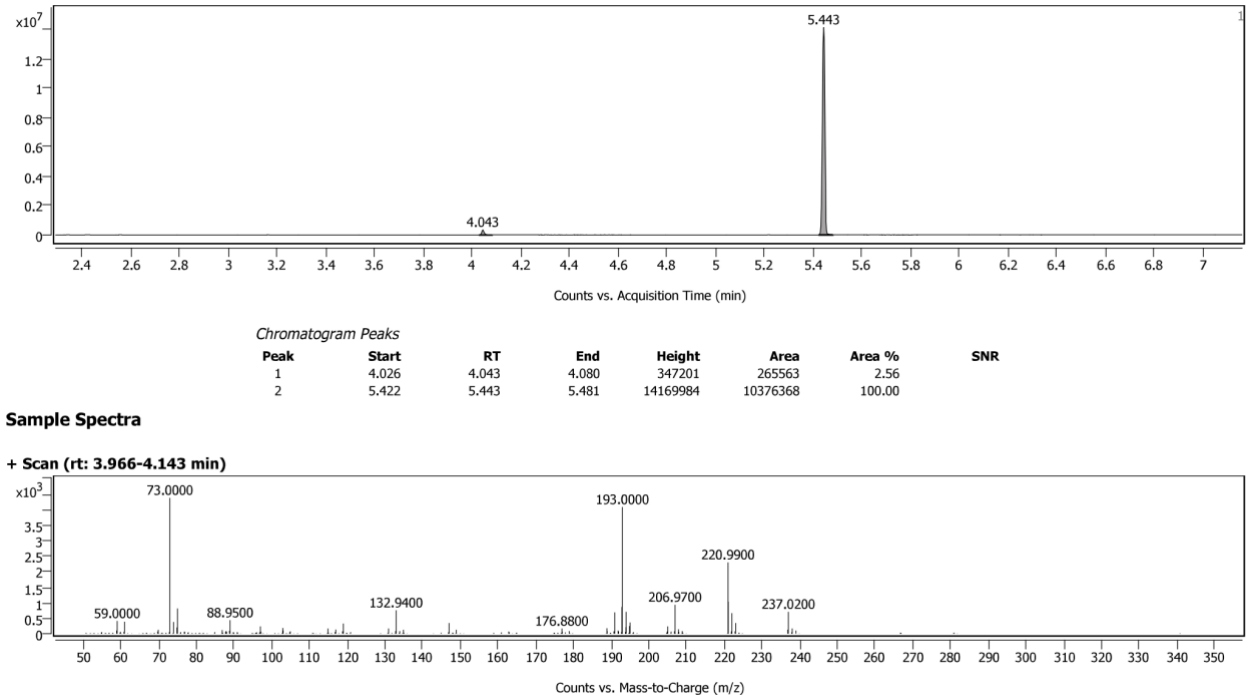

Figure S13. Representative gas chromatogram and EI mass spectrum of a 0.222 mM sample of carbinol **S1** (4.04 min) with 1,3,5-trimethoxybenzene (5.44 min).

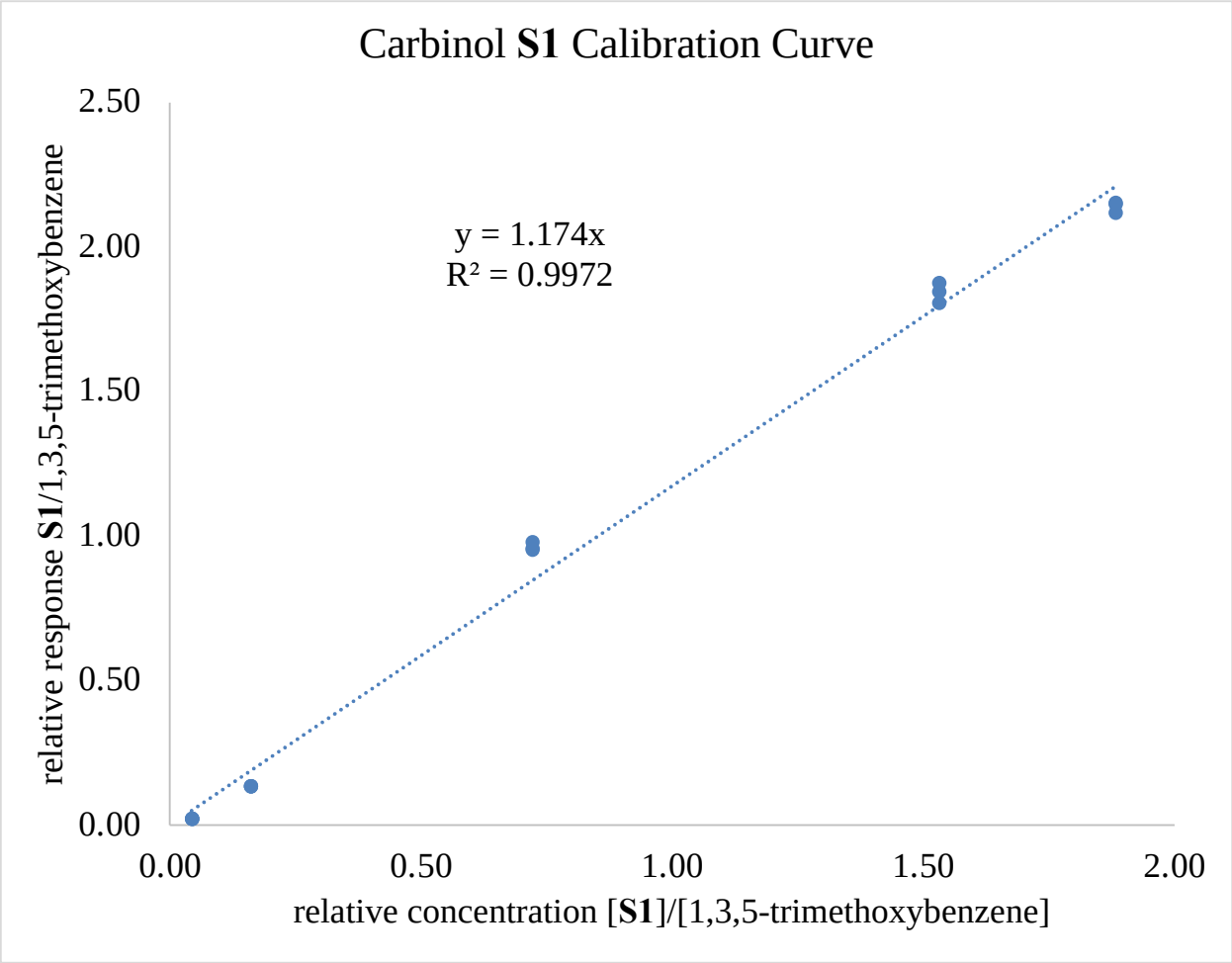

Figure S14. Calibration curve for carbinol **S1**.

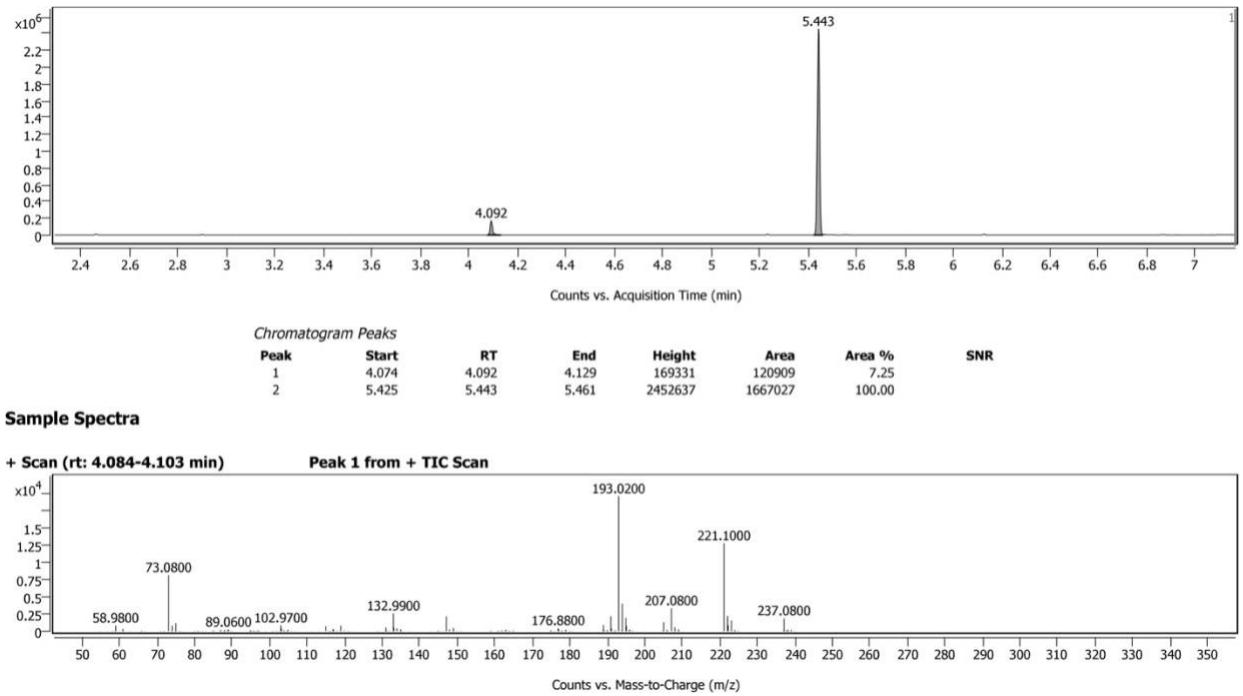

Figure S15. Representative gas chromatogram and EI mass spectrum of a 0.328 mM sample of carbinol **6** with 5 mM 1,3,5-trimethoxybenzene.

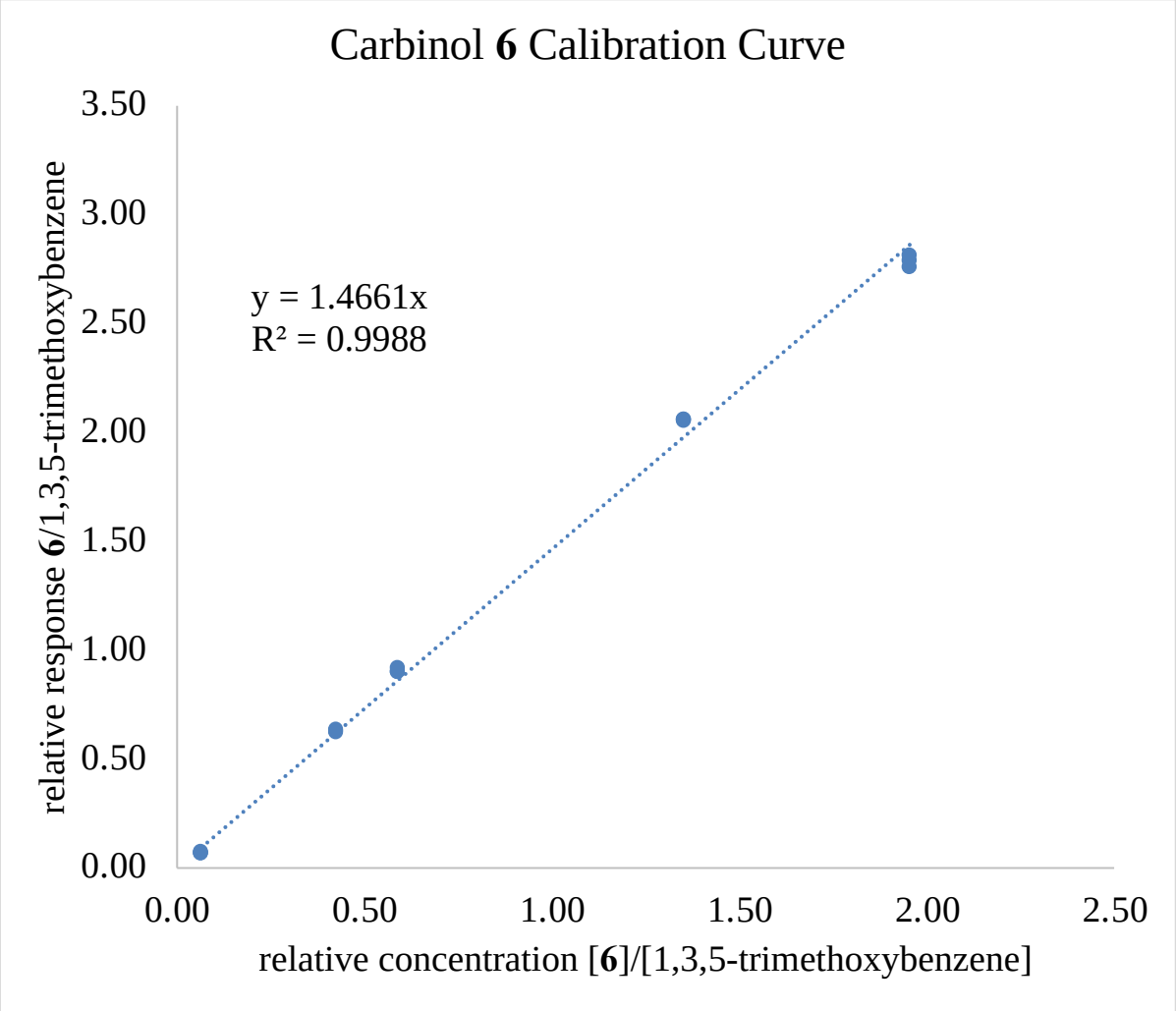

Figure S16. Calibration curve for carbinol **6**.

3.2 GC/MS Analysis of Octamethyltrisiloxane (**2**) Biocatalytic Reactions

The following tables outline GC/MS parameters relevant to the analysis of biocatalytic reactions involving siloxane substrate **3**, carbinol **8**, and silanol **9**.

	Rate (ºC/min)	Value (ºC)	Hold Time (min)
Initial		120	0
Gradient	75	300	1.2

Table S16. GC/MS oven parameters.

Solvent Delay (min)	Start Mass (*m*/*z*)	End Mass (*m*/*z*)	Scan Speed (u/s)
1.30	50	350	3.125

Table S17. Mass spectrometer parameters (scan mode).

Analyte	Retention Time (min)	Qualifier Ions (*m*/*z*) (relative abundance)
Carbinol **8**	1.87	281.1 (100), 252.9 (71.6), 265.1 (12.0)
Silanol **9**	1.66	267.1 (100), 251.0 (15.9), 283.1 (13.7), 193.0 (12.9)

Table S18. Summary of analytes.

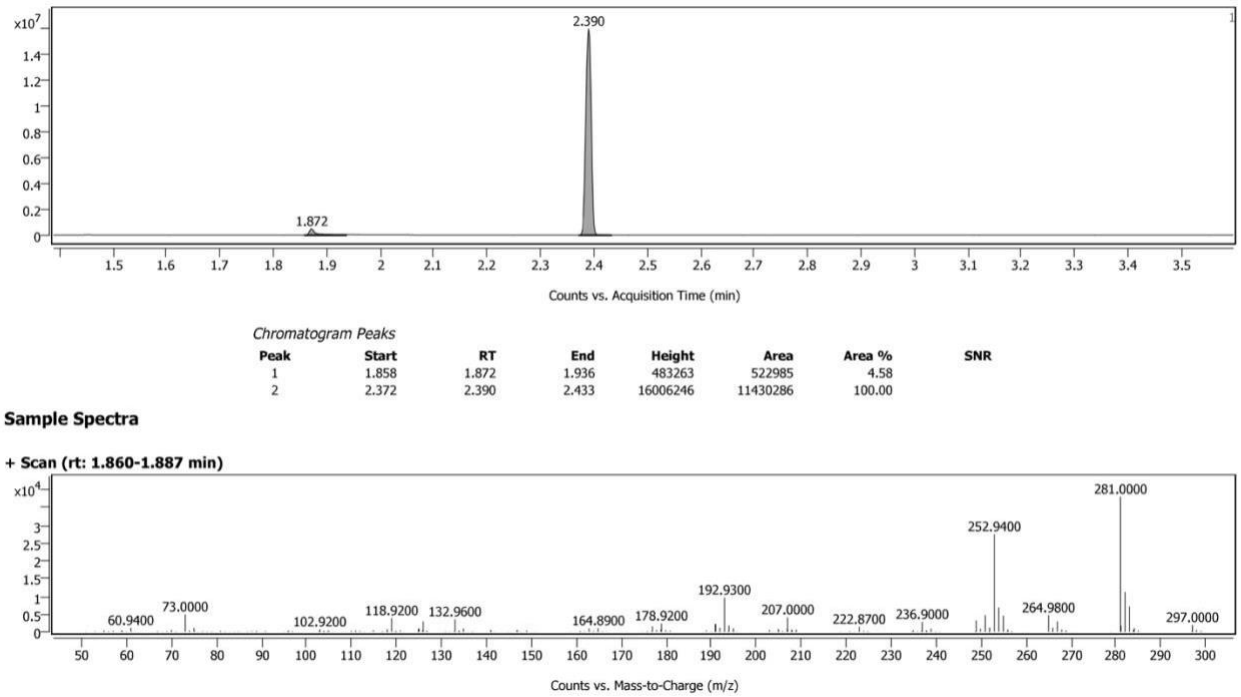

Figure S17. Representative gas chromatogram and EI mass spectrum of a 0.320 mM sample of carbinol **8** (1.87 min) with 5 mM 1,3,5-trimethoxybenzene (2.39 min).

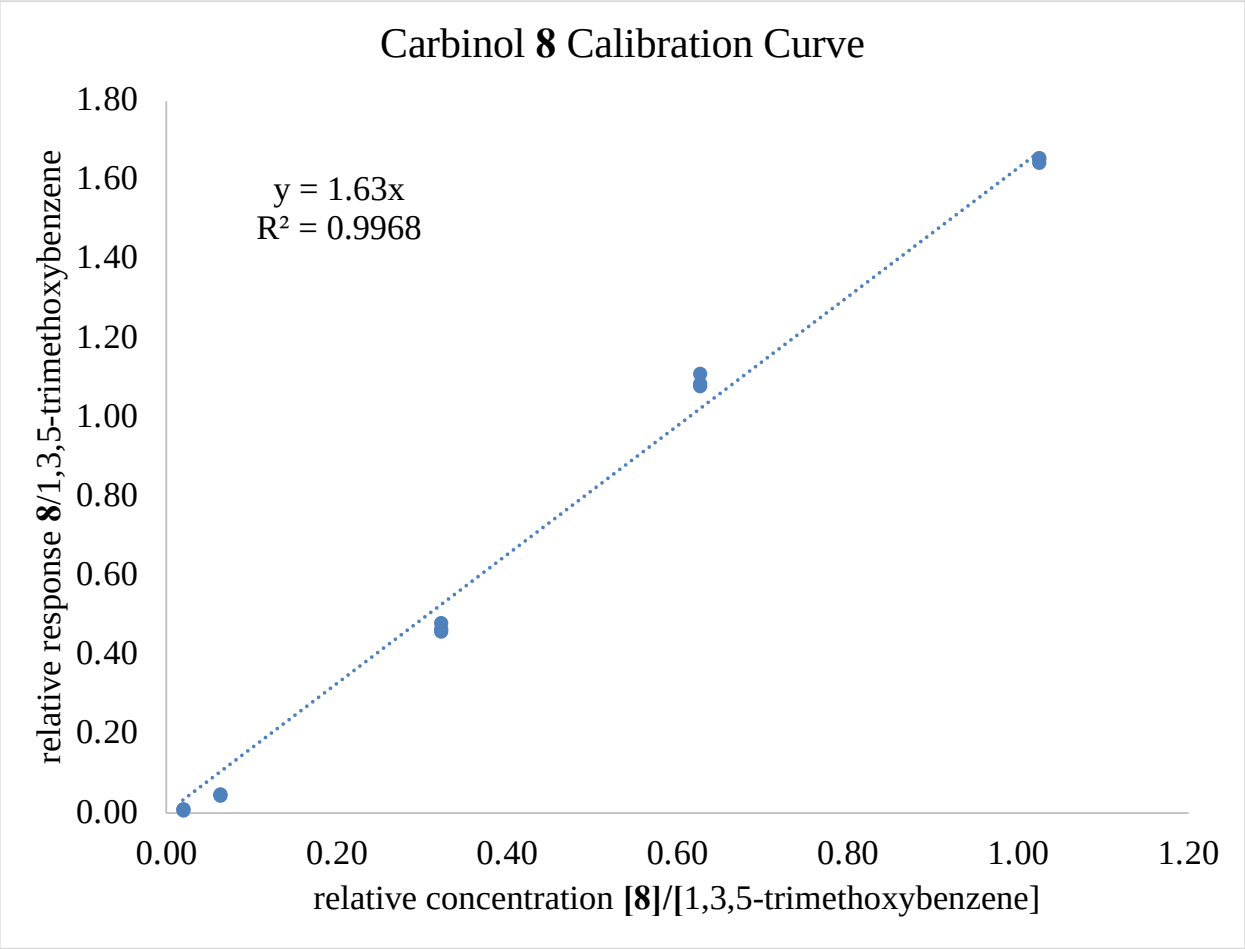

Figure S18. Calibration curve for carbinol **8**.

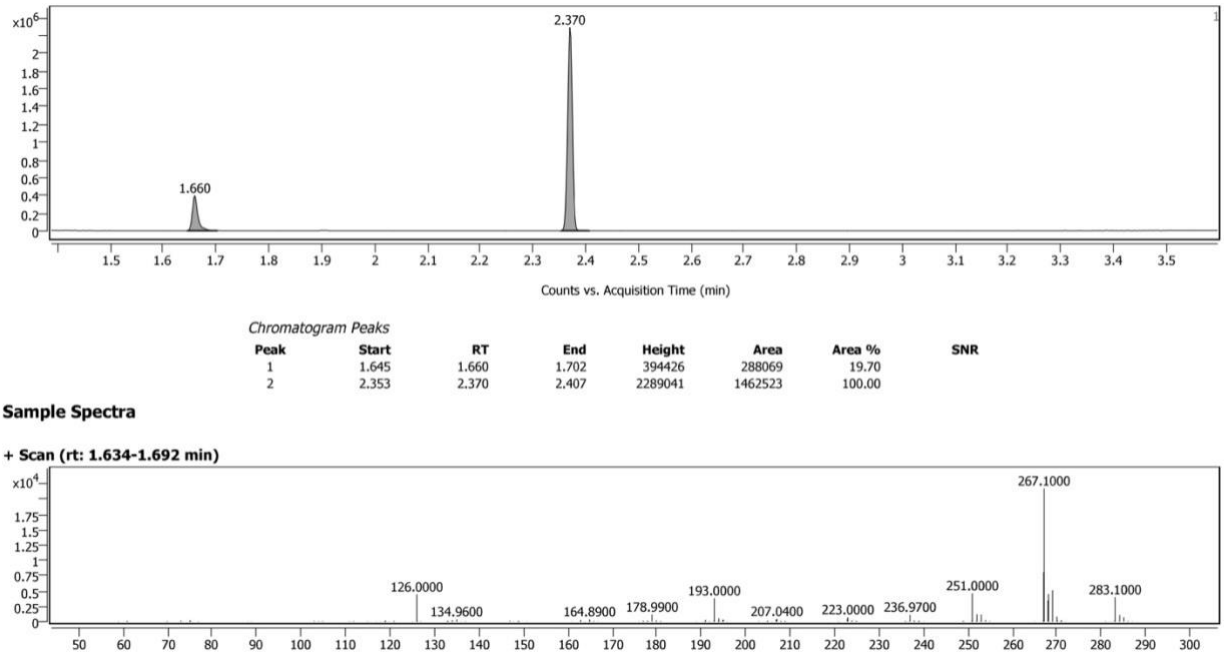

Figure S19. Representative gas chromatogram and EI mass spectrum of a 0.362 mM sample of silanol **9** (1.66 min) with 5 mM 1,3,5-trimethoxybenzene (2.37 min).

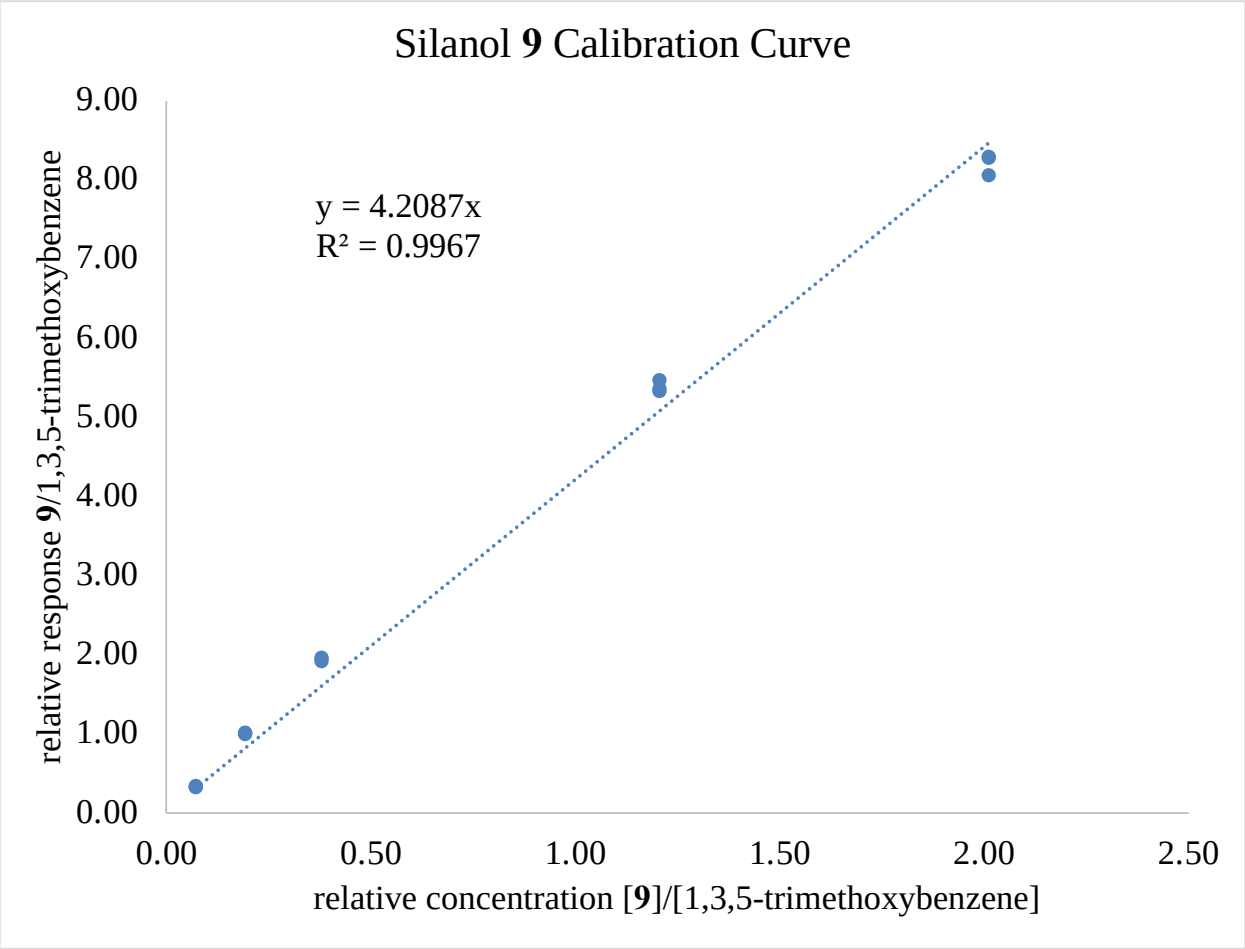

Figure S20. Calibration curve for silanol **9**.

4. Experimental Data Relevant to Figure 2A

Leading Variant	Mutations from Parent	Method of Mutagenesis
*L*SilOx1	–	
*L*SilOx2	T327M, A328F	dSSM (327X, 328X)
*L*SilOx3	D34G, I122T	epPCR and StEP recombination
*L*SilOx4	G252E	StEP recombination
*L*SilOx4 (lyophilized)	–	

Table S19. Summary of enzyme lineage for hexamethyldisiloxane (**1**).

Leading Variant (Mutations)	**[Enzyme] (μM)**	**[Carbinol 4] (μM)**	**[Silanol 5] (μM)**	**Total Product [Enzyme]**
wild-type P450$_{BM3}$	4.63	0	0	0
	4.63	0	0	0
	4.63	0	0	0
*L*SilOx1	4.76	trace	86.1	18.1
	4.76	trace	86.1	18.1
	4.76	trace	85.5	18.0
*L*SilOx2	3.83	trace	150	39.1
	3.83	trace	136	35.4
	3.83	trace	141	36.8
*L*SilOx3	1.72	trace	74.6	43.4
	1.72	trace	79.3	46.1
	1.72	trace	78.8	45.8
*L*SilOx4	2.59	trace	136	52.5
	2.59	trace	132	51.0
	2.59	trace	126	48.5
*L*SilOx4 (lyophilized)	7.26	24.5	231	35.2
	7.26	23.2	218	33.3
	7.26	17.1	214	31.8

Table S20. Experimental data relevant to **Figure 2A**.

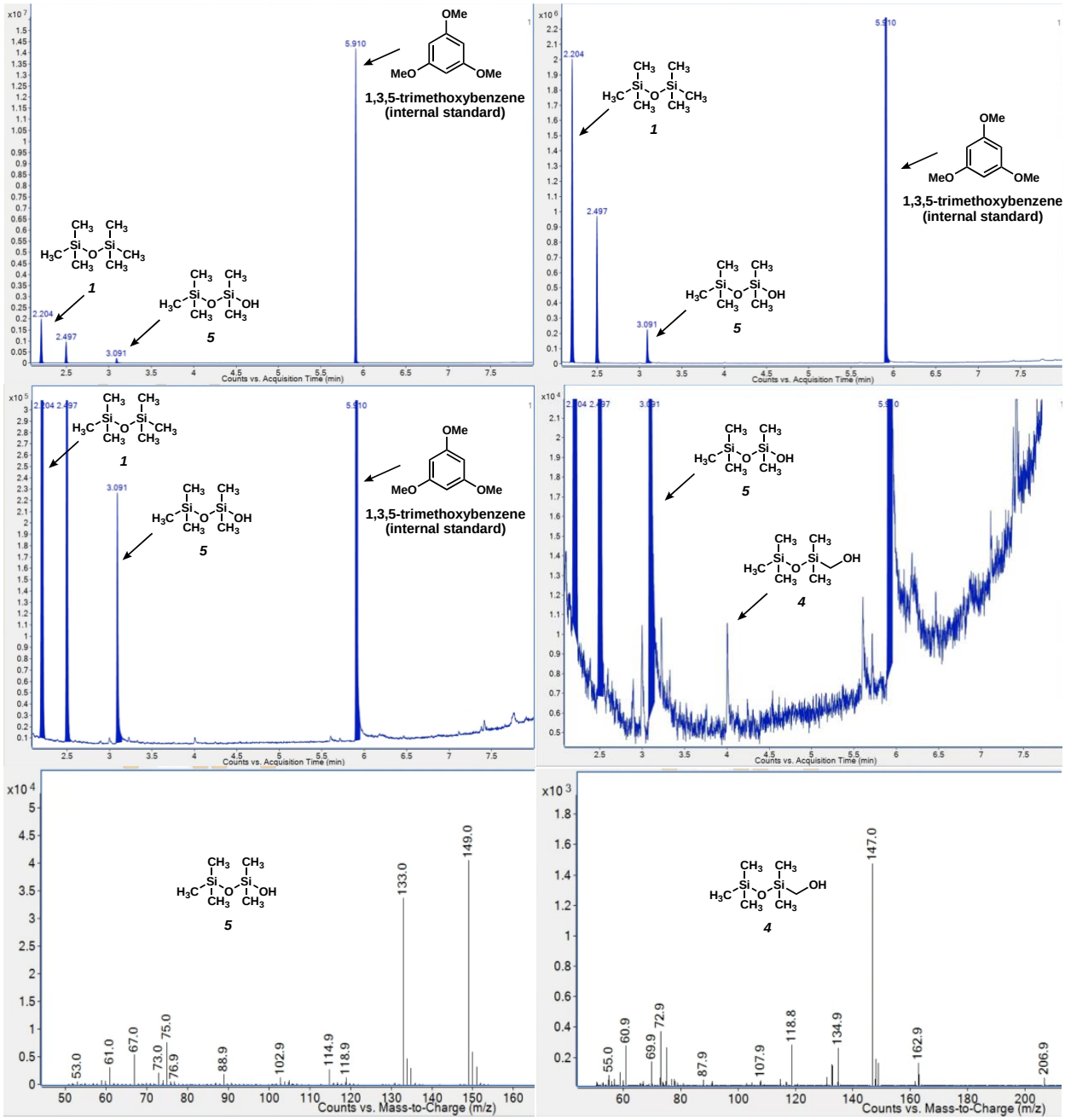

Figure S21. Representative example of a reaction trace of siloxane **1** with *L*SilOx4 with progressive levels of zoom showing silanol **5** and trace levels of carbinol **4**. The peak present at 2.50 is ethyl propionoate, an impurity present in the ethyl acetate extraction solvent.

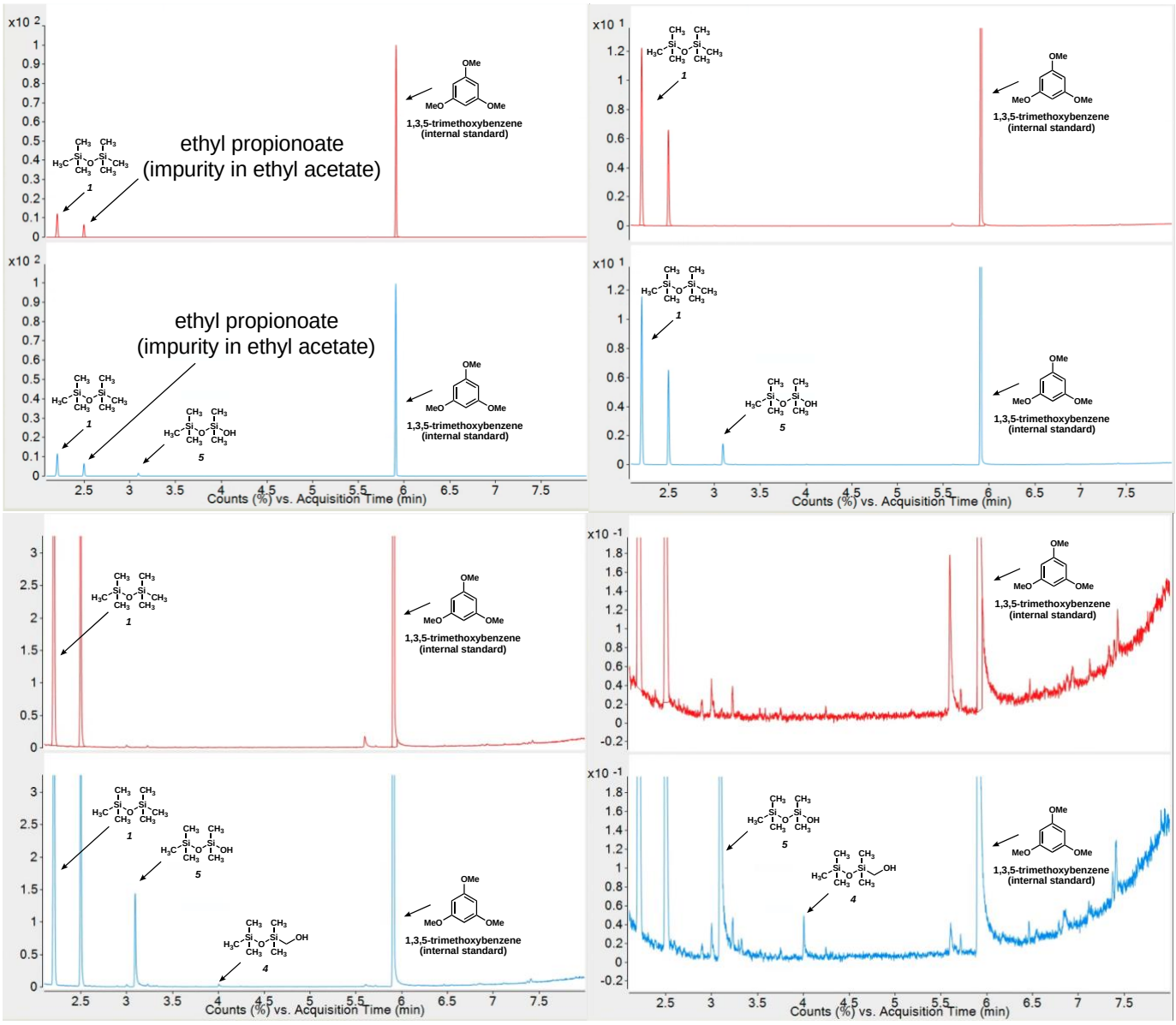

Figure S22. Stacked GC chromatograms of representative enzymatic reactions with siloxane **1** using wild-type P450$_{BM3}$ (red, top) and *L*SilOx4 (blue). The wild-type enzyme has no detectable activity whereas the engineered *L*SilOx4 enzyme generates silanol **5** and trace amounts of carbinol **6**.

5. Experimental Data Relevant to Figure 2B

Leading Variant	Mutations from Parent	Method of Mutagenesis
*L*SilOx4	–	–
*L*SilOx5	F328S	epPCR
*L*SilOx6	F165L	epPCR, then StEP recombination
*L*SilOx7	Y51V, V184M	SSM of sites F42, R47, Y51, A78, G87, L181, V184, A330, then StEP recombination

Table S21. Summary of enzyme lineage for octamethyltrisiloxane (**2**).

Leading Variant	[Enzyme] (μM)	[Carbinol 6] (μM)	[Silanol 7] (μM)	[Silanol 5] (μM)	**Total Product** Enzyme
wild-type P450$_{BM3}$	7.50	0	0	0	0
	7.50	0	0	0	0
	7.50	0	0	0	0
	7.50	0	0	0	0
	7.50	0	0	0	0
*L*SilOx4	11.0	trace	53.9	trace	4.90
	11.0	trace	41.7	trace	3.79
	11.0	trace	27.8	trace	2.52
	11.0	trace	34.7	trace	3.16
	11.0	trace	29.7	trace	2.70
*L*SilOx5	9.20	trace	66.5	23.8	9.82
	9.20	trace	51.9	17.3	7.52
	9.20	trace	62.4	23.9	9.38
	9.20	trace	59.4	22.5	8.91
	9.20	trace	56.4	25.1	8.86
*L*SilOx6	8.16	trace	90.3	31.4	14.9
	8.16	trace	83.2	28.6	13.7
	8.16	trace	66.2	21.2	10.7
	8.16	trace	74.8	23.4	12.0
	8.16	trace	66.3	26.6	11.4
*L*SilOx7	4.47	trace	144	41.0	41.5
	4.47	trace	141	42.5	41.1
	4.47	trace	112	34.7	32.9
	4.47	trace	114	39.9	34.4
	4.47	trace	91.9	29.8	27.2
*L*SilOx7 (lyophilized)	3.09	trace	65.0	trace	21.0
	3.09	trace	59.2	trace	19.2
	3.09	trace	59.0	trace	19.1

Table S22. Experimental data relevant to **Figure 2B**. Carbinol **S1**, silanol **S2**, and carbinol **4** were not detected in any reactions and are therefore omitted from the table.

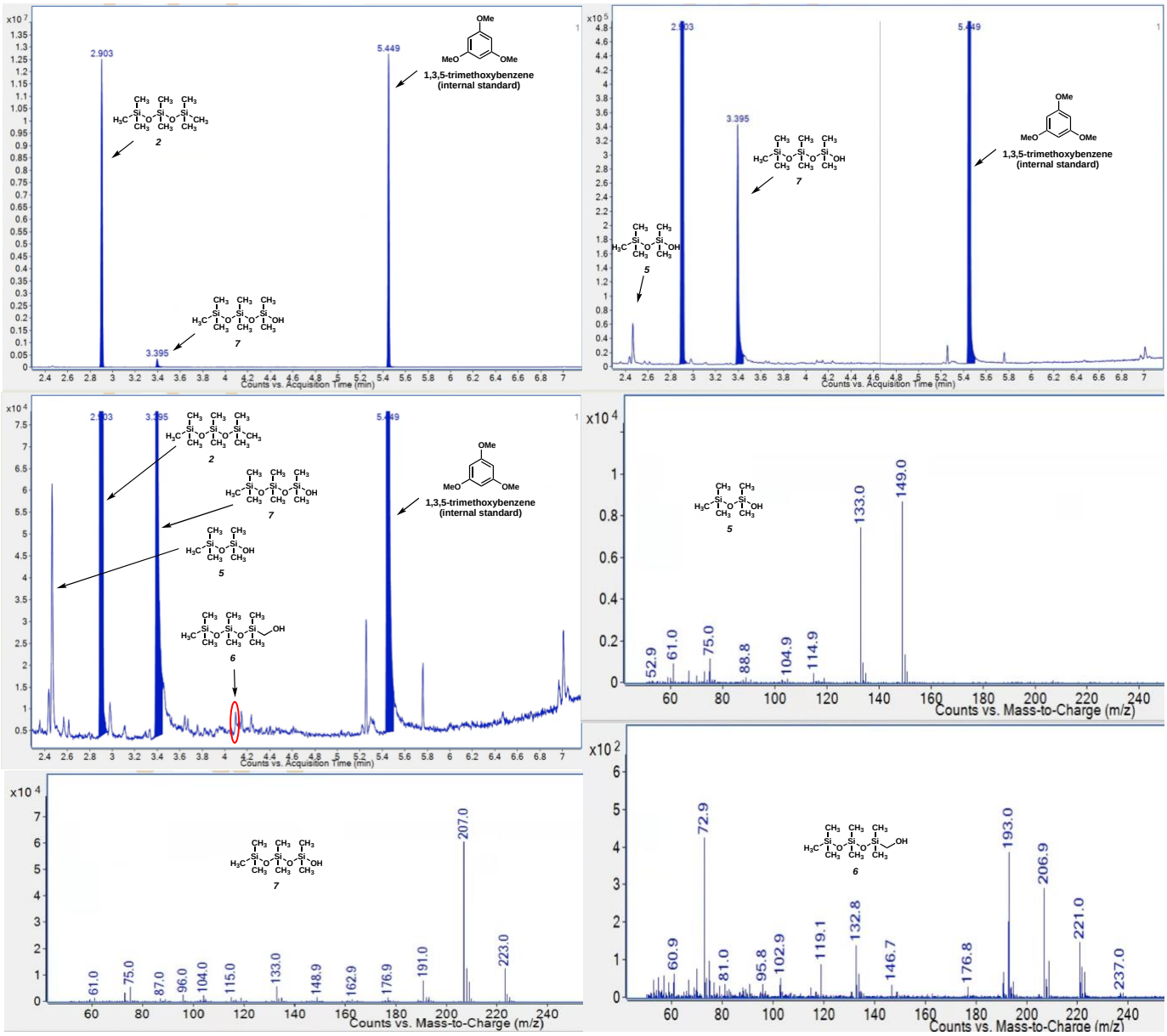

Figure S23. Representative example of a reaction trace of siloxane **2** with *L*SilOx7 with progressive levels of zoom showing silanol **7**, silanol **5** (via hydrolysis), and trace levels of carbinol **6**.

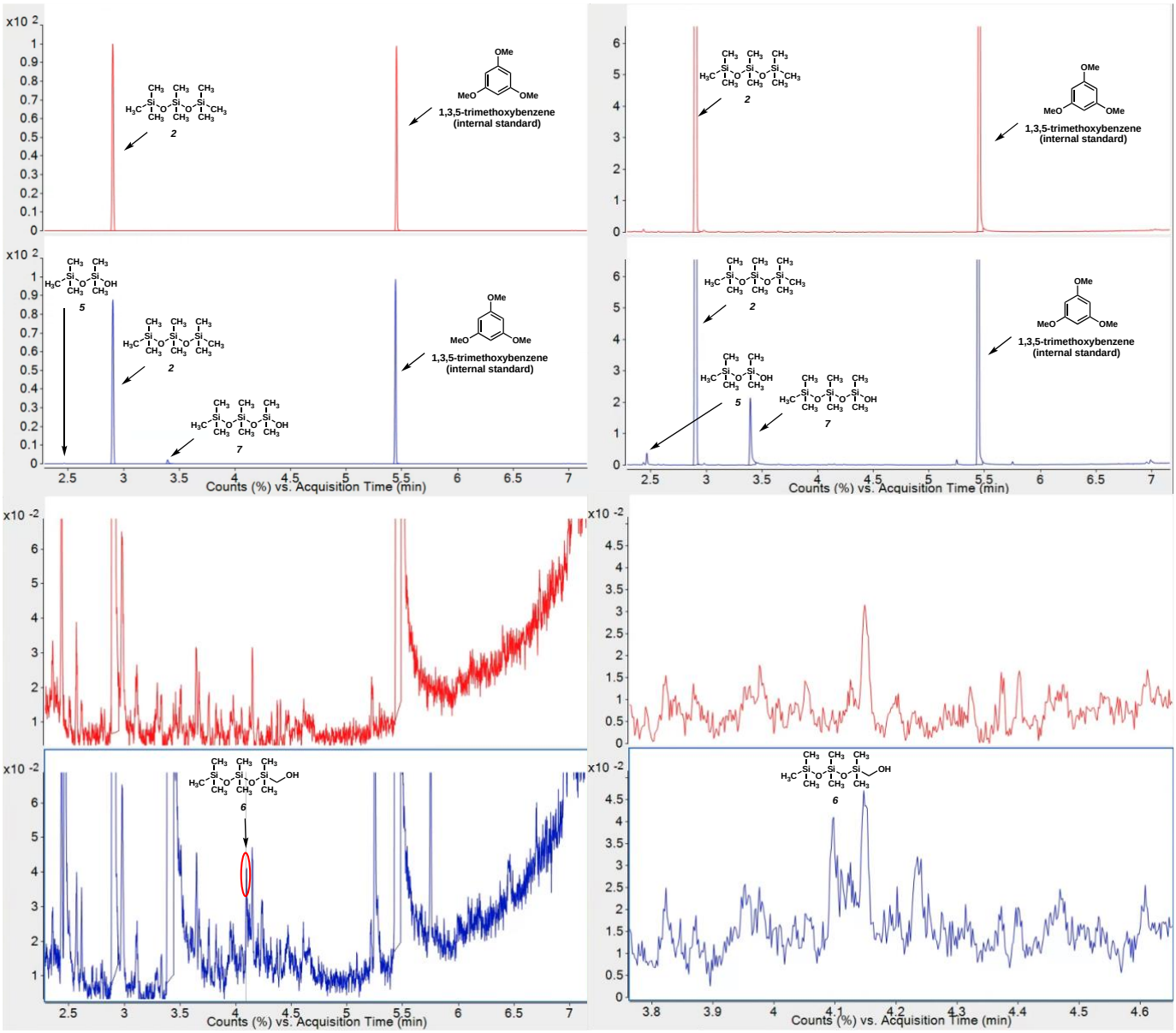

Figure S24. Stacked GC chromatograms of representative enzymatic reactions with siloxane **2** using wild-type P450$_{BM3}$ (red, top) and *L*SilOx7 (blue). The wild-type enzyme has no detectable activity whereas the engineered *L*SilOx7 enzyme generates silanol **7,** silanol **5** (from hydrolysis), and trace amounts of carbinol **6**.

6. Experimental Data Relevant to Figure 2C

Leading Variant	Mutations from Parent	Method of Mutagenesis
*L*SilOx5	–	–
*C*SilOx	N95S, D214G, T438S	epPCR, then StEP recombination
*C*SilOx2	S72G, G85A	epPCR, then targeted recombination
*C*SilOx3	R47G	epPCR and SSM of sites F42, R47, Y51, A78, G87, L181, V184, A330, then StEP recombination

Table S23. Summary of enzyme lineage for octamethylcyclotetrasiloxane (**3**).

Leading Variant	[Enzyme] (μM)	[Carbinol 8] (μM)	[Silanol 9] (μM)	[Total Product] / [Enzyme]
wild-type P450$_{BM3}$	5.03	0	0	0
	5.03	0	0	0
	5.03	0	0	0
	5.03	0	0	0
	5.03	0	0	0
*L*SilOx5	4.20	trace	11.6	2.77
	4.20	trace	8.78	2.09
	4.20	trace	9.14	2.18
	4.20	trace	7.92	1.89
	4.20	trace	8.97	2.14
*C*SilOx1	5.82	trace	37.5	6.44
	5.82	trace	27.6	4.74
	5.82	trace	27.4	4.70
	5.82	trace	24.0	4.13
	5.82	trace	24.9	4.28
*C*SilOx2	2.38	trace	32.0	13.4
	2.38	trace	20.6	8.64
	2.38	trace	33.0	13.9
	2.38	trace	32.1	13.5
	2.38	trace	37.8	15.9
*C*SilOx3	0.36	trace	12.1	33.6
	0.36	trace	8.99	25.0
	0.36	trace	11.2	31.2
	0.36	trace	12.8	35.5
	0.36	trace	10.1	28.1
*C*SilOx3 (lyophilized)	1.10	trace	18.6	16.9
	1.10	trace	19.0	17.3
	1.10	trace	19.2	17.4

Table S24. Experimental data relevant to **Figure 2C**. Carbinol **S1**, silanol **S2**, and carbinol **4** were not detected in any reactions and are therefore omitted from the table.

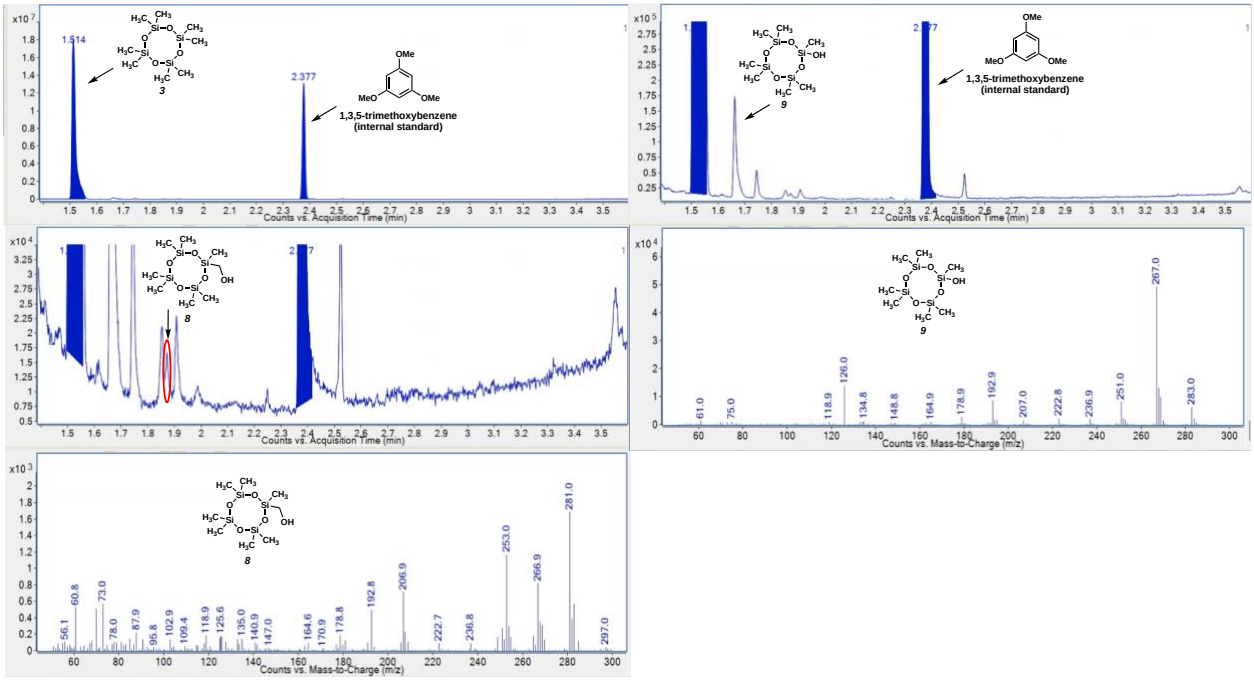

Figure S25. Representative example of a reaction trace of siloxane **3** with *C*SilOx2 with progressive levels of zoom showing silanol **9** and trace levels of carbinol **8**. Although *C*SilOx3 has higher activity per unit of enzyme, the traces shown are an example of *C*SilOx2 because of the increased protein expression and higher overall product.

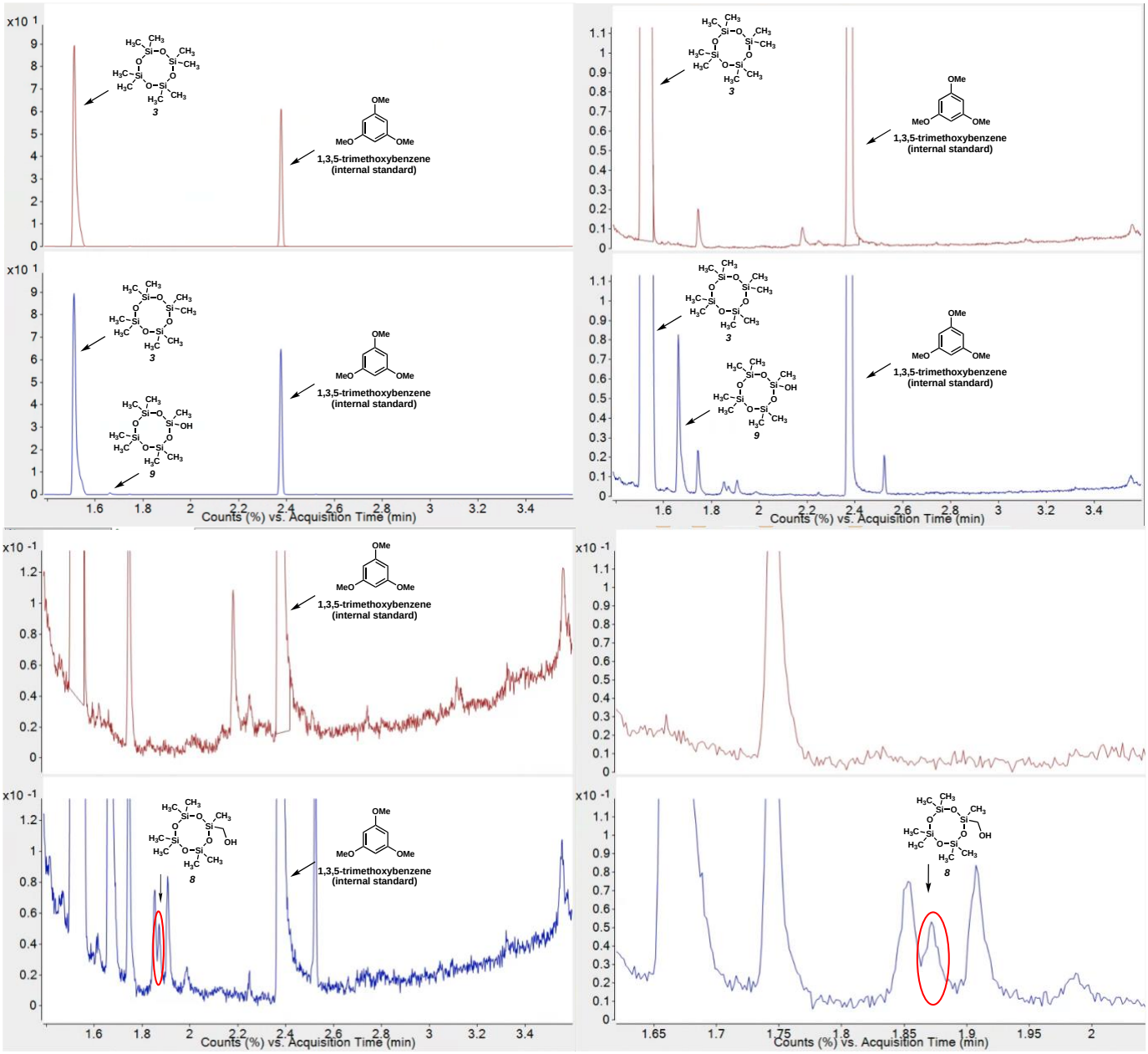

Figure S26. Stacked GC chromatograms of representative enzymatic reactions with siloxane **3** using wild-type P450$_{BM3}$ (red, top) and *C*SilOx2 (blue). The wild-type enzyme has no detectable activity whereas the engineered *C*SilOx2 enzyme generates silanol **9** and trace amounts of carbinol **8**.

7. Experimental Data Relevant to Figure 3A

[NADPH] (mM)	[Carbinol 4] (mM)	[Silanol 5] (mM)	[Total Product] (mM)
0	0.013	0.000	0.013
	0.000	0.000	0.000
	0.000	0.000	0.000
0.01	0.053	0.000	0.053
	0.008	0.000	0.008
	0.007	0.000	0.007
0.05	0.029	0.001	0.030
	0.019	0.001	0.020
	0.017	0.001	0.019
0.1	0.030	0.000	0.030
	0.020	0.000	0.020
	0.023	0.000	0.023
0.5	0.062	0.011	0.072
	0.040	0.011	0.051
	0.042	0.012	0.054
1.0	0.070	0.026	0.095
	0.056	0.026	0.082
	0.060	0.024	0.084
2.5	0.102	0.060	0.162
	0.081	0.059	0.139
	0.074	0.052	0.126
5.0	0.105	0.106	0.210
	0.098	0.118	0.216
	0.094	0.108	0.202

Table S25. Experimental data relevant to **Figure 3A** with siloxane **1** as substrate. The concentration of *L*SilOx4 was 4.7 µM.

[NADPH] (µM)	[Silanol 5] (mM)
0	0.00
	0.00
	0.00
0.01	0.01
	0.02
	0.02
0.05	0.04
	0.04
	0.04
0.1	0.05
	0.05
	0.04
0.5	0.10
	0.10
	0.10
1.0	0.20
	0.20
	0.18
2.5	0.40
	0.39
	0.37
5.0	0.60
	0.56
	0.62

Table S26. Experimental data relevant to **Figure 3A** with carbinol **4** as substrate. The concentration of *L*SilOx4 was 4.7 µM.

8. Experimental Data Relevant to Figure 3B

*L*SilOx4ΔFAD was prepared according to Section 1.3 Cloning, Mutagenesis, and Plasmid Isolation, Site-saturation mutagenesis, with the following primers, instead of those listed in **Table S2**.

Primer	Amplicon	Sequence (5' to 3')
RLO007	BB1 reverse (use with Amp_int_forward)	CATATGTATATCTCCTTCTTAAAGTTAAACAAAATTATTTCTAGAGGGGAATTGTTATCC
RLO005	Heme + FMN domain forward	GGATAACAATTCCCCTCTAGAAATAATTTTGTTTAACTTTAAGAAGGAGATATACATATG
Amp_int_forward	BB1 forward	GCTAACCGCTTTTTTGCACAACATG
Amp_int_reverse	BB2 reverse	TTGTGCAAAAAAGCGGTTAGCTCC
TruncationF_v2	BB2 forward	ACGTCGTAGCAAGCAAAGAACTTCAACACCACCACCACCACCACTGAGAT
TruncationR_v2	Heme + FMN (use with RLO005)	ATCTCAGTGGTGGTGGTGGTGGTGTTGAAGTTCTTTGCTTGCTACGACGT
L4_HemeTruncationR	BB1, heme domain (use with Amp_int_forward)	TCAGTGGTGGTGGTGGTGGTGAAAGCCTTTAGGTTTTAACG
L4_HemeTruncationF	BB2, heme domain (use with Amp_int_reverse)	CGTTAAAACCTAAAGGCTTTCACCACCACCACCACCACTGA

Table S27. Primers used for truncation of *L*SilOx4 to prepare variant *L*SilOx4ΔFAD with the FAD domain removed.

Cofactor System	Enzyme Variant	[Enzyme] (μM)	[Carbinol 4] (mM)	[Silanol 5] (mM)	[Total Product] / [Enzyme]
NADPH	wild-type $P450_{BM3}$	3.70	0.000	0.000	0.00
		3.70	0.000	0.000	0.00
		3.70	0.000	0.000	0.00
	wild-type $P450_{BM3}$ heme domain	27.3	0.000	0.000	0.00
		27.3	0.000	0.000	0.00
		27.3	0.000	0.000	0.00
	*L*SilOx4	4.80	0.253	0.209	96.2
		4.80	0.169	0.172	71.1
		4.80	0.160	0.162	67.0
	*L*SilOx4ΔFAD	8.50	0.068	0.026	11.02
		8.50	0.070	0.034	12.23
		8.50	0.059	0.025	9.93
NADPH Regeneration System	wild-type $P450_{BM3}$	3.70	0.000	0.000	0.00
		3.70	0.000	0.000	0.00
		3.70	0.000	0.000	0.00
	wild-type $P450_{BM3}$ heme domain	27.3	0.000	0.000	0.00
		27.3	0.000	0.000	0.00
		27.3	0.000	0.000	0.00
	*L*SilOx4	4.80	0.023	0.475	104
		4.80	0.021	0.462	101
		4.80	0.020	0.419	91.4
	*L*SilOx4ΔFAD	8.50	0.064	0.051	13.5
		8.50	0.058	0.046	12.3
		8.50	0.060	0.045	12.3

Table S28. Experimental data relevant to **Figure 3B** with siloxane **1** as substrate**.**

Cofactor System	Enzyme Variant	[Enzyme] (μM)	[Silanol 5] (mM)	[Total Product] / [Enzyme]
NADPH	wild-type $P450_{BM3}$	3.70	0.143	38.7
		3.70	0.105	28.4
		3.70	0.115	31.0
	wild-type $P450_{BM3}$ heme domain	27.3	0.000	0.00
		27.3	0.000	0.00
		27.3	0.000	0.00
	*L*SilOx4	4.80	0.769	160
		4.80	0.733	153
		4.80	0.646	135
	*L*SilOx4ΔFAD	8.50	0.443	52.1
		8.50	0.498	58.6
		8.50	0.432	50.8
NADPH Regeneration System	wild-type $P450_{BM3}$	3.70	0.140	37.9
		3.70	0.156	42.0
		3.70	0.142	38.5
	wild-type $P450_{BM3}$ heme domain	27.3	0.014	0.52
		27.3	0.014	0.50
		27.3	0.012	0.45
	*L*SilOx4	4.80	0.789	164
		4.80	0.759	158
		4.80	0.723	150
	*L*SilOx4ΔFAD	8.50	0.522	61.6
		8.50	0.512	60.2
		8.50	0.503	59.1

Table S29. Experimental data relevant to **Figure 3B** with carbinol **4** as substrate.

9. Experimental Data Relevant to Figure 3C

9.1 Enzymatic ABTS Assay for Methanol

All reactions were performed in 2.0-mL snap-cap microtubes on a 350-µL scale. This assay was performed in KPi buffer for direct comparison to the formaldehyde assay. For a direct comparison of KPi and Tris buffer, see section 17. Comparison of Tris and KPi buffers. MeCN was used as a cosolvent as EtOH will be detected by this assay. Purified *L*SilOx4 (41.0 µM in 100 mM pH 7.00 KPi) was diluted to prepare a 5.38 µM solution in 100 mM pH 7.00 KPi buffer. The reaction vessels were charged with 12.5 µL of NADPH solution (140 mM in 100 mM pH 7.00 KPi), 325 µL of the 5.38 µM solution of *L*SilOx4, and 12.5 µL of siloxane **1** or carbinol **4** solution. For methanol and formaldehyde, 7.5 µL of solution were added followed by an additional 5 µL of MeCN. For this assay, substrates siloxane **1** or carbinol **4** were separately prepared as 140 mM solutions in MeCN (final concentrations of 5 mM), and methanol and formaldehyde were prepared as 14 mM solutions in MeCN (final concentrations of 300 µM). An additional control with no substrate was performed with the addition of 12.5 µL of 100 mM pH 7.00 KPi instead of substrate solution. After substrate addition, the reaction vessels were sealed and shaken at 800 rpm for 4 h at 23 ºC. Six replicates of the siloxane **1** and carbinol **4** reactions were performed for parallel GC/MS and ABTS analysis. After 4 h, the reactions for ABTS analysis were heat treated at 60 ºC for 20 min with shaking at 800 rpm to degrade excess NADPH which can quench the colorimetric ABTS dication. After heat treatment, the vessels were centrifuged at 20,817 *g* for 15 min and 4 ºC to pellet denatured protein. After centrifugation, 100 µL aliquots of each sample were transferred to a 96-well microtiter plate. The samples were diluted with 100 µL of 100 mM pH 7.00 KPi buffer and 70 µL of a freshly prepared solution of 1.3 mg/mL ABTS, 3.0 mg/mL horseradish peroxidase, and 0.5 U/mL alcohol oxidase in 100 mM pH 7.00 KPi buffer were added to each well. The microtiter plate was shaken in a plate reader for 10 min, and the absorbance was measured at 420 nm. Simultaneously, three replicates of siloxane **1** and carbinol **4** reactions were opened and 450 µL of 5 mM 1,3,5-trimethoxybenzene in EtOAc were added. The reactions were vortexed for 10 s, and the layers were separated by centrifugation at 20,817 *g* and 4 ºC for 15 min. Aliquots of the organic phase (200–300 µL /reaction) were then transferred to individual 400-µL flat-bottom glass inserts in 2-mL screw-cap vials which were sealed with septum screw caps. Analysis was then performed using GC/MS with product concentrations determined by response relative to the 1,3,5-trimethoxybenzene internal standard using a calibration curve.

In parallel, an ABTS methanol calibration curve was prepared by using the 14 mM methanol solution from above. This stock was vortexed and then added to 2.0-mL snap-cap microtubes with MeCN and purified *L*SilOx4 (5.38 µM in 100 mM pH 7.00 KPi) following the table below to give calibration points of

500, 300, 200, 100, 50, and 0 μM methanol. From these calibration points, 100 μL aliquots were transferred to a 96-well microtiter plate and diluted with 100 μL of 100 mM pH 7.00 KPi buffer, and 70 μL of 1.3 mg/mL ABTS, 3.0 mg/mL horseradish peroxidase, and 0.5 U/mL alcohol oxidase in 100 mM pH 7.00 KPi were added to each sample. The samples were shaken in a plate reader for 10 min, and the absorbance was measured at 420 nm.

Methanol Calibration Point (µM)	**500**	**300**	**200**	**100**	**50**	**0**
Volume of 14 mM Methanol (µL)	12.5	7.5	5	2.5	1.25	0
Volume of MeCN (µL)	0	5.0	7.5	10	11.25	12.5
Volume of 100 mM pH 7.00 KPi (µL)	12.5	12.5	12.5	12.5	12.5	12.5
Volume of 5.38 µM *L*SilOx4 (µL)	325	325	325	325	325	325
Total Volume (µL)	350	350	350	350	350	350

Table S30. Preparation of ABTS methanol calibration points.

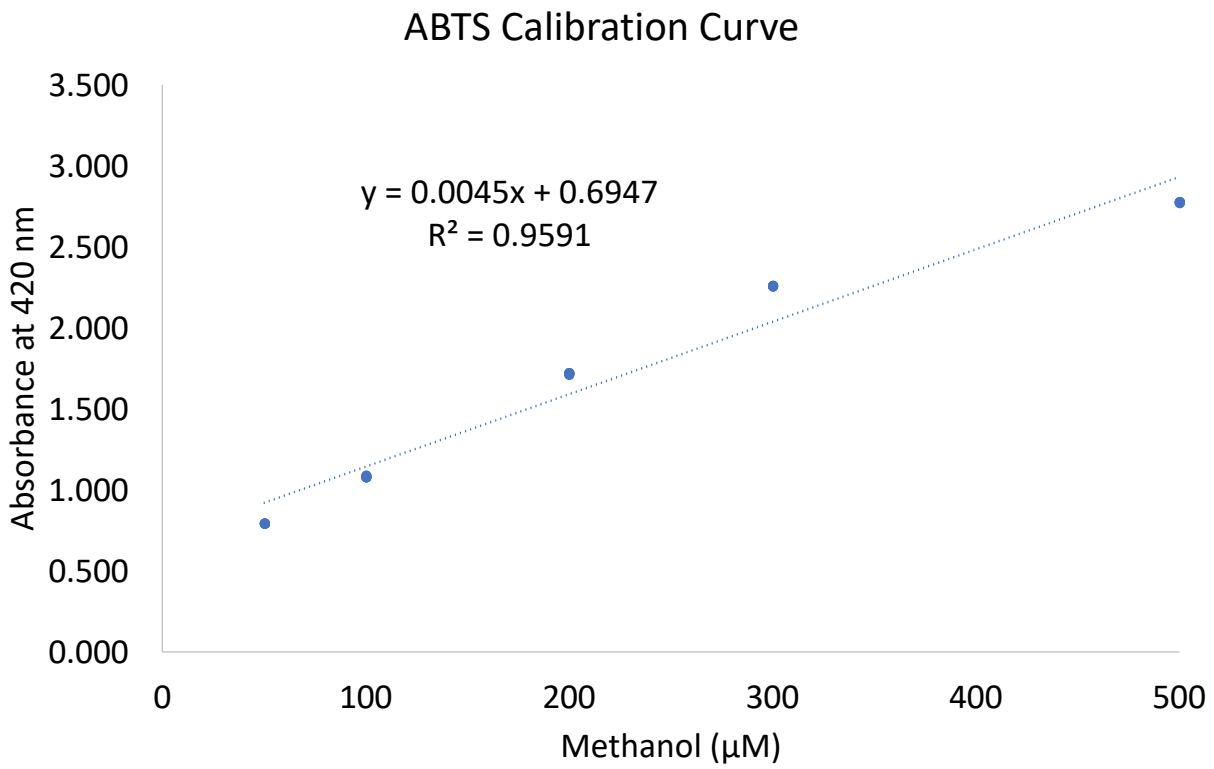

Figure S27. ABTS calibration curve for detection of methanol.

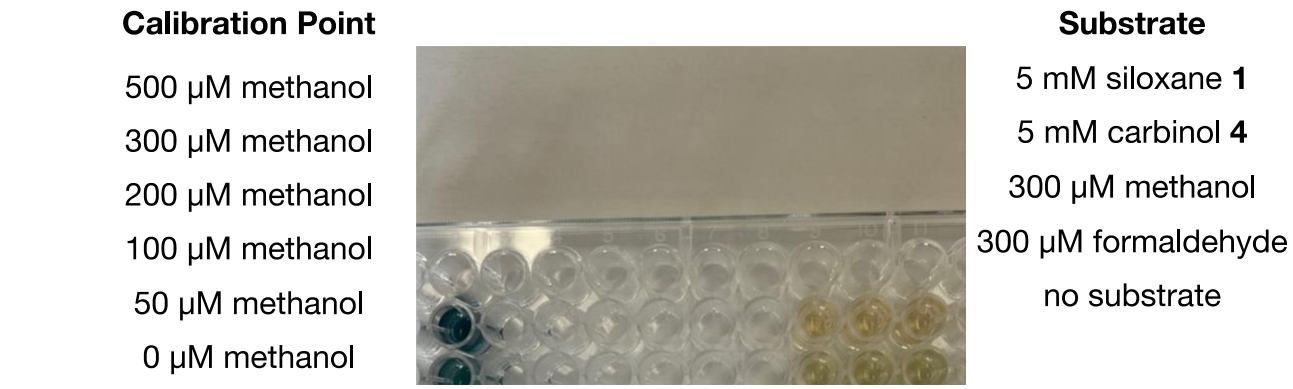

Figure S28. ABTS assay calibration points (left) and reaction analysis with siloxane **1**, carbinol **4**, methanol, formaldehyde, and no substrate (right).

Substrate	Average Calculated Methanol (ABTS)	Average Calculated Silanol 5 (GC/MS) (μM)
Siloxane **1**	–22.0	122
Carbinol **4**	–15.3	630
Methanol	313.6	–
Formaldehyde	44.9	–
No Substrate	–21.5	–

Table S31. Methanol detected by the ABTS assay and silanol **5** detected in parallel reactions analyzed by GC/MS. Note: Formaldehyde solution contains 10–15% methanol as stabilizer. While the ABTS assay is selective for methanol, it can detect other alcohols and may detect carbinol **4** with low activity.

9.2 Purpald Assay for Formaldehyde

All reactions were performed in 2.0-mL snap-cap microtubes on a 350-µL scale. Purified *L*SilOx4 (41.0 µM in 100 mM pH 7.00 KPi) was diluted to prepare a 5.38 µM solution in 100 mM pH 7.00 KPi buffer. The reaction vessels were charged with 12.5 µL of NADPH solution (140 mM in 100 mM pH 7.00 KPi), 325 µL of the 5.38 µM solution of *L*SilOx4, and 12.5 µL of substrate solution. For this assay, substrates siloxane **1** or carbinol **4** were separately prepared as 140 mM solutions in MeCN, and methanol and formaldehyde (formalin, 37 wt% with 10–15% methanol as stabilizer) were prepared as 14 mM solutions in MeCN. An additional control with no substrate was performed with the addition of 12.5 µL of 100 mM pH 7.00 KPi instead of substrate solution. After substrate addition, the reaction vessels were sealed and shaken at 800 rpm for 4 h at 23 ºC. Six replicates of the siloxane **1** and carbinol **4** reactions were performed for parallel GC/MS and Purpald analysis. After 4 h, the reactions for Purpald analysis were centrifuged at 20,817 *g* for 5 min and 4 ºC to pellet denatured protein. After centrifugation, 100 µL aliquots of each sample were transferred to a 96-well microtiter plate. The samples were diluted with 100 µL of 100 mM pH 7.00 KPi buffer, and 50 µL of 168 mM Purpald in 2 M NaOH were added to each sample. The samples were shaken in a plate reader for 10 min, and the absorbance was measured at 550 nm. Simultaneously, three replicates of siloxane **1** and carbinol **4** reactions were opened and 450 µL of 5 mM 1,3,5-trimethoxybenzene in EtOAc were added. The reactions were vortexed for 10 s, and the layers were separated by centrifugation at 20,817 *g* and 4 ºC for 15 min. Aliquots of the organic phase (200–300 µL /reaction) were then transferred to individual 400-µL flat-bottom glass inserts in 2-mL screw-cap vials which were sealed with septum screw caps. Analysis was then performed using GC/MS with product concentrations determined by response relative to the 1,3,5-trimethoxybenzene internal standard using a calibration curve.

In parallel, a Purpald formaldehyde calibration curve was prepared by using the 14 mM formaldehyde solution from above. This stock was vortexed and then added to 2.0-mL snap-cap microtubes with MeCN and purified *L*SilOx4 (5.38 µM in 100 mM pH 7.00 KPi) following the table below to give calibration points of 500, 300, 200, 100, 50, and 0 µM formaldehyde. From these calibration points, 100 µL aliquots were transferred to a 96-well microtiter plate and diluted with 100 µL of 100 mM pH 7.00 KPi buffer, and 50 µL of 168 mM Purpald in 2 M NaOH were added to each sample. The samples were shaken in a plate reader for 10 min, and the absorbance was measured at 550 nm.

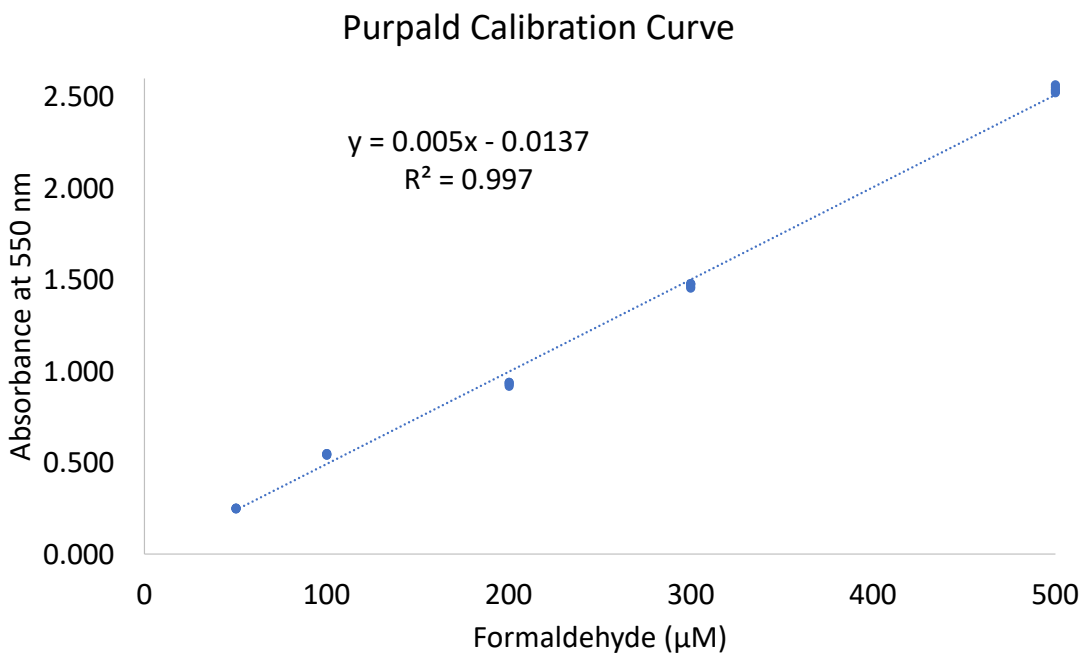

Figure S29. Calibration curve for formaldehyde detection using the Purpald reagent.

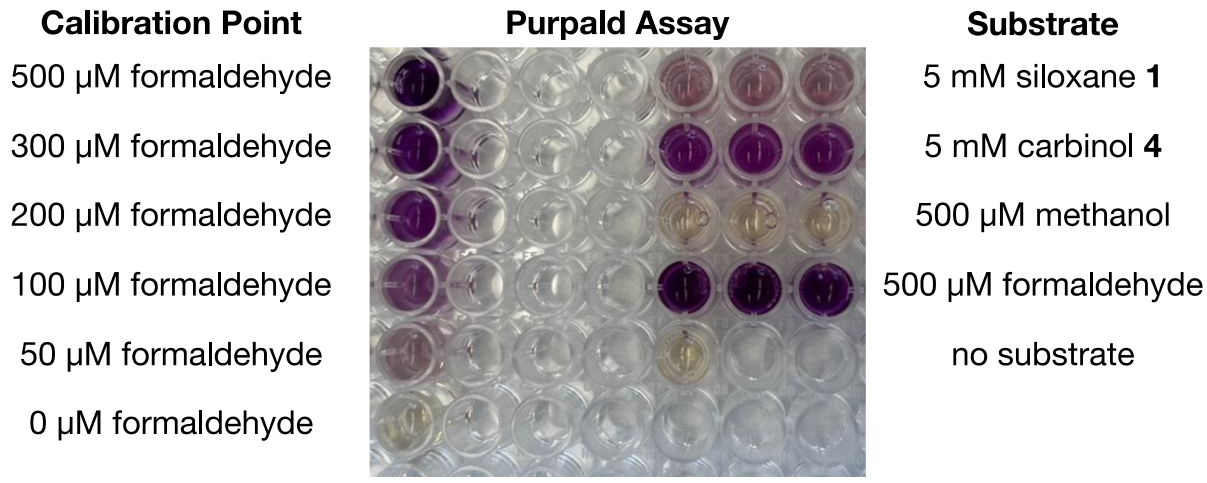

Figure S30. Purpald assay calibration points (left) and reaction analysis with siloxane **1**, carbinol **4**, methanol, formaldehyde, and no substrate (right).

Substrate	Average Calculated Formaldehyde (Purpald)	Average Calculated Silanol **5** (GC/MS)
Siloxane **1**	65	114
Carbinol **4**	170	540
Methanol	26	–
Formaldehyde	440	–
No Substrate	25	–

Table S32. Formaldehyde detected by the Purpald reagent assay and silanol **5** detected in parallel reactions analyzed by GC/MS.

10. Experimental Data Relevant to Figure 3D

Timepoint (min)	[Carbinol 4] (mM)	[Silanol 5] (mM)
0	0.022	0.007
	0.017	0.007
	0.025	0.007
2	0.033	0.051
	0.030	0.052
	0.025	0.054
5	0.036	0.104
	0.034	0.112
	0.033	0.119
10	0.045	0.221
	0.038	0.233
	0.040	0.260
20	0.029	0.275
	0.033	0.323
	0.041	0.328
30	0.033	0.419
	0.034	0.459
	0.031	0.493
60	0.036	0.495
	0.036	0.512
	0.030	0.525
120	0.042	0.594
	0.032	0.607
	0.039	0.635
180	0.033	0.645
	0.031	0.658
	0.033	0.660
240	0.038	0.682
	0.037	0.687
	0.035	0.698
300	0.029	0.734
	0.027	0.778
	0.028	0.786

Table S33. Experimental data relevant to **Figure 3D** with siloxane **1** as substrate. The concentration of *L*SilOx4 was 9.35 µM.

Timepoint (min)	[Silanol 5] (mM)
0	0.105
	0.085
	0.112
2	0.198
	0.180
	0.169
5	0.334
	0.342
	0.363
10	0.526
	0.534
	0.514
20	0.675
	0.696
	0.677
30	0.810
	0.820
	0.766
60	0.855
	0.909
	0.811
120	1.07
	1.08
	1.09
180	1.09
	1.21
	1.15
240	1.35
	1.22
	1.17
300	1.18
	1.12
	1.16

Table S34. Experimental data relevant to **Figure 3D** with carbinol **4** as substrate. The concentration of LSilOx4 was 9.35 µM.

11. Hydrolysis in the Siloxane 1 Reaction Manifold

All reactions were performed in crimp-cap GC/MS vials. A culture of *E. coli* transformed with a pUC19 vector (no expressed P450) was grown and lysed as described above (see 1.5 Large-Scale Protein Expression for Validation and Mechanistic Experiments). To the reaction vials were added 325 μL of the *E. coli* lysate and 12.5 μL of 100 mM Tris pH 7.00 buffer followed by 12.5 μL siloxane **1**, carbinol **4**, or silanol **5** (all prepared separately as 140 mM solutions in EtOH, final concentrations of 5 mM each). After the addition of substrate, the reaction vessels were crimp capped and shaken at 800 rpm. After the specified time, 1,3,5-trimethoxybenzene (5 mM in EtOAc) were added to each reaction. The microtubes were sealed, vortexed for 10 s, and the aqueous and organic phases were separated by centrifugation at 20,817 g and 4 ºC for 20 min. If phase separation did not occur after initial centrifugation, the sample was vortexed again for 10 s and centrifuged for an additional 20 min at 20,817 g and 4 ºC. Aliquots of the organic phase (200–300 μL/reaction) were then transferred to individual 400-μL flat bottom glass inserts in 2-mL screw-cap vials which were sealed with septum screw caps. Analysis was then performed using GC/MS with product concentrations determined by response relative to the 1,3,5-trimethoxybenzene internal standard using a calibration curve. In the case of siloxane **1**, the calibration range is non-linear for the response observed, therefore siloxane **1** is plotted as relative response to the 1,3,5-trimethoxybenzene internal standard over time.

Timepoint (min)	Siloxane 1 Peak Area	1,3,5-trimethoxybenzene Peak Area	Relative Response
0	11843952.46	4924939.722	2.40
	11257881.14	4984504.944	2.26
	11871337.63	4958550.954	2.39
10	11741319.72	4849432.004	2.42
	10976832.99	4818593.437	2.28
	11780588.65	4850177.717	2.43
30	13494651.01	4909453.528	2.75
	12296692.17	4844710.916	2.54
	11404408.15	4921743.244	2.32
60	11602360.39	4923681.435	2.36
	11822219.61	4863646.015	2.43
	11627235.45	4892950.802	2.38
120	13095228.72	5018950.446	2.61
	13077490.99	4894407.154	2.67
	12464742.85	5033695.572	2.48
180	11847224.12	4946712.246	2.39
	11692822.17	4967194.664	2.35
	11682428.19	4784001.66	2.44
240	12047310.32	4841095.683	2.49
	11493904.27	4888717.268	2.35
	11858506.91	4824709.379	2.46
360	12006511.24	4764938.427	2.52
	11943918.79	4749294.63	2.51
	11164040.84	4546517.011	2.46
1,440	11291001.19	4634012.285	2.44
	11009865.49	4799217.429	2.29
	11407731.91	4620519.038	2.47
2,880	11657292.44	4856262.851	2.40
	11764194.51	4841066.348	2.43
	11582822.64	4650407.263	2.49
4,320	11655020.06	4646060.759	2.51
	10698746.46	4660393.872	2.30
	11404222.88	4765579.966	2.39

Table S35. Experimental data for siloxane **1** response relative to internal standard 1,3,5-trimethoxybenzene over time in *E. coli* lysate.

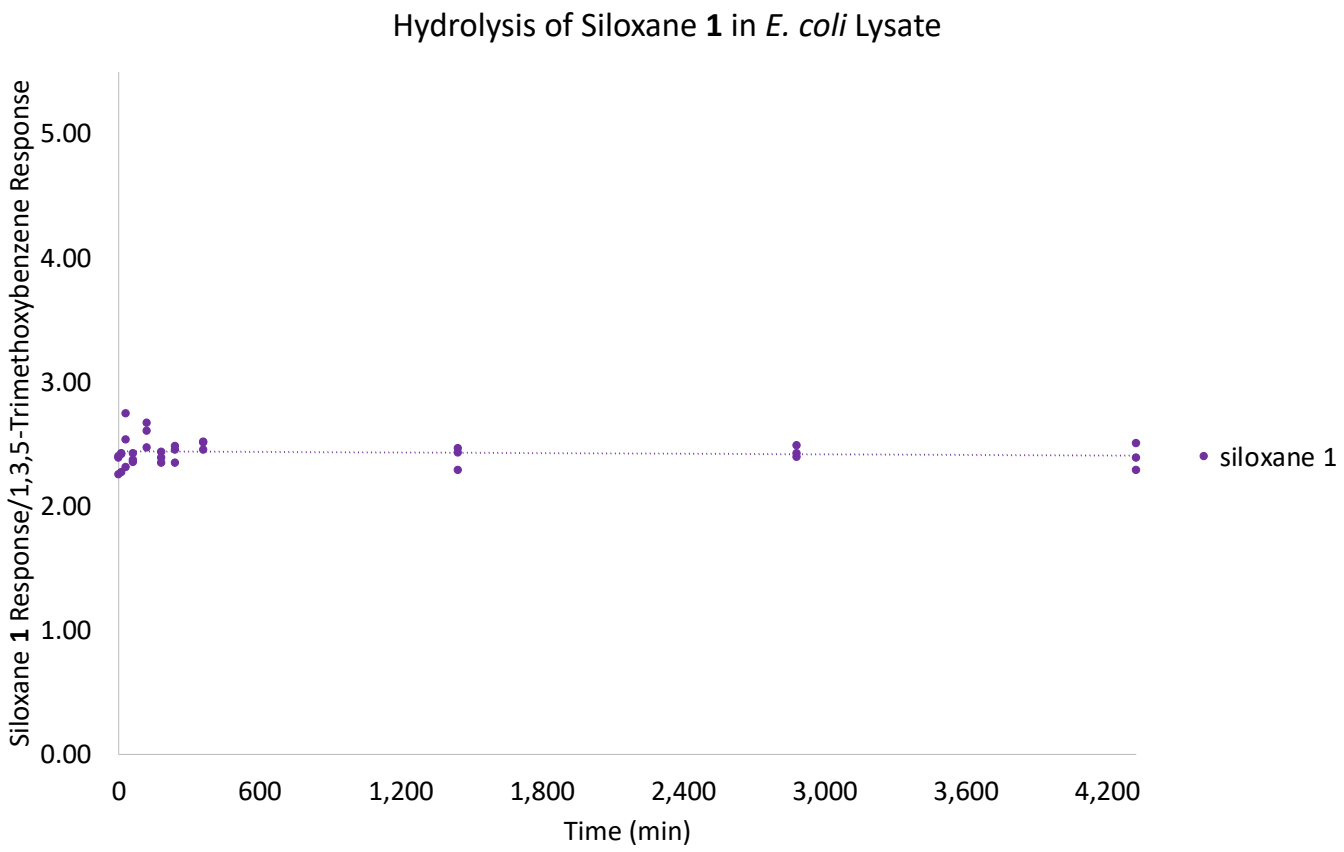

Figure S31. Response of siloxane **1** vs. 1,3,5-trimethoxybenzene internal standard over time in *E. coli* lysate at pH 7.00.

Timepoint (min)	[carbinol 4] (mM)	[silanol 5] (mM)
0	5.20	5.36
	5.50	4.95
	5.12	5.17
10	5.35	4.89
	5.11	5.21
	5.04	4.82
30	4.98	4.68
	5.24	5.87
	5.18	4.61
60	5.17	5.00
	4.86	4.85
	5.16	4.61
120	5.05	4.92
	5.03	5.01
	4.86	5.22
180	5.32	4.82
	5.07	5.00
	5.40	4.76
240	4.98	4.35
	5.80	4.98
	5.16	5.21
360	4.51	6.03
	4.28	5.00
	4.42	4.82
1,440	2.84	4.72
	2.63	4.45
	2.61	4.74
2,880	1.23	4.41
	1.17	4.45
	0.97	4.26
4,320	0.27	3.85
	0.35	4.10
	0.32	3.97

Table S36. Experimental data for carbinol **4** and silanol **5** concentration over time in *E. coli* lysate at pH 7.00.

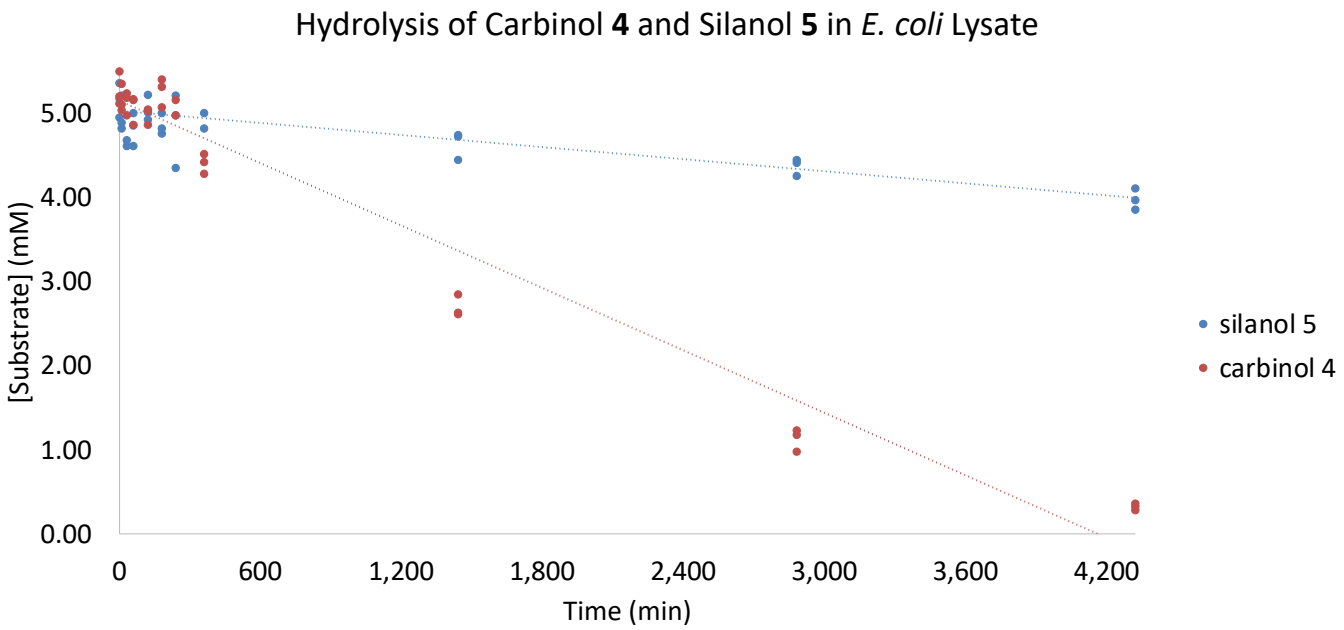

Figure S32. Plot for the change in concentration of carbinol **4** and silanol **5** over time in *E. coli* lysate at pH 7.00.

12. pH-Dependent Hydrolysis of Carbinol 4

All reactions were performed in crimp-cap GC/MS vials following the procedure outlined in 1.9 Enzymatic Reactions for Mechanistic Studies. To the reaction vials were added 337.5 μL of the 100 mM Tris buffer at the noted pH followed by 12.5 μL carbinol **4** (140 mM in EtOH). After the addition of carbinol **4**, the reaction vessels were crimp capped and shaken at 800 rpm. After the specified time, a 5 mM 1,3,5-trimethoxybenzene stock in EtOAc was added. The microtubes were sealed, vortexed for 10 s, and aliquots of the organic phase (200–300 μL/reaction) were then transferred to individual 400-μL flat bottom glass inserts in 2-mL screw-cap vials which were sealed with septum screw caps. Analysis was then performed using GC/MS with product concentrations determined by response relative to the 1,3,5-trimethoxybenzene internal standard using a calibration curve.

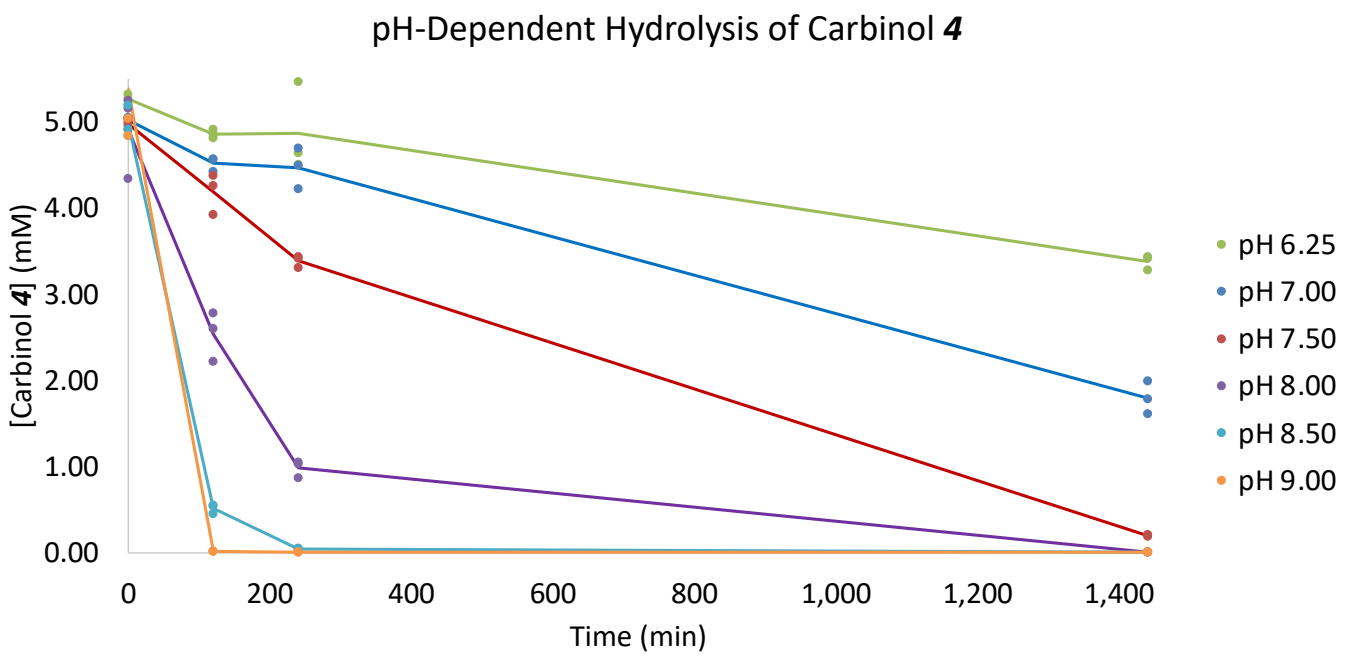

Figure S33. Hydrolysis of carbinol ***4*** at varying pH in 100 mM Tris buffer.

pH	Time (min)	[Carbinol 4]	[Silanol 5]	pH	[Carbinol 4]	[Silanol 5]
6.25	0	5.27	0	8.00	0	4.34
		5.32	0			5.15
		5.19	0			5.25
	120	4.81	0		120	2.60
		4.90	0			2.78
		4.86	0			2.22
	240	4.64	0		240	1.06
		4.50	0			0.88
		5.46	0			1.04
	1440	3.43	0		1440	0.0096
		3.28	0			0.0093
		3.41	0			0.0091
7.00	0	4.96	0	8.50	0	5.19
		5.04	0			4.91
		5.05	0			4.83
	120	4.42	0		120	0.56
		4.56	0			0.45
		4.56	0			0.54
	240	4.22	0		240	0.058
		4.50	0			0.042
		4.69	0			0.046
	1440	1.61	0		1440	0.012
		1.78	0			0.0095
		2.00	0			0.0095
7.50	0	5.03	0	9.00	0	4.84
		4.99	0			5.04
		4.91	0			6.27
	120	3.92	0		120	0.019
		4.38	0			0.023
		4.26	0			0.017
	240	3.41	0		240	0.011
		3.30	0			0.0094
		3.44	0			0.0091
	1440	0.21	0		1440	0.011
		0.21	0			0.0096
		0.19	0			0.011

Table S37. pH-dependent hydrolysis of carbinol **4** data. Formation of silanol **5** is not observed at any pH.

13. Protein-Concentration Dependence

All reactions were performed in 2.0-mL snap-cap microtubes on a 350-μL scale with specific conditions outlined below. A frozen aliquot of purified *L*SilOx4 in 100 mM pH 7.00 Tris buffer (67.1 μM) was thawed on ice, and serial dilutions of 8.1, 5.38, 2.7, and 1.1 μM *L*SilOx4 were prepared in 100 mM pH 7.00 Tris buffer. An additional control of 5.38 μM *L*SilOx4 with 5.38 mM imidazole was prepared to determine the effect of residual imidazole from protein purification. All reaction vessels were charged with 12.5 μL of NADPH (140 mM in 100 mM pH 7.00 Tris buffer) followed by 325 μL of purified *L*SilOx4 stock to give final protein concentrations of 7.5, 5.0, 2.5, and 1.0 μM *L*SilOx4. Buffer controls were performed by adding 325 μL of 100 mM pH 7.00 Tris buffer or 325 μL of 5.38 mM imidazole in 100 mM pH 7.00 Tris buffer. The reactions were then charged with 12.5 μL of carbinol **4** (140 mM in EtOH). After the addition of substrate, the microtubes were rapidly sealed and shaken at 800 rpm at 23 ºC in for 4 h. After 4 h, the reaction vessels were unsealed and 450 μL of a 5 mM 1,3,5- trimethoxybenzene stock in EtOAc were added. The microtubes were sealed again, vortexed for 10 s, and the aqueous and organic phases were separated by centrifugation at 20,817 *g* and 4 ºC for 20 min. If phase separation did not occur after initial centrifugation, the sample was vortexed again for 10 s and centrifuged for an additional 20 min at 20,817 *g* and 4 ºC. Aliquots of the organic phase (200–300 μL/reaction) were then transferred to individual 400-μL flat-bottom glass inserts in 2-mL screw-cap vials which were sealed with septum screw caps. Analysis was then performed using GC/MS with product concentrations determined by response relative to the 1,3,5-trimethoxybenzene internal standard using a calibration curve.

Enzyme Variant or Condition	[Enzyme] (μM)	[Silanol 5] (mM)
100 mM pH 7.00 Tris buffer	–	0.00
	–	0.00
	–	0.00
*L*SilOx4	0	0.00
	0	0.00
	0	0.00
*L*SilOx4	1.0	0.21
	1.0	0.19
	1.0	0.19
*L*SilOx4	2.5	0.49
	2.5	0.44
	2.5	0.43
heat-treated *L*SilOx4	2.5	0.00
	2.5	0.00
	2.5	0.00
*L*SilOx4	5.0	0.92
	5.0	0.87
	5.0	0.82
*L*SilOx4 + 5 mM imidazole	5.0	0.97
	5.0	0.91
	5.0	0.85
*L*SilOx4	7.5	1.28
	7.5	1.22
	7.5	1.20

Table S38. Protein concentration dependence data with carbinol **4** as substrate including imidazole, heat treatment, and buffer only controls.

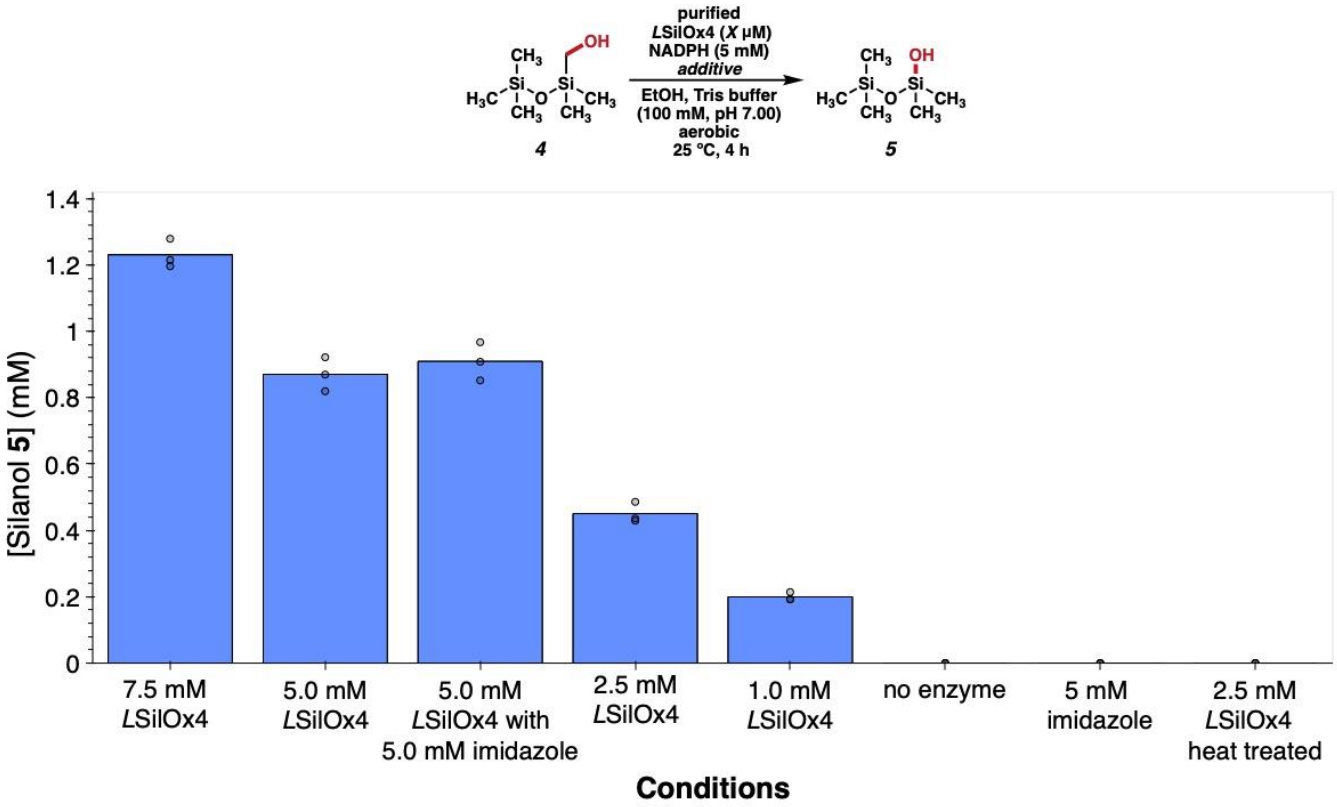

Figure S34. Plot for protein concentration dependence data of reactions with carbinol **4** as substrate including imidazole, heat treatment, and buffer controls.

14. Oxygen-Dependence Studies

All reactions were performed in 2.0-mL snap-cap microtubes on a 350-μL scale with specific conditions are outlined below. Purified *L*SilOx4 or buffer were added to the reaction vessels which were then pumped into an anaerobic Coy chamber (35 ppm O_2) under an atmosphere of 2.5% H_2/N_2. The remaining reaction components were added in the Coy chamber as noted below. All reactions had final concentrations of 5 mM carbinol **4**, 5 mM NADPH, 5.0 μM *L*SilOx4. Controls with glucose oxidase/catalase had final concentrations of 0.15 mg/mL glucose oxidase, 0.10 mg/mL catalase, and 73 mM glucose. The reactions were shaken at 800 rpm at 23 ºC for 4 h under the atmosphere noted below. After 4 h, the reaction vessels were unsealed and 450 μL of a 5 mM 1,3,5-trimethoxybenzene stock in EtOAc were added. The microtubes were resealed, vortexed for 10 s, and the aqueous and organic phases were separated by centrifugation at 20,817 *g* and 4 ºC for 20 min. If phase separation did not occur after initial centrifugation, the sample was vortexed again for 10 s and centrifuged for an additional 20 min at 20,817 *g* and 4 ºC. Aliquots of the organic phase (200–300 μL/reaction) were then transferred to individual 400-μL flat-bottom glass inserts in 2-mL screw-cap vials which were sealed with septum screw caps. Analysis was performed using GC/MS with product concentrations determined by response relative to the 1,3,5-trimethoxybenzene internal standard using a calibration curve.

14.1 Aerobic

Frozen aliquots of purified *L*SilOx4 (67.1 μM) were thawed on ice, and a stock of 5.38 μM *L*SilOx4 in 100 mM pH 7.00 Tris buffer was prepared and 325 μL of the *L*SilOx4 stock were added to the reaction vessels. The vessel was then pumped into an anaerobic Coy chamber, and 12.5 μL of NADPH solution (140 mM in 100 mM pH 7.00 Tris buffer) were added followed by 12.5 μL of carbinol **4** (140 mM in EtOH). The reactions had final concentrations of 5 mM substrate, 5 mM NADPH, and 5.0 μM *L*SilOx4. After the addition of substrate, the reaction was removed from the Coy chamber, opened to aerobic atmosphere for 10 s, then sealed and shaken sealed at 800 rpm and 23 ºC for 4 h.

14.2 Aerobic with catalase/GOX

Frozen aliquots of purified *L*SilOx4 (67.1 μM) were thawed on ice, and a stock of 6.83 μM *L*SilOx4 in 100 mM pH 7.00 Tris buffer was prepared of which 257 μL were added to the reaction vessels. The vessel was then pumped into an anaerobic Coy chamber, and 17 μL of 6.0 mg/mL glucose oxidase/4.0 mg/mL catalase solution, 51 μL of a glucose solution, and 12.5 μL of 140 mM NADPH solution, all prepared in 100 mM pH 7.00 Tris buffer, were added sequentially followed by 12.5 μL of carbinol **4** (140 mM in EtOH). The reactions had final concentrations of 5 mM carbinol **4**, 5 mM NADPH, 5.0 μM *L*SilOx4, 0.15 mg/mL glucose oxidase, 0.10 mg/mL catalase, and 73 mM glucose. After the addition of substrate, the reaction was removed from the Coy chamber, opened to aerobic atmosphere for 10 s, and shaken sealed at 800 rpm and 23 ºC for 4 h.

14.3 35 ppm O_2 Atmosphere

Frozen aliquots of purified *L*SilOx4 (67.1 μM) were thawed on ice, and a stock of 5.38 μM *L*SilOx4 in 100 mM pH 7.00 Tris buffer was prepared of which 325 μL were added to the reaction vessels. The vessels were pumped into an anaerobic Coy chamber, and 12.5 μL of NADPH solution (140 mM in 100 mM pH 7.00 Tris buffer) were added followed by 12.5 μL of carbinol **4** (140 mM in EtOH). The reactions had final concentrations of 5 mM carbinol **4**, 5 mM NADPH, and 5.0 μM *L*SilOx4. After the addition of substrate, the reaction was shaken in the Coy chamber at 800 rpm and 23 ºC for 4 h.

13.4 35 ppm O_2 with catalase/GOX

Frozen aliquots of purified *L*SilOx4 (67.1 μM) were thawed on ice, and a stock of 6.83 μM *L*SilOx4 in 100 mM pH 7.00 Tris buffer was prepared of which 257 μL were added to the reaction vessels. The vessels were pumped into an anaerobic Coy chamber, and 17 μL of 6.0 mg/mL glucose oxidase/4.0 mg/mL catalase solution, 51 μL of a glucose solution, and 12.5 μL of 140 mM NADPH solution, all prepared in 100 mM pH 7.00 Tris buffer, were added sequentially followed by 12.5 μL of carbinol **4** (140 mM in EtOH). The reactions had final concentrations of 5 mM carbinol **4**, 5 mM NADPH, 5.0 μM *L*SilOx4, 0.15 mg/mL glucose oxidase, 0.10 mg/mL catalase, and 73 mM glucose. After the addition of substrate, the reaction was shaken in the Coy chamber at 800 rpm and 23 ºC for 4 h.

14.5 35 ppm O_2, then recovery after 1 h

Frozen aliquots of purified *L*SilOx4 (67.1 μM) were thawed on ice, and a stock of 5.38 μM *L*SilOx4 in 100 mM pH 7.00 Tris buffer was prepared of which 325 μL were added to the reaction vessels. The vessels were ,pumped into an anaerobic Coy chamber and 12.5 μL of NADPH solution (140 mM in 100 mM pH 7.00 Tris buffer) were added followed by 12.5 μL of carbinol **4** (140 mM in EtOH). The reactions had final concentrations of 5 mM carbinol **4**, 5 mM NADPH, and 5.0 μM *L*SilOx4. After the addition of substrate, the reaction was shaken in the Coy chamber at 800 rpm and 23 ºC for 1 h. The reaction was then removed from the Coy chamber, opened to aerobic atmosphere for 10 s, and shaken sealed at 800 rpm and 23 ºC in for 3 h.

14.6 Buffer with catalase/GOX

To the microtube was added 257 μL of 100 mM pH 7.00 Tris buffer. The vessels were pumped into a Coy anaerobic chamber, and 17 μL of 6.0 mg/mL glucose oxidase/4.0 mg/mL catalase solution, 51 μL of a glucose solution, and 12.5 μL of 140 mM NADPH solution, all prepared in 100 mM pH 7.00 Tris buffer, were added sequentially followed by 12.5 μL of carbinol **4** (140 mM in EtOH). The reactions had final concentrations of 5 mM carbinol **4**, 5 mM NADPH, 0.15 mg/mL glucose oxidase, 0.10 mg/mL catalase, and 73 mM glucose. After the addition of substrate, the reactions were removed from the Coy chamber, opened to aerobic atmosphere for 10 s, and shaken sealed at 800 rpm and 23 ºC for 4 h.

Conditions	Replicant	[Carbinol 4] (mM)	[Silanol 5] (mM)	Total Product Enzyme
aerobic	1	0.053	0.150	41
	2	0.043	0.125	34
	3	0.039	0.113	30
aerobic with catalase/GOX	1	0.000	0.016	3.1
	2	0.000	0.017	3.4
	3	0.000	0.015	3.0
35 ppm O_2	1	0.015	0.011	5.1
	2	0.013	0.011	4.8
	3	0.013	0.013	5.2
35 ppm O_2 with catalase/GOX	1	0.012	0.009	4.1
	2	0.011	0.009	4.0
	3	0.012	0.008	4.0
buffer with catalase/GOX	1	0.000	0.000	0.0
	2	0.000	0.000	0.0
	3	0.000	0.000	0.0
35 ppm O_2, then recovery after 1 h	1	0.043	0.132	35
	2	0.045	0.111	31
	3	0.034	0.105	28

Table S39. Oxygen dependence data for reactions with siloxane **1** as a substrate with 5 μM *L*SilOx4.

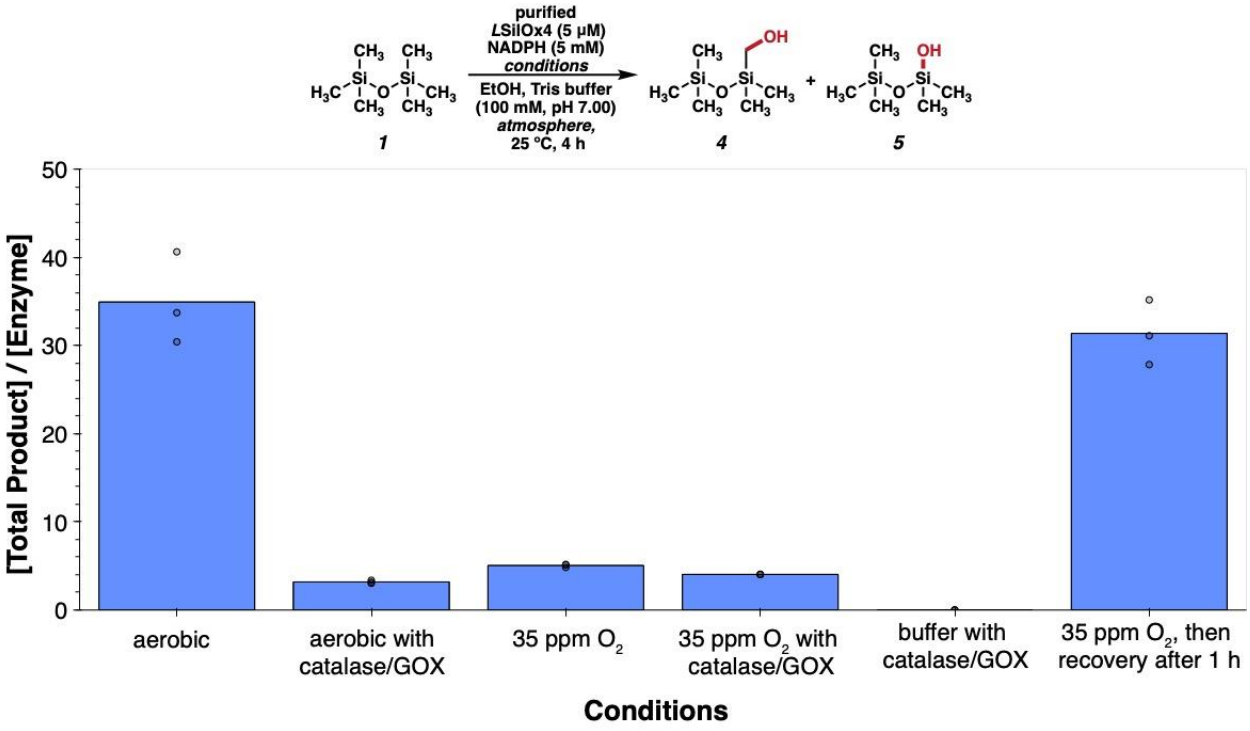

Figure S35. Bar graph of oxygen-dependence experiments with siloxane **1** as substrate.

Conditions	Replicant	[Silanol 5] (mM)	Total Product / Enzyme
aerobic	1	0.582	116
	2	0.520	104
	3	0.497	99.4
aerobic with catalase/GOX	1	0.055	11.1
	2	0.040	7.9
	3	0.059	11.7
35 ppm O_2	1	0.144	28.9
	2	0.138	27.7
	3	0.139	27.8
35 ppm O_2 with catalase/GOX	1	0.108	21.7
	2	0.101	20.1
	3	0.100	19.9
buffer with catalase/GOX	1	0.000	0.00
	2	0.000	0.00
	3	0.000	0.00
35 ppm O_2, then recovery after 1 h	1	0.302	60.5
	2	0.285	57.0
	3	0.283	56.5

Table S40. Oxygen dependence data for reactions with carbinol **4** as a substrate with 5.0 μM *L*SilOx4.

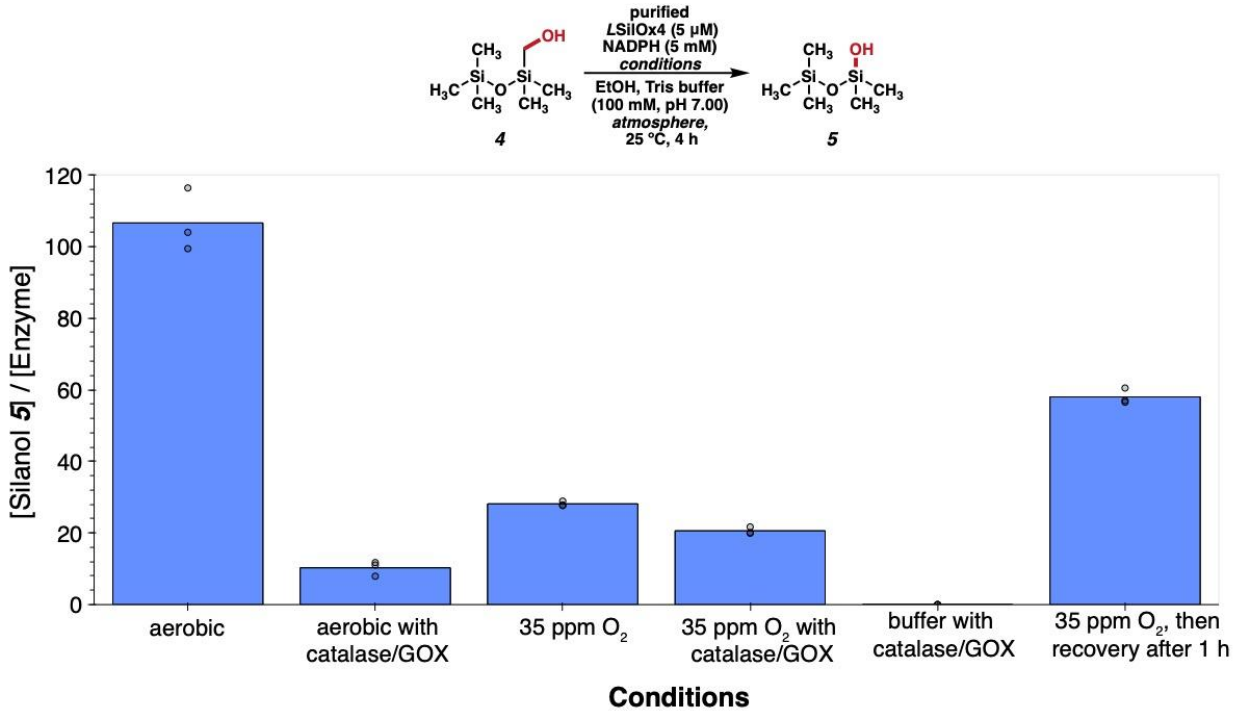

Figure S36. Bar graph of oxygen-dependence experiments with carbinol **4** as substrate.

15. Experimental Data Relevant to Figure 4

15.1 Observation of Formylsiloxane **10** in GC/MS Traces

Early time-points in enzymatic reaction time-course data (**Figure 3D**) show the formation of a trace peak at 3.55 min when the rate of the enzymatic reaction is fastest (**Figure S37**) with a mass spectrum showing fragments *m/z* 147.1 and 133.0 (**Figure S38**). After the enzymatic reaction slows, this peak is no longer observed in GC/MS traces. This trace peak could be observed with multiple injections, however, with complete decay (**Figure S39**). This peak was tentatively assigned as formylsiloxane **10** pending additional evidence (vide infra, sections 15.2 and 15.3).

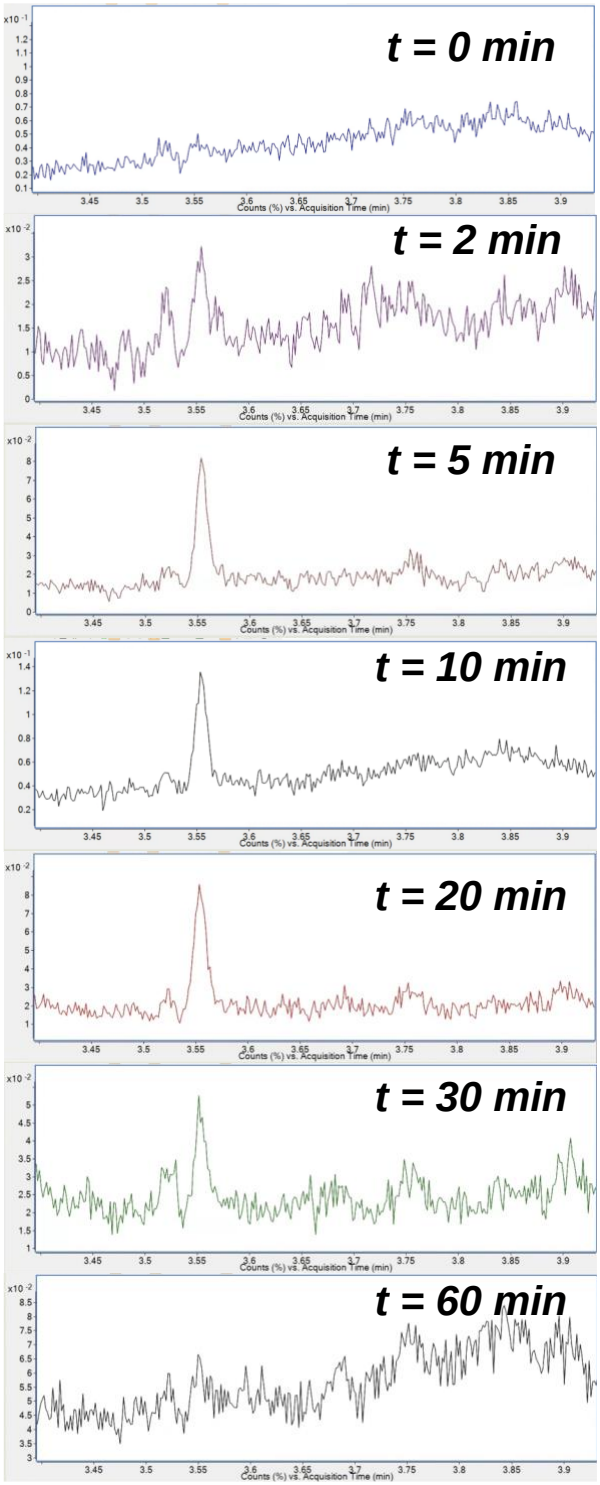

Figure S37. Appearance of a trace peak at 3.55 min in an enzymatic reaction time-course with carbinol **4** (Figure 3D).

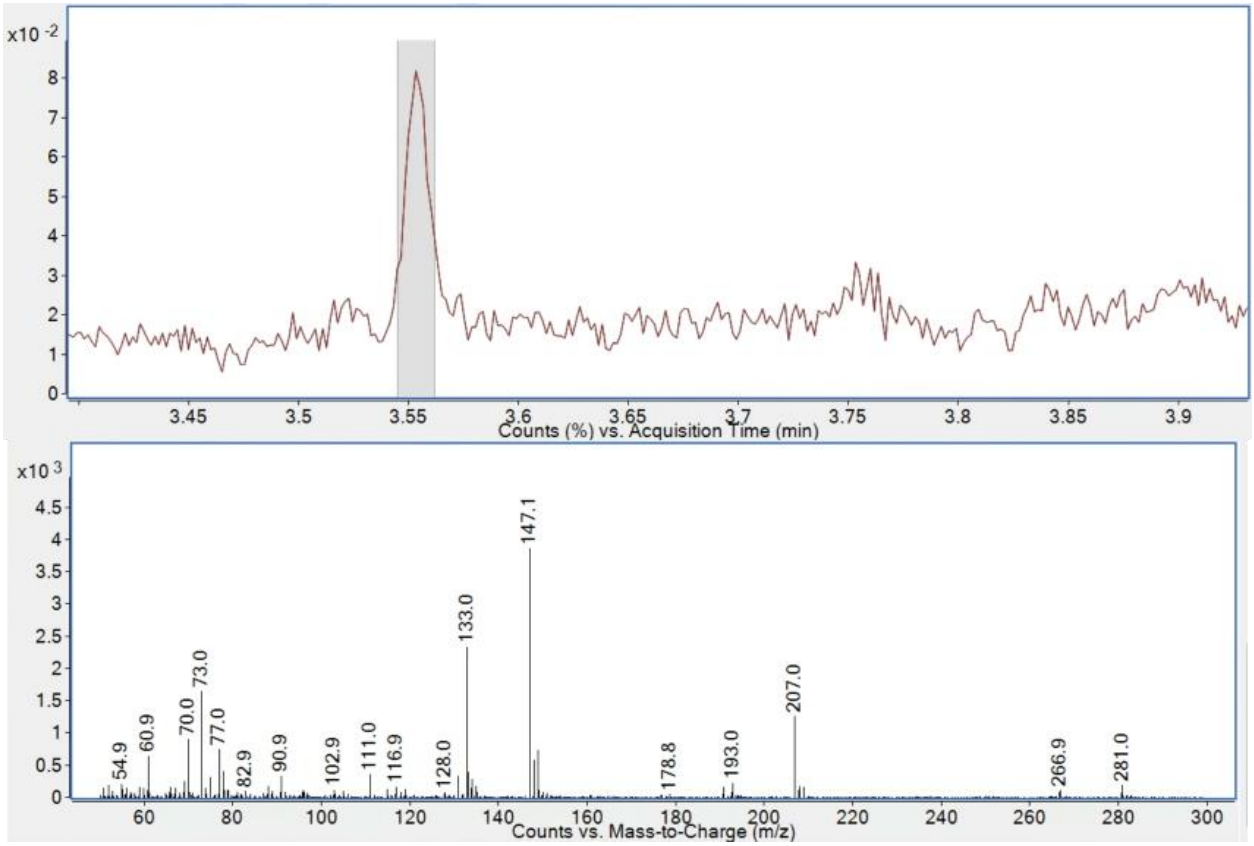

Figure S38. Mass spectrum of the trace peak observed with 3.55 min retention time in a 5 min timepoint of an enzymatic reaction with carbinol **4** as substrate.

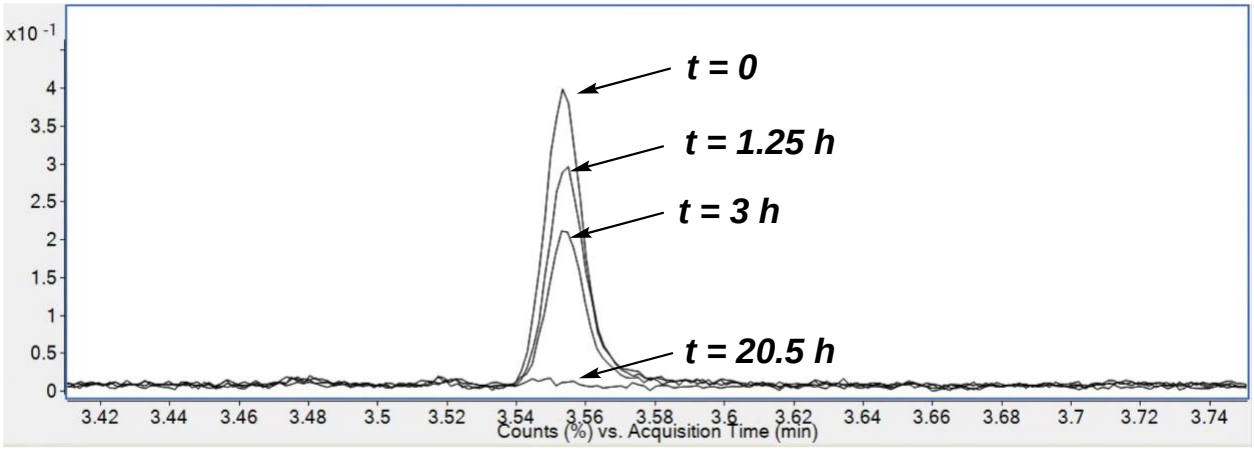

Figure S39. Decay of the 3.55 min peak over time is observed by analyzing an enzymatic reaction sample on GC/MS over time.

15.2 High-Resolution Mass Spectrometry of Carbinol **4** Enzymatic Reactions

Identification of this peak necessitated the collection of high-resolution mass spectral data. Enzymatic reactions from **Figure 3D** were repeated, and the reactions were extracted with ethyl acetate (no internal standard) as described in Experimental Data Relevant to Figure 3D after 5 min in triplicate. The organic extracts were immediately frozen on dry ice and thawed immediately before analysis on a JEOL JMS-T2000 GC AccuTOF GC-Alpha. Samples were analyzed by Gas Chromatography (GCI with Chemical Ionization (CI) using a JEOL AccuTOF GC-Alpha (JMS-T2000GC) mass spectrometer interfaced with an Agilent 8890 GC system. The CI gas was methane with 5% ammonia. Additionally, the samples were also analyzed with EI+ ionization on the same instrument. In these samples the formylsiloxane could be observed by high resolution mass spectrometry in both CI+ and EI+ ionization modes, eluting between silanol **5** and carbinol **4**.

Analyte	Retention Time (min)	Ionization Method	Observed *m/z*	Formula	Calculated *m/z* (difference, ppm)
silanol **5**	3.38–3.49	CI+	165.07674	$[M+H]^+$ $C_5H_{17}O_2Si_2$	165.07671 (0.17)
			182.10320	$[M+NH_4]^+$ $C_5H_{20}NO_2Si_2$	182.10326 (–0.32)
formylsiloxane **10**	4.00–4.04	CI+	177.07740	$[M+H]^+$ $C_6H_{17}O_2Si_2$	177.07671 (3.88)
			194.10266	$[M+NH_4]^+$ $C_6H_{20}NO_2Si_2$	194.10326 (–3.06)
		EI+	147.06550	$[M–CHO]^+$ $C_5H_{15}OSi_2$	147.06614 (–4.38)
carbinol **4**	4.54–4.64	CI+	179.09237	$[M+H]^+$ $C_6H_{19}O_2Si_2$	179.09236 (0.07)
siloxane **S4**[a]	4.72–4.92	CI+	177.07680	$[M+H]^+$ $C_6H_{17}O_2Si_2$	177.07671 (0.53)

Table S41. High-resolution mass spectrometry data for enzymatic reaction analytes. [a]Siloxane **S4** is a trace impurity in carbinol **4** which is a constitutional isomer of formylsiloxane **10**.

15.2 Studies of Formylsiloxane **10** Prepared *in situ* via Swern Oxidation of Carbinol **4**

To further confirm this sensitive, trace enzymatic product, we attempted chemical synthesis of formylsiloxane **10** through oxidation of carbinol **4**. This was most successful using rigorously anhydrous Swern oxidation conditions which allowed for the direct observation of formylsiloxane **10** by NMR spectroscopy. While formylsiloxane **10** could be observed under these conditions, attempts to isolate it further were thwarted by its sensitivity. Notably, a small amount of formaldehyde is observed in the formation of formylsiloxane **10**, presumably via hydrolysis with trace water.

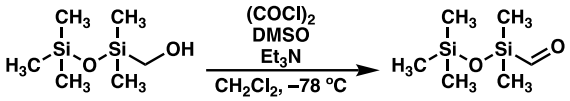

An oven-dried NMR tube with a septum cap was purged and evacuated with Ar 3x. To the NMR tube was added a solution of $(COCl)_2$ (6.3 μL, 0.075 mmol, 1.5 equiv) and CD_2Cl_2 (300 μL). The NMR tube was immersed in a dry ice/acetone bath for 10 min, then a solution of DMSO (10.7 μL, 0.150 mmol, 3.0 equiv) in 50 μL CD_2Cl_2 was added. The solution was mixed by gently flicking the NMR tube. After 1 h, a solution of carbinol **4** (8.9 mg, 0.050 mmol, 1.0 equiv) in CD_2Cl_2 (100 μL) was added and the reaction mixture became slightly white and opaque. The solution was again mixed by gently flicking the NMR tube. After 1 h, Et_3N (35 μL, 0.25 mmol, 5.0 equiv) was added. The NMR tube septum cap was quickly exchanged for a plastic cap under flow of Ar. The NMR tube was then quickly transferred to an NMR spectrometer, precooled to –80 ºC. A single scan ^1H–^{29}Si HMBC was acquired and showed a signal at ca δ 11.7 ppm with correlation to an Si atom bearing methyl groups. The sample was warmed to –40 ºC and a 64 scan ^1H–^{29}Si HMBC was acquired, revealing the key formyl C–H proton (**Figure S37**) which could be observed in a ^1H NMR spectrum, albeit with a broad peak obscuring it slightly (**Figure S38**). The sample was then warmed to 25 ºC and another ^1H NMR was acquired (**Figure S39**), showing the clear presence of the characteristic formyl C–H with J = 37.2 Hz and the formation of additional formaldehyde, presumably as a hydrolysis byproduct. Observation of formylsiloxane **10** via GC/MS analysis shows the same characteristic peak at 3.56 min with an identical mass fragmentation pattern to enzymatic samples containing this peak (**Figure S40**).

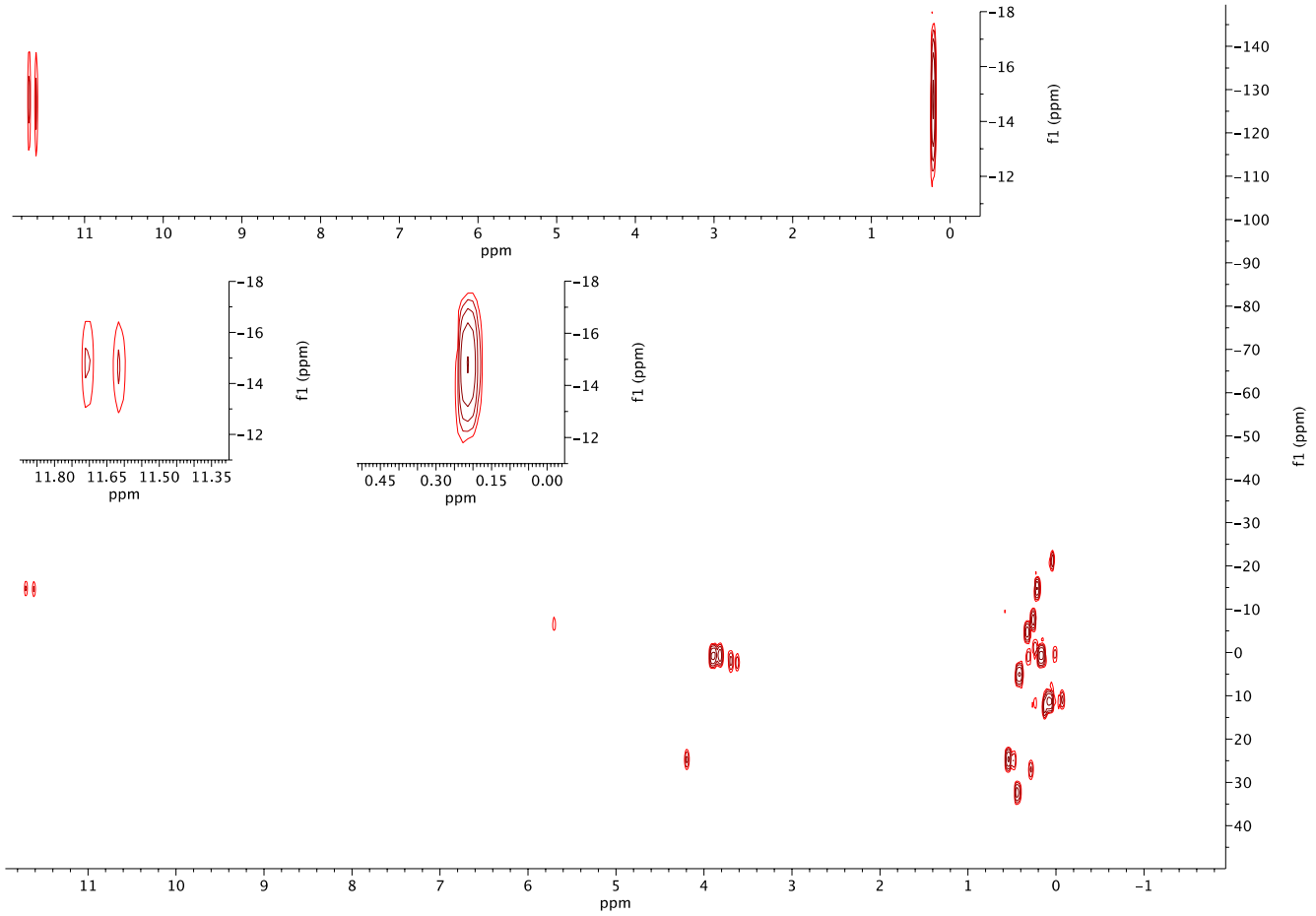

Figure S40. $^{1}H–^{29}Si$ HMBC at –40 ºC showing correlation of the formyl C–H δ 11.66 (s, 1H) to a Si center with methyl groups.

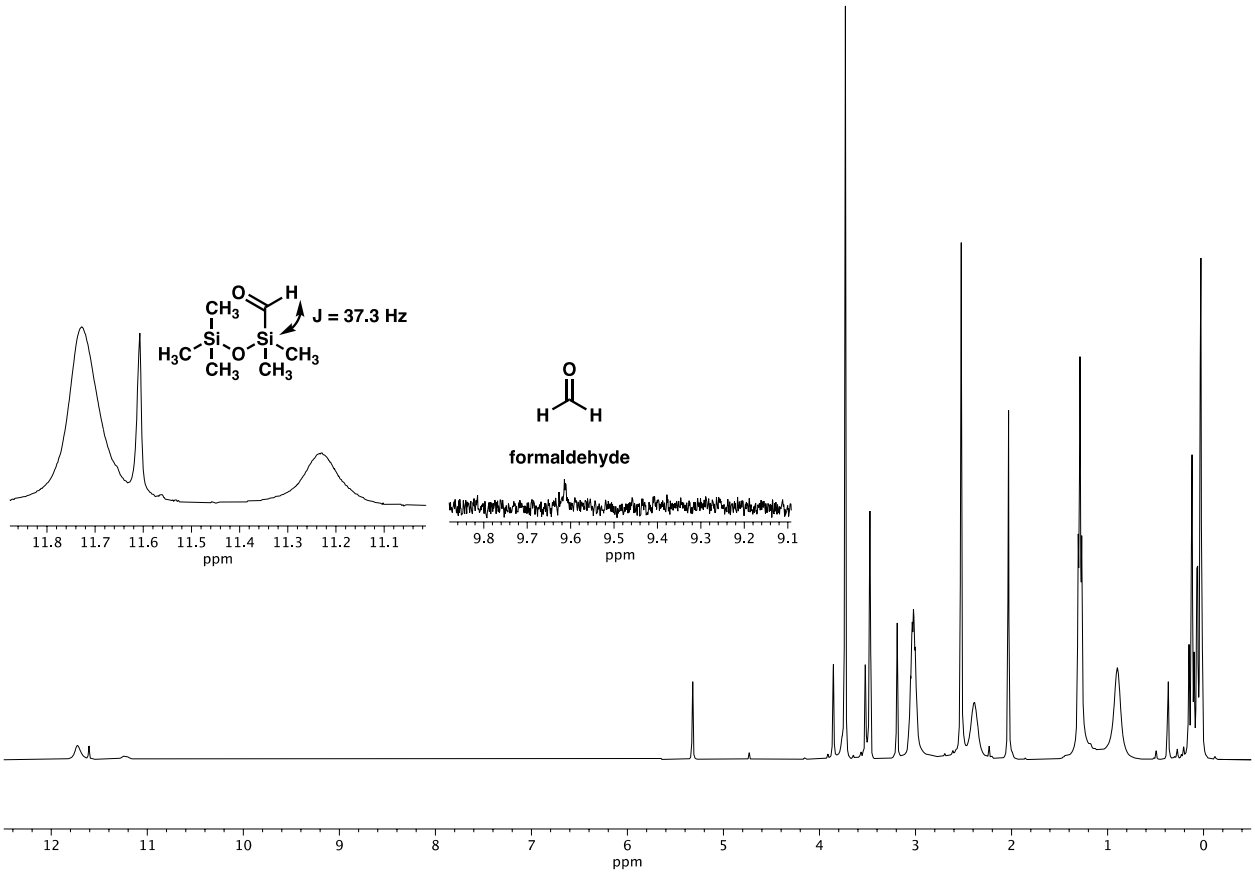

Figure S41. ^{1}H NMR (400 MHz, CD_2Cl_2, –40 ºC) of the Swern reaction mixture, showing the formylsiloxane **10** and trace amounts of formaldehyde as a byproduct.

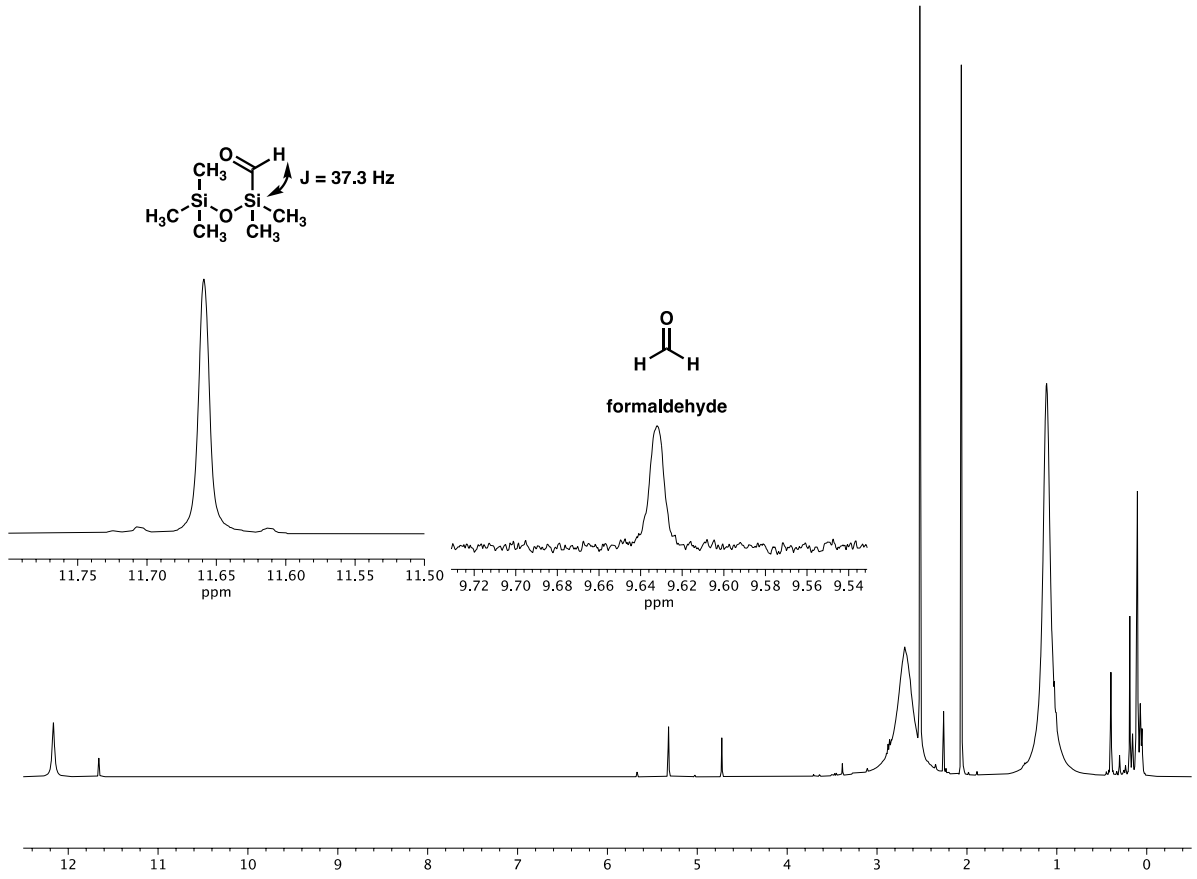

Figure S42. ^{1}H NMR (400 MHz, CD_2Cl_2, 25 ºC) of the Swern reaction mixture, showing the formylsiloxane **10** and small amounts of formaldehyde as a byproduct.

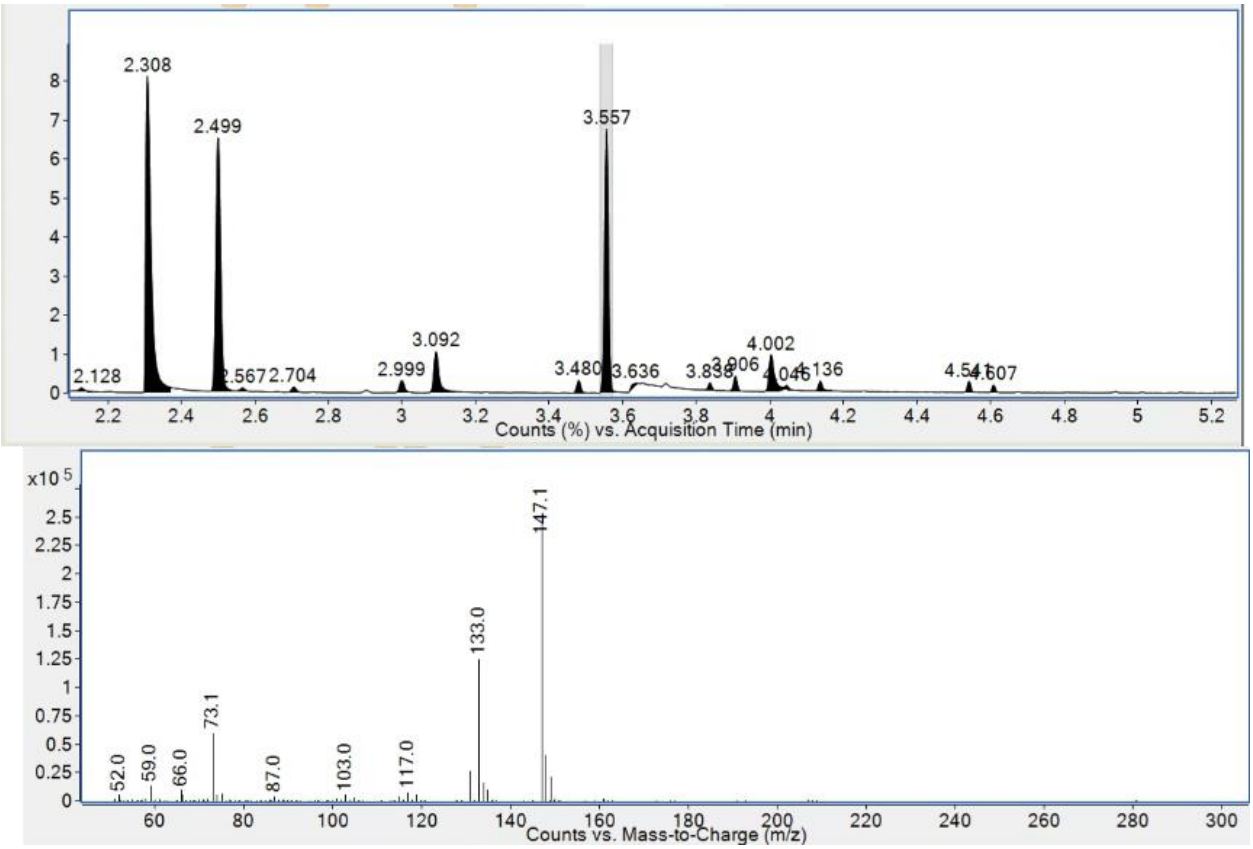

Figure S43. A GC/MS trace and mass fragmentation pattern of the formylsiloxane (**10**) peak corresponding to the same peak in both retention time and mass fragmentation as observed in enzymatic reactions. The signal present at 3.09 corresponds to silanol **5**.

17. Comparison of Tris and KPi Buffers

All reactions were performed in 2.0-mL snap-cap microtubes on a 350-µL scale in *E. coli* lysate with 5 mM substrate (siloxane **1** or carbinol **4**), following the general procedure outlined in 1.9 Enzymatic Reactions for Mechanistic Studies with either NADPH or the NADPH cofactor regeneration system. Lysis was performed using either 100 mM pH 7.00 Tris or 100 mM pH 7.00 KPi buffer.

Cofactor System	Buffer	[Carbinol 4] (mM)	[Silanol 5] (mM)	Total Product Enzyme
NADPH	100 mM pH 7.00 Tris	0.176	0.164	53
		0.169	0.149	48
		0.153	0.139	45
	100 mM pH 7.00 Kpi	0.163	0.196	63
		0.151	0.165	53
		0.147	0.159	51
NADPH Regeneration System	100 mM pH 7.00 Tris	0.026	0.441	142
		0.028	0.430	139
		0.027	0.413	133
	100 mM pH 7.00 Kpi	0.018	0.391	126
		0.016	0.366	118
		0.017	0.374	121

Table S42. Comparison of Tris and KPi buffers and NADPH cofactor and cofactor regeneration with siloxane **1** as a substrate. *L*SilOx4 was 3.1 µM in Tris buffer and 4.2 µM in KPi buffer.

Cofactor System	Buffer	[Silanol 5] (mM)	Total Product / Enzyme
NADPH	100 mM pH 7.00 Tris	0.558	133
		0.482	115
		0.523	124
	100 mM pH 7.00 Kpi	0.586	140
		0.545	130
		0.556	132
NADPH Regeneration System	100 mM pH 7.00 Tris	0.553	132
		0.542	129
		0.538	128
	100 mM pH 7.00 Kpi	0.629	150
		0.642	153
		0.636	152

Table S43. Comparison of Tris and KPi buffers and NADPH cofactor and cofactor regeneration with carbinol **4** as a substrate. *L*SilOx4 was 3.1 µM in Tris buffer and 4.2 µM in KPi buffer.

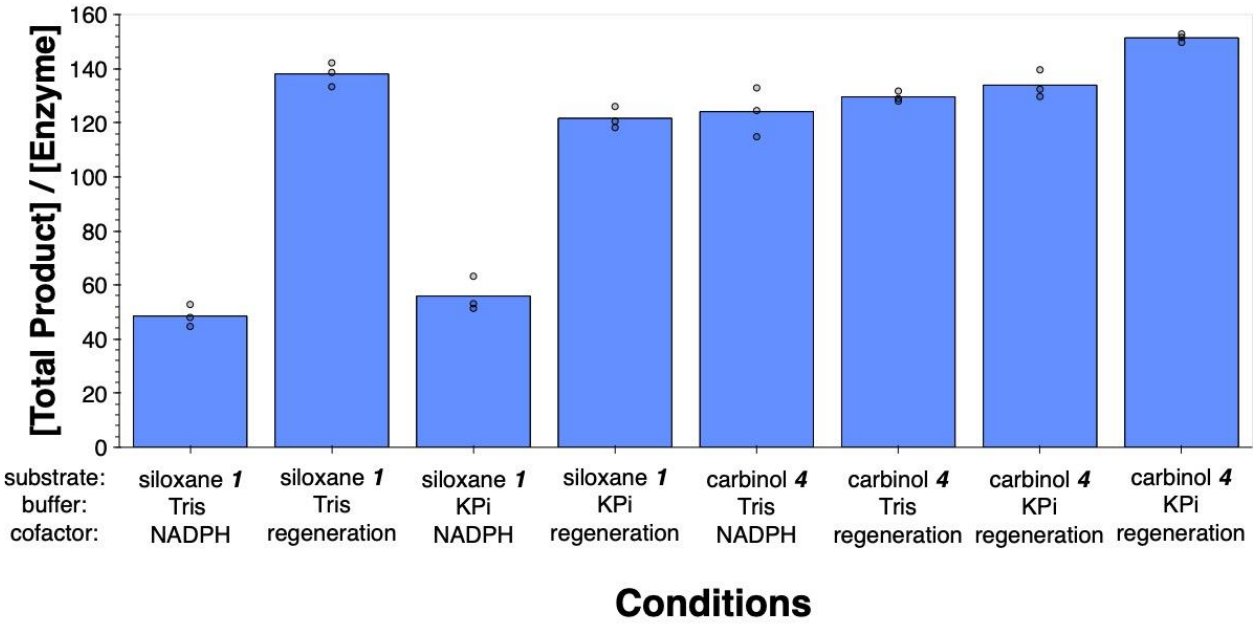

Figure S44. Comparion of Tris and KPi buffers and NADPH and NADPH cofactor regeneration for reactions with siloxane **1** and carbinol **4** as substrates.

18. Enzymatic Reaction Time-Course with Siloxane 2

Enzymatic reaction time-course data were collected as described in Experimental Data Relevant to Figure 3D using siloxane **2** as a substrate.

Timepoint (min)	[Carbinol 6] (mM)	[Silanol 7] (mM)	[Silanol 5] (mM)
0	trace	0.00	0.00
	trace	0.00	0.00
	trace	0.00	0.00
2	trace	0.02	0.00
	trace	0.02	0.00
	trace	0.02	0.00
5	trace	0.02	0.01
	trace	0.02	0.00
	trace	0.02	0.00
10	trace	0.05	0.01
	trace	0.06	0.01
	trace	0.05	0.01
20	trace	0.11	0.02
	trace	0.06	0.01
	trace	0.04	0.01
30	trace	0.13	0.03
	trace	0.10	0.02
	trace	0.11	0.02
60	trace	0.25	0.04
	trace	0.14	0.03
	trace	0.17	0.03
120	trace	0.18	0.04
	trace	0.15	0.04
	trace	0.19	0.04
180	trace	0.11	0.03
	trace	0.10	0.03
	trace	0.10	0.04
240	trace	0.17	0.05
	trace	0.15	0.04
	trace	0.13	0.04
300	trace	0.10	0.04
	trace	0.12	0.04
	trace	0.13	0.04
1,440	trace	0.11	0.04
	trace	0.09	0.05
	trace	0.10	0.04

Table S44. Experimental data relevant to Figure S44 with siloxane **2** as substrate. *L*SilOx7 was measured at 3.7 µM.

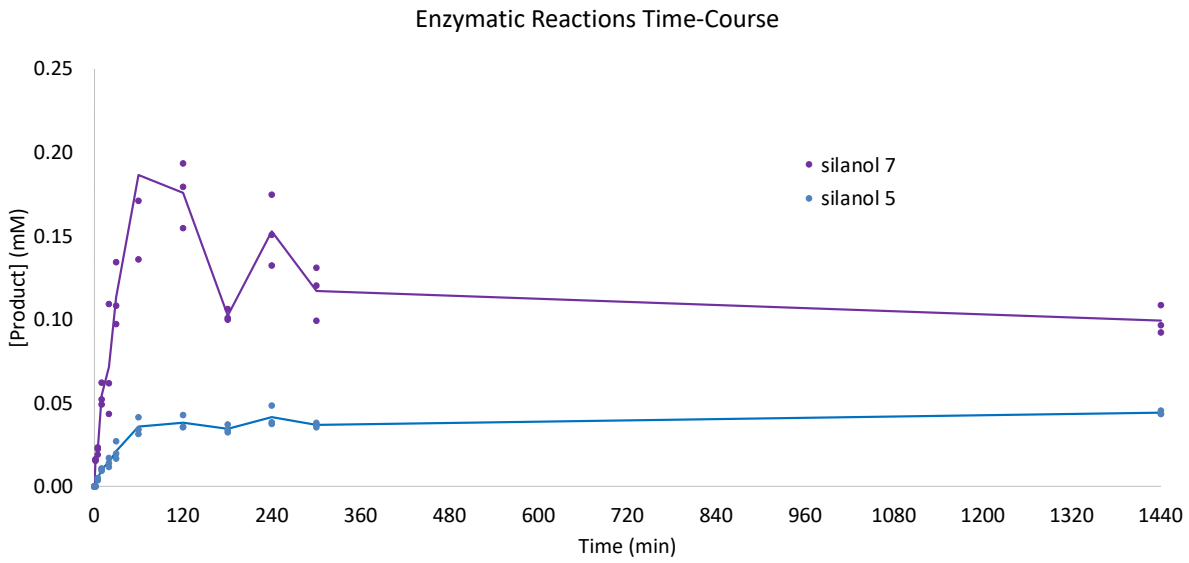

Figure S45. Enzymatic reaction time-course for siloxane **2** at 3.7 µM *L*SilOx7.

19. Enzymatic Reaction Time-Course with Siloxane 3

Enzymatic reaction time-course data were collected as described in Experimental Data Relevant to Figure 3D using siloxane **3** as a substrate.

Timepoint (min)	[carbinol **8**] (mM)	[silanol **9**] (mM)
0	trace	0.007
	trace	0.008
	trace	0.007
2	trace	0.007
	trace	0.007
	trace	0.007
5	trace	0.010
	trace	0.010
	trace	0.008
10	trace	0.010
	trace	0.010
	trace	0.009
20	trace	0.002
	trace	0.002
	trace	0.002
30	trace	0.003
	trace	0.003
	trace	0.003
60	trace	0.010
	trace	0.008
	trace	0.007
120	trace	0.015
	trace	0.016
	trace	0.015
180	trace	0.020
	trace	0.022
	trace	0.020
240	trace	0.030
	trace	0.024
	trace	0.026
300	trace	0.027
	trace	0.026
	trace	0.031
1,440	trace	0.040
	trace	0.036
	trace	0.034

Table S45. Experimental data relevant to Figure S44 with siloxane **3** as substrate. *C*SilOx3 was measured at 0.19 µM.

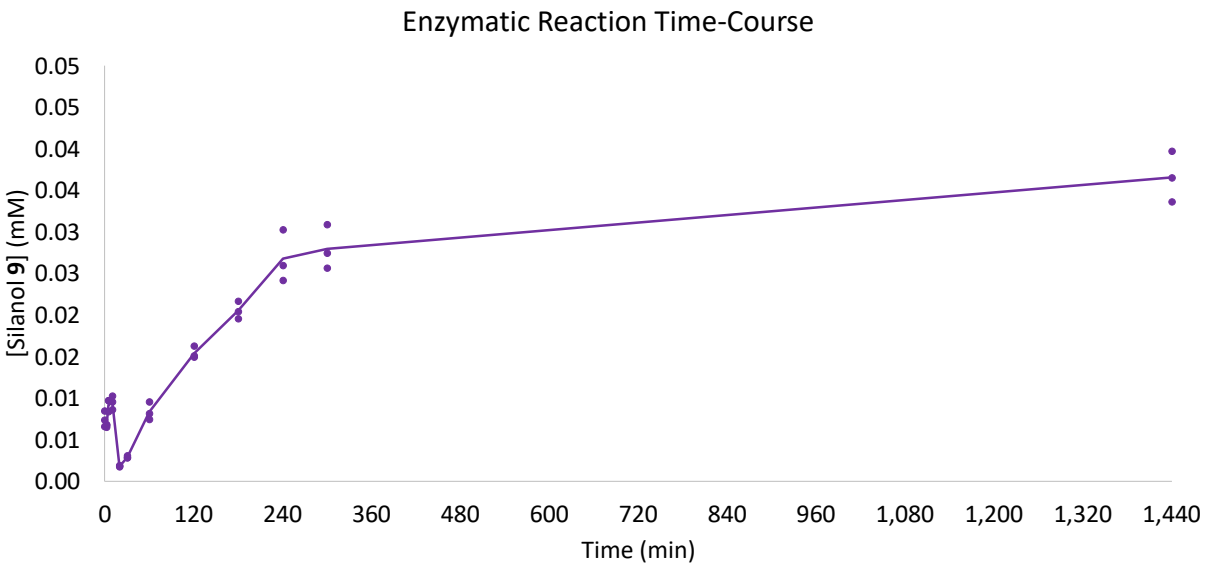

Figure S46. Enzymatic reaction time-course for siloxane **2** at 0.19 µM *C*SilOx3.

20. DNA Sequences of Engineered Enzymes

14.1 DNA Sequence of *L*SilOx1

ACAATTAAAGAAATGCCTCAGCCAAAAACGTTTGGAGAGCTTAAAAATTTACCGTT
ATTAAACACAGATAAACCGGTTCAAGCTTTGATGAAAATTGCGGATGAATTAGGAG
AAATCTTTAAATTCGAGGCGCCTGGTCGTGTAACGCGCTACTTATCAAGTCAGCGTC
TAATTAAAGAAGCATGCGATGAATCACGCTTTGATAAAAACTTAAGTCAAGCGCTTA
AATTTGCACGTGATTTTGTTGGAGACGGGTTAGGTACAAGCTGGACGCATGAAAAA
AATTGGAAAAAAGCGCATAATATCTTACTTCCAAGCTTTAGTCAGCAGGCAATGAA
AGGCTATCATGCGATGATGGTCGATATCGCCGTGCAGCTTGTTCAAAAGTGGGAGCG
TCTAAATGCAGATGAGCATATTGAAGTATCGGAAGACATGACACGTTTAACGCTTGA
TACAATTGGTCTTTGCGGCTTTAACTATCGCTTTAACAGCTTTTACCGAGATCAGCCT
CATCCATTTATTATAAGTATGGTCCGTGCACTGGATGAAGTAATGAACAAGCTGCAG
CGAGCAAATCCAGACGACCCAGCTTATGATGAAAACAAGCGCCAGTTTCAAGAAGA
TATCAAGGTGATGAACGACCTAGTAGATAAAATTATTGCAGATCGCAAAGCAAGGG
GTGAACAAAGCGATGATTTATTAACGCAGATGCTAAACGGAAAAGATCCAGAAACG
GGTGAGCCGCTTGATGACGGGAACATTCGCTATCAAATTATTACATTCTTAATTGCG
GGACACGAAACAACAAGTGGTCTTTTATCATTTGCGCTGTATTTCTTAGTGAAAAAT
CCACATGTATTACAAAAAGTAGCAGAAGAAGCAGCACGAGTTCTAGTAGATCCTGT
TCCAAGCTACAAACAAGTCAAACAGCTTAAATATGTCGGCATGGTCTTAAACGAAG
CGCTGCGCTTATGGCCAACTGCTCCTGCGTTTTCCCTATATGCAAAAGAAGATACGG
TGCTTGGAGGAGAATATCCTTTAGAAAAAGGCGACGAAGTAATGGTTCTGATTCCTC
AGCTTCACCGTGATAAAACAGTTTGGGGAGACGATGTGGAGGAGTTCCGTCCAGAG
CGTTTTGAAAATCCAAGTGCGATTCCGCAGCATGCGTTTAAACCGTTTGGAAACGGT
CAGCGTGCGTGTATCGGTCAGCAGTTCGCTCTTCATGAAGCAACGCTGGTACTTGGT
ATGATGCTAAAACACTTTGACTTTGAAGATCATACAAACTACGAGCTCGATATTAAA
GAAACTTTAACGTTAAAACCTAAAGGCTTT

14.2 DNA Sequence of *L*SilOx2

ACAATTAAAGAAATGCCTCAGCCAAAAACGTTTGGAGAGCTTAAAAATTTACCGTT
ATTAAACACAGATAAACCGGTTCAAGCTTTGATGAAAATTGCGGATGAATTAGGAG
AAATCTTTAAATTCGAGGCGCCTGGTCGTGTAACGCGCTACTTATCAAGTCAGCGTC
TAATTAAAGAAGCATGCGATGAATCACGCTTTGATAAAAACTTAAGTCAAGCGCTTA
AATTTGCACGTGATTTTGTTGGAGACGGGTTAGGTACAAGCTGGACGCATGAAAAA
AATTGGAAAAAAGCGCATAATATCTTACTTCCAAGCTTTAGTCAGCAGGCAATGAA
AGGCTATCATGCGATGATGGTCGATATCGCCGTGCAGCTTGTTCAAAAGTGGGAGCG
TCTAAATGCAGATGAGCATATTGAAGTATCGGAAGACATGACACGTTTAACGCTTGA
TACAATTGGTCTTTGCGGCTTTAACTATCGCTTTAACAGCTTTTACCGAGATCAGCCT
CATCCATTTATTATAAGTATGGTCCGTGCACTGGATGAAGTAATGAACAAGCTGCAG
CGAGCAAATCCAGACGACCCAGCTTATGATGAAAACAAGCGCCAGTTTCAAGAAGA
TATCAAGGTGATGAACGACCTAGTAGATAAAATTATTGCAGATCGCAAAGCAAGGG
GTGAACAAAGCGATGATTTATTAACGCAGATGCTAAACGGAAAAGATCCAGAAACG
GGTGAGCCGCTTGATGACGGGAACATTCGCTATCAAATTATTACATTCTTAATTGCG
GGACACGAAACAACAAGTGGTCTTTTATCATTTGCGCTGTATTTCTTAGTGAAAAAT
CCACATGTATTACAAAAAGTAGCAGAAGAAGCAGCACGAGTTCTAGTAGATCCTGT
TCCAAGCTACAAACAAGTCAAACAGCTTAAATATGTCGGCATGGTCTTAAACGAAG
CGCTGCGCTTATGGCCAATGTTTCCTGCGTTTTCCCTATATGCAAAAGAAGATACGG

TGCTTGGAGGAGAATATCCTTTAGAAAAAGGCGACGAAGTAATGGTTCTGATTCCTC
AGCTTCACCGTGATAAAACAGTTTGGGGAGACGATGTGGAGGAGTTCCGTCCAGAG
CGTTTTGAAAATCCAAGTGCGATTCCGCAGCATGCGTTTAAACCGTTTGGAAACGGT
CAGCGTGCGTGTATCGGTCAGCAGTTCGCTCTTCATGAAGCAACGCTGGTACTTGGT
ATGATGCTAAAACACTTTGACTTTGAAGATCATACAAACTACGAGCTCGATATTAAA
GAAACTTTAACGTTAAAACCTAAAGGCTTT

14.3 DNA Sequence of *L*SilOx3

ACAATTAAAGAAATGCCTCAGCCAAAAACGTTTGGAGAGCTTAAAAATTTACCGTT
ATTAAACACAGATAAACCGGTTCAAGCTTTGATGAAAATTGCGGGTGAATTAGGAG
AAATCTTTAAATTCGAGGCGCCTGGTCGTGTAACGCGCTACTTATCAAGTCAGCGTC
TAATTAAAGAAGCATGCGATGAATCACGCTTTGATAAAAACTTAAGTCAAGCGCTTA
AATTTGCACGTGATTTTGTTGGAGACGGGTTAGGTACAAGCTGGACGCATGAAAAA
AATTGGAAAAAAGCGCATAATATCTTACTTCCAAGCTTTAGTCAGCAGGCAATGAA
AGGCTATCATGCGATGATGGTCGATACCGCCGTGCAGCTTGTTCAAAAGTGGGAGC
GTCTAAATGCAGATGAGCATATTGAAGTATCGGAAGACATGACACGTTTAACGCTTG
ATACAATTGGTCTTTGCGGCTTTAACTATCGCTTTAACAGCTTTTACCGAGATCAGCC
TCATCCATTTATTATAAGTATGGTCCGTGCACTGGATGAAGTAATGAACAAGCTGCA
GCGAGCAAATCCAGACGACCCAGCTTATGATGAAAACAAGCGCCAGTTTCAAGAAG
ATATCAAGGTGATGAACGACCTAGTAGATAAAATTATTGCAGATCGCAAAGCAAGG
GGTGAACAAAGCGATGATTTATTAACGCAGATGCTAAACGGAAAAGATCCAGAAAC
GGGTGAGCCGCTCGATGACGGGAACATTCGCTATCAAATTATTACATTCTTAATTGC
GGGACACGAAACAACAAGTGGTCTTTTATCATTTGCGCTGTATTTCTTAGTGAAAAA
TCCACATGTATTACAAAAAGTAGCAGAAGAAGCAGCACGAGTTCTAGTAGATCCTG
TTCCAAGCTACAAACAAGTCAAACAGCTTAAATATGTCGGCATGGTCTTAAACGAA
GCGCTGCGCTTATGGCCAATGTTTCCTGCGTTTTCCCTATATGCAAAAGAGGATACG
GTGCTAGGAGGAGAATATCCTTTAGAAAAAGGCGACGAAGTAATGGTTCTGATTCC
TCAGCTTCACCGTGATAAAACAGTTTGGGGAGACGATGTGGAGGAGTTCCGTCCAG
AGCGTTTTGAGAATCCAAGTGCGATTCCACAGCATGCGTTTAAACCGTTTGGAAACG
GTCAGCGTGCGTGTATCGGTCAGCAGTTCGCTCTTCATGAAGCAACGCTGGTACTTG
GTATGATGCTAAAACACTTTGACTTTGAAGATCATACAAACTACGAGCTCGATATTA
AAGAAACTTTAACGTTAAAACCTAAAGGCTTT

14.4 DNA Sequence of *L*SilOx4

ACAATTAAAGAAATGCCTCAGCCAAAAACGTTTGGAGAGCTTAAAAATTTACCGTT
ATTAAACACAGATAAACCGGTTCAAGCTTTGATGAAAATTGCGGGTGAATTAGGAG
AAATCTTTAAATTCGAGGCGCCTGGTCGTGTAACGCGCTACTTATCAAGTCAGCGTC
TAATTAAAGAAGCATGCGATGAATCACGCTTTGATAAAAACTTAAGTCAAGCGCTTA
AATTTGCACGTGATTTTGTTGGAGACGGGTTAGGTACAAGCTGGACGCATGAAAAA
AATTGGAAAAAAGCGCATAATATCTTACTTCCAAGCTTTAGTCAGCAGGCAATGAA
AGGCTATCATGCGATGATGGTCGATACCGCCGTGCAGCTTGTTCAAAAGTGGGAGC
GTCTAAATGCAGATGAGCATATTGAAGTATCGGAAGACATGACACGTTTAACGCTTG
ATACAATTGGTCTTTGCGGCTTTAACTATCGCTTTAACAGCTTTTACCGAGATCAGCC
TCATCCATTTATTATAAGTATGGTCCGTGCACTGGATGAAGTAATGAACAAGCTGCA
GCGAGCAAATCCAGACGACCCAGCTTATGATGAAAACAAGCGCCAGTTTCAAGAAG
ATATCAAGGTGATGAACGACCTAGTAGATAAAATTATTGCAGATCGCAAAGCAAGGG

GTGAACAAAGCGATGATTTATTAACGCAGATGCTAAACGGAAAAGATCCAGAAAC
GGGTGAGCCGCTTGATGACGAGAACATTCGCTATCAAATTATTACATTCTTAATTGC
GGGACACGAAACAACAAGTGGTCTTTTATCATTTGCGCTGTATTTCTTAGTGAAAAA
TCCACATGTATTACAAAAAGTAGCAGAAGAAGCAGCACGAGTTCTAGTAGATCCTG
TTCCAAGCTACAAACAAGTCAAACAGCTTAAATATGTCGGCATGGTCTTAAACGAA
GCGCTGCGCTTATGGCCAATGTTTCCTGCGTTTTCCCTATATGCAAAAGAAGATACG
GTGCTTGGAGGAGAATATCCTTTAGAAAAAGGCGACGAAGTAATGGTTCTGATTCCT
CAGCTTCACCGTGATAAAACAGTTTGGGGAGACGATGTGGAGGAGTTCCGTCCAGA
GCGTTTTGAAAATCCAAGTGCGATTCCGCAGCATGCGTTTAAACCGTTTGGAAACGG
TCAGCGTGCGTGTATCGGTCAGCAGTTCGCTCTTCATGAAGCAACGCTGGTACTTGG
TATGATGCTAAAACACTTTGACTTTGAAGATCATACAAACTACGAGCTCGATATTAA
AGAAACTTTAACGTTAAAACCTAAAGGCTTT

14.5 DNA Sequence of *L*SilOx5

ACAATTAAAGAAATGCCTCAGCCAAAAACGTTTGGAGAGCTTAAAAATTTACCGTT
ATTAAACACAGATAAACCGGTTCAAGCTTTGATGAAAATTGCGGGTGAATTAGGAG
AAATCTTTAAATTCGAGGCGCCTGGTCGTGTAACGCGCTACTTATCAAGTCAGCGTC
TAATTAAAGAAGCATGCGATGAATCACGCTTTGATAAAAACTTAAGTCAAGCGCTTA
AATTTGCACGTGATTTTGTTGGAGACGGGTTAGGTACAAGCTGGACGCATGAAAAA
AATTGGAAAAAAGCGCATAATATCTTACTTCCAAGCTTTAGTCAGCAGGCAATGAA
AGGCTATCATGCGATGATGGTCGATACCGCCGTGCAGCTTGTTCAAAAGTGGGAGC
GTCTAAATGCAGATGAGCATATTGAAGTATCGGAAGACATGACACGTTTAACGCTTG
ATACAATTGGTCTTTGCGGCTTTAACTATCGCTTTAACAGCTTTTACCGAGATCAGCC
TCATCCATTTATTATAAGTATGGTCCGTGCACTGGATGAAGTAATGAACAAGCTGCA
GCGAGCAAATCCAGACGACCCAGCTTATGATGAAAACAAGCGCCAGTTTCAAGAAG
ATATCAAGGTGATGAACGACCTAGTAGATAAAATTATTGCAGATCGCAAAGCAAGG
GGTGAACAAAGCGATGATTTATTAACGCAGATGCTAAACGGAAAAGATCCAGAAAC
GGGTGAGCCGCTTGATGACGAGAACATTCGCTATCAAATTATTACATTCTTAATTGC
GGGACACGAAACAACAAGTGGTCTTTTATCATTTGCGCTGTATTTCTTAGTGAAAAA
TCCACATGTATTACAAAAAGTAGCAGAAGAAGCAGCACGAGTTCTAGTAGATCCTG
TTCCAAGCTACAAACAAGTCAAACAGCTTAAATATGTCGGCATGGTCTTAAACGAA
GCGCTGCGCTTATGGCCAATGTCTCCTGCGTTTTCCCTATATGCAAAAGAAGATACG
GTGCTTGGAGGAGAATATCCTTTAGAAAAAGGCGACGAAGTAATGGTTCTGATTCCT
CAGCTTCACCGTGATAAAACAGTTTGGGGAGACGATGTGGAGGAGTTCCGTCCAGA
GCGTTTTGAAAATCCAAGTGCGATTCCGCAGCATGCGTTTAAACCGTTTGGAAACGG
TCAGCGTGCGTGTATCGGTCAGCAGTTCGCTCTTCATGAAGCAACGCTGGTACTTGG
TATGATGCTAAAACACTTTGATTTTGAAGATCATACAAACTACGAGCTCGATATTAA
AGAAACTTTAACGTTAAAACCTAAAGGCTTT

14.6 DNA Sequence of *L*SilOx6

ACAATTAAAGAAATGCCTCAGCCAAAAACGTTTGGAGAGCTTAAAAATTTACCGTT
ATTAAACACAGATAAACCGGTTCAAGCTTTGATGAAAATTGCGGGTGAATTAGGAG
AAATCTTTAAATTCGAGGCGCCTGGTCGTGTAACGCGCTACTTATCAAGTCAGCGTC
TAATTAAAGAAGCATGCGATGAATCACGCTTTGATAAAAACTTAAGTCAAGCGCTTA
AATTTGCACGTGATTTTGTTGGAGACGGGTTAGGTACAAGCTGGACGCATGAAAAA
AATTGGAAAAAAGCGCATAATATCTTACTTCCAAGCTTTAGTCAGCAGGCAATGAA

AGGCTATCATGCGATGATGGTCGATACCGCCGTGCAGCTTGTTCAAAAGTGGGAGC
GTCTAAATGCAGATGAGCATATTGAAGTATCGGAAGACATGACACGTTTAACGCTTG
ATACAATTGGTCTTTGCGGCTTTAACTATCGCTTTAACAGCCTTTACCGAGATCAGCC
TCATCCATTTATTATAAGTATGGTCCGTGCACTGGATGAAGTAATGAACAAGCTGCA
GCGAGCAAATCCAGACGACCCAGCTTATGATGAAAACAAGCGCCAGTTTCAAGAAG
ATATCAAGGTGATGAACGACCTAGTAGATAAAATTATTGCAGATCGCAAAGCAAGG
GGTGAACAAAGCGATGATTTATTAACGCAGATGCTAAACGGAAAAGATCCAGAAAC
GGGTGAGCCGCTTGATGACGAGAACATTCGCTATCAAATTATTACATTCTTAATTGC
GGGACACGAAACAACAAGTGGTCTTTTATCATTTGCGCTGTATTTCTTAGTGAAAAA
TCCACATGTATTACAAAAAGTAGCAGAAGAAGCAGCACGAGTTCTAGTAGATCCTG
TTCCAAGCTACAAACAAGTCAAACAGCTTAAATATGTCGGCATGGTCTTAAACGAA
GCGCTGCGCTTATGGCCAATGTCTCCTGCGTTTTCCCTATATGCAAAAGAAGATACG
GTGCTTGGAGGAGAATATCCTTTAGAAAAAGGCGACGAAGTAATGGTTCTGATTCCT
CAGCTTCACCGTGATAAAACAGTTTGGGGAGACGATGTGGAGGAGTTCCGTCCAGA
GCGTTTTGAAAATCCAAGTGCGATTCCGCAGCATGCGTTTAAACCGTTTGGAAACGG
TCAGCGTGCGTGTATCGGTCAGCAGTTCGCTCTTCATGAAGCAACGCTGGTACTTGG
TATGATGCTAAAACACTTTGATTTTGAAGATCATACAAACTACGAGCTCGATATTAA
AGAAACTTTAACGTTAAAACCTAAAGGCTTT

14.7 DNA Sequence of *L*SilOx7

ACAATTAAAGAAATGCCTCAGCCAAAAACGTTTGGAGAGCTTAAAAATTTACCGTT
ATTAAACACAGATAAACCGGTTCAAGCTTTGATGAAAATTGCGGGTGAATTAGGAG
AAATCTTTAAATTCGAGGCGCCTGGTCGTGTAACGCGCGTTTTATCAAGTCAGCGTC
TAATTAAAGAAGCATGCGATGAATCACGCTTTGATAAAAACTTAAGTCAAGCGCTTA
AATTTGCACGTGATTTTGTTGGAGACGGGTTAGGTACAAGCTGGACGCATGAAAAA
AATTGGAAAAAAGCGCATAATATCTTACTTCCAAGCTTTAGTCAGCAGGCAATGAA
AGGCTATCATGCGATGATGGTCGATACCGCCGTGCAGCTTGTTCAAAAGTGGGAGC
GTCTAAATGCAGATGAGCATATTGAAGTATCGGAAGACATGACACGTTTAACGCTTG
ATACAATTGGTCTTTGCGGCTTTAACTATCGCTTTAACAGCCTTTACCGAGATCAGCC
TCATCCATTTATTATAAGTATGGTCCGTGCACTGGATGAAATGATGAACAAGCTGCA
GCGAGCAAATCCAGACGACCCAGCTTATGATGAAAACAAGCGCCAGTTTCAAGAAG
ATATCAAGGTGATGAACGACCTAGTAGATAAAATTATTGCAGATCGCAAAGCAAGG
GGTGAACAAAGCGATGATTTATTAACGCAGATGCTAAACGGAAAAGATCCAGAAAC
GGGTGAGCCGCTTGATGACGAGAACATTCGCTATCAAATTATTACATTCTTAATTGC
GGGACACGAAACAACAAGTGGTCTTTTATCATTTGCGCTGTATTTCTTAGTGAAAAA
TCCACATGTATTACAAAAAGTAGCAGAAGAAGCAGCACGAGTTCTAGTAGATCCTG
TTCCAAGCTACAAACAAGTCAAACAGCTTAAATATGTCGGCATGGTCTTAAACGAA
GCGCTGCGCTTATGGCCAATGTCTCCTGCGTTTTCCCTATATGCAAAAGAAGATACG
GTGCTTGGAGGAGAATATCCTTTAGAAAAAGGCGACGAAGTAATGGTTCTGATTCCT
CAGCTTCACCGTGATAAAACAGTTTGGGGAGACGATGTGGAGGAGTTCCGTCCAGA
GCGTTTTGAAAATCCAAGTGCGATTCCGCAGCATGCGTTTAAACCGTTTGGAAACGG
TCAGCGTGCGTGTATCGGTCAGCAGTTCGCTCTTCATGAAGCAACGCTGGTACTTGG
TATGATGCTAAAACACTTTGATTTTGAAGATCATACAAACTACGAGCTCGATATTAA
AGAAACTTTAACGTTAAAACCTAAAGGCTTT

14.8 DNA Sequence of *C*SilOx1

ACAATTAAAGAAATGCCTCAGCCAAAAACGTTTGGAGAGCTTAAAAATTTACCGTT
ATTAAACACAGATAAACCGGTTCAAGCTTTGATGAAAATTGCGGGTGAATTAGGAG
AAATCTTTAAATTCGAGGCGCCTGGTCGTGTAACGCGCTACTTATCAAGTCAGCGTC
TAATTAAAGAAGCATGCGATGAATCACGCTTTGATAAAAACTTAAGTCAAGCGCTTA
AATTTGCACGTGATTTTGTTGGAGACGGGTTAGGTACAAGCTGGACGCATGAAAAA
AGTTGGAAAAAAGCGCATAATATCTTACTTCCAAGCTTTAGTCAGCAGGCAATGAA
AGGCTATCATGCGATGATGGTCGATACCGCCGTGCAGCTTGTTCAAAAGTGGGAGC
GTCTAAATGCAGATGAGCATATTGAAGTATCGGAAGACATGACACGTTTAACGCTTG
ATACAATTGGTCTTTGCGGCTTTAACTATCGCTTTAACAGCTTTTACCGAGATCAGCC
TCATCCATTTATTATAAGTATGGTCCGTGCACTGGATGAAGTAATGAACAAGCTGCA
GCGAGCAAATCCAGACGACCCAGCTTATGATGAAAACAAGCGCCAGTTTCAAGAAG
ATATCAAGGTGATGAACGGCCTAGTAGATAAAATTATTGCAGATCGCAAAGCAAGG
GGTGAACAAAGCGATGATTTATTAACGCAGATGCTAAACGGAAAAGATCCAGAAAC
GGGTGAGCCGCTTGATGACGAGAACATTCGCTATCAAATTATTACATTCTTAATTGC
GGGACACGAAACAACAAGTGGTCTTTTATCATTTGCGCTGTATTTCTTAGTGAAAAA
TCCACACGTATTACAAAAAGTAGCAGAAGAAGCAGCACGAGTTCTAGTAGATCCTG
TTCCAAGCTACAAACAAGTCAAACAGCTTAAATATGTCGGCATGGTCTTAAACGAA
GCGCTGCGCTTATGGCCAATGTCTCCTGCGTTTTCCCTATATGCAAAAGAAGATACG
GTGCTTGGAGGAGAATATCCTTTAGAAAAAGGCGACGAAGTAATGGTTCTGATTCCT
CAGCTTCACCGTGATAAAACAGTTTGGGGAGACGATGTGGAGGAGTTCCGTCCAGA
GCGTTTTGAAAATCCAAGTGCGATTCCGCAGCATGCGTTTAAACCGTTTGGAAACGG
TCAGCGTGCGTGTATCGGTCAGCAGTTCGCTCTTCATGAAGCAACGCTGGTACTTGG
TATGATGCTAAAACACTTTGATTTTGAAGATCATACAAACTACGAGCTCGATATTAA
AGAAACTTTATCGTTAAAACCTAAAGGCTTT

14.9 DNA Sequence of *C*SilOx2

ACAATTAAAGAAATGCCTCAGCCAAAAACGTTTGGAGAGCTTAAAAATTTACCGTT
ATTAAACACAGATAAACCGGTTCAAGCTTTGATGAAAATTGCGGGTGAATTAGGAG
AAATCTTTAAATTCGAGGCGCCTGGTCGTGTAACGCGCTACTTATCAAGTCAGCGTC
TAATTAAAGAAGCATGCGATGAATCACGCTTTGATAAAAACTTAGGTCAAGCGCTTA
AATTTGCACGTGATTTTGTTGGAGACGCGTTAGGTACAAGCTGGACGCATGAAAAA
AGTTGGAAAAAAGCGCATAATATCTTACTTCCAAGCTTTAGTCAGCAGGCAATGAA
AGGCTATCATGCGATGATGGTCGATACCGCCGTGCAGCTTGTTCAAAAGTGGGAGC
GTCTAAATGCAGATGAGCATATTGAAGTATCGGAAGACATGACACGTTTAACGCTTG
ATACAATTGGTCTTTGCGGCTTTAACTATCGCTTTAACAGCTTTTACCGAGATCAGCC
TCATCCATTTATTATAAGTATGGTCCGTGCACTGGATGAAGTAATGAACAAGCTGCA
GCGAGCAAATCCAGACGACCCAGCTTATGATGAAAACAAGCGCCAGTTTCAAGAAG
ATATCAAGGTGATGAACGGCCTAGTAGATAAAATTATTGCAGATCGCAAAGCAAGG
GGTGAACAAAGCGATGATTTATTAACGCAGATGCTAAACGGAAAAGATCCAGAAAC
GGGTGAGCCGCTTGATGACGAGAACATTCGCTATCAAATTATTACATTCTTAATTGC
GGGACACGAAACAACAAGTGGTCTTTTATCATTTGCGCTGTATTTCTTAGTGAAAAA
TCCACACGTATTACAAAAAGTAGCAGAAGAAGCAGCACGAGTTCTAGTAGATCCTG
TTCCAAGCTACAAACAAGTCAAACAGCTTAAATATGTCGGCATGGTCTTAAACGAA
GCGCTGCGCTTATGGCCAATGTCTCCTGCGTTTTCCCTATATGCAAAAGAAGATACG
GTGCTTGGAGGAGAATATCCTTTAGAAAAAGGCGACGAAGTAATGGTTCTGATTCCT

CAGCTTCACCGTGATAAAACAGTTTGGGGAGACGATGTGGAGGAGTTCCGTCCAGA
GCGTTTTGAAAATCCAAGTGCGATTCCGCAGCATGCGTTTAAACCGTTTGGAAACGG
TCAGCGTGCGTGTATCGGTCAGCAGTTCGCTCTTCATGAAGCAACGCTGGTACTTGG
TATGATGCTAAAACACTTTGATTTTGAAGATCATACAAACTACGAGCTCGATATTAA
AGAAACTTTATCGTTAAAACCTAAAGGCTTT

14.10 DNA Sequence of *C*SilOx3

ATGACAATTAAAGAAATGCCTCAGCCAAAAACGTTTGGAGAGCTTAAAAATTTACC
GTTATTAAACACAGATAAACCGGTTCAAGCTTTGATGAAAATTGCGGGTGAATTAGG
AGAAATCTTTAAATTCGAGGCGCCTGGTGGTGTAACGCGCTACTTATCAAGTCAGCG
TCTAATTAAAGAAGCATGCGATGAATCACGCTTTGATAAAAACTTAGGTCAAGCGCT
TAAATTTGCACGTGATTTTGTTGGAGACGCGTTAGGTACAAGCTGGACGCATGAAAA
AAGTTGGAAAAAAGCGCATAATATCTTACTTCCAAGCTTTAGTCAGCAGGCAATGA
AAGGCTATCATGCGATGATGGTCGATACCGCCGTGCAGCTTGTTCAAAAGTGGGAG
CGTCTAAATGCAGATGAGCATATTGAAGTATCGGAAGACATGACACGTTTAACGCTT
GATACAATTGGTCTTTGCGGCTTTAACTATCGCTTTAACAGCTTTTACCGAGATCAGC
CTCATCCATTTATTATAAGTATGGTCCGTGCACTGGATGAAGTAATGAACAAGCTGC
AGCGAGCAAATCCAGACGACCCAGCTTATGATGAAAACAAGCGCCAGTTTCAAGAA
GATATCAAGGTGATGAACGGCCTAGTAGATAAAATTATTGCAGATCGCAAAGCAAG
GGGTGAACAAAGCGATGATTTATTAACGCAGATGCTAAACGGAAAAGATCCAGAAA
CGGGTGAGCCGCTTGATGACGAGAACATTCGCTATCAAATTATTACATTCTTAATTG
CGGGACACGAAACAACAAGTGGTCTTTTATCATTTGCGCTGTATTTCTTAGTGAAAA
ATCCACACGTATTACAAAAAGTAGCAGAAGAAGCAGCACGAGTTCTAGTAGATCCT
GTTCCAAGCTACAAACAAGTCAAACAGCTTAAATATGTCGGCATGGTCTTAAACGA
AGCGCTGCGCTTATGGCCAATGTCTCCTGCGTTTTCCCTATATGCAAAAGAAGATAC
GGTGCTTGGAGGAGAATATCCTTTAGAAAAAGGCGACGAAGTAATGGTTCTGATTC
CTCAGCTTCACCGTGATAAAACAGTTTGGGGAGACGATGTGGAGGAGTTCCGTCCA
GAGCGTTTTGAAAATCCAAGTGCGATTCCGCAGCATGCGTTTAAACCGTTTGGAAAC
GGTCAGCGTGCGTGTATCGGTCAGCAGTTCGCTCTTCATGAAGCAACGCTGGTACTT
GGTATGATGCTAAAACACTTTGATTTTGAAGATCATACAAACTACGAGCTCGATATT
AAAGAAACTTTATCGTTAAAACCTAAAGGCTTT

20. Materials and Methods for the Preparation of Analytical Standards

Unless otherwise stated, reactions were performed in flame-dried glassware under an argon or nitrogen atmosphere using anhydrous solvents. Anhydrous solvents were purchased in septum-sealed bottles from Sigma-Aldrich or Tokyo Chemical Industry and used as received. Reaction progress was monitored by gas chromatography/mass spectrometry (GC/MS) or thin-layer chromatography (TLC). GC/MS analysis was performed on an Agilent 8890 gas chromatograph equipped with a 5977B mass spectrometer detector and a DB-5MS capillary column (30 m length, 0.250 mm diameter, 0.25 μm film thickness using split-mode capillary injection and electron- impact ionization). TLC was performed using E. Merck silicagel 60 F254 precoated glass plates (0.25 mm) and visualized by UV fluorescence quenching, *p*-anisaldehyde, or $KMnO_4$ staining.

Silicycle SiliaFlash P60 Academic Silica gel (particle size 40–63 μm) was used for flash column chromatography. ^{1}H NMR spectra were recorded on Varian Inova 500 MHz spectrometer with an auto-x pfg broadband probe or a Bruker 400 MHz spectrometer with a Prodigy broadband cyrobprobe, broadband Smart Probe and are reported relative to residual C_6H_6 (δ 7.16 ppm). ^{13}C NMR spectra were recorded on a Bruker 400 MHz spectrometer (100 MHz) with a Prodigy broadband cyrobprobe, broadband Smart Probe and are reported relative to C_6H_6 (δ 128.1 ppm). ^{1}H–^{29}Si HMBC spectra were recorded on a Bruker 400 MHz spectrometer with a Prodigy broadband cyrobprobe, broadband Smart Probe or a Bruker 400 MHz Spectrometer with a broadband iProbe and ^{29}Si peaks are reported relative to associated ^{1}H NMR shifts. Data for ^{1}H NMR are reported as follows: chemical shift (δ ppm) (multiplicity, coupling constant (Hz), integration). Multiplicities are reported as follows: s = singlet, d = doublet, t = triplet, q = quartet, p = pentet, sept = septuplet, m = multiplet, br s = broad singlet, br d = broad doublet. Data for ^{13}C NMR are reported in terms of chemical shifts (δ ppm). All NMR data were processed using MestReNova version 14.2.0. ^{1}H NMR spectra were phase corrected and baseline corrected along f1 using a Bernstein polynomial fit. ^{13}C NMR spectra were phase corrected and baseline corrected along f1 using a Whittacker smoother fit. ^{1}H–^{29}Si HMBC NMR spectra t1 noise was reduced in MestReNova. High resolution mass spectra (HRMS) were obtained at the Caltech CCE Multiuser Mass Spectrometry lab using a JMS-T2000GC AccuTOF GC-Alpha in field ionization (FI+) mode. Reagents were purchased from commercial sources and used as received. 2,2,5,5-Tetramethyl-1,4-dioxa-2,5-disilacyclohexane was prepared as previously described (*46*).

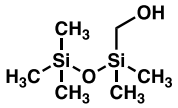

4

Carbinol **4**

Prepared as previously described (*49*) and isolated as a clear, colorless oil; ^{1}H NMR (400 MHz, C_6D_6) δ 3.15 (s, 1H), 0.15 (s, 9H), 0.13 (s, 6H); ^{13}C NMR (100 MHz, C_6D_6) δ 56.0, 2.0, –1.1; ^{29}Si (via ^{1}H–^{29}Si HMBC, 79 MHz, C_6D_6) δ 8.6, 3.1; HRMS (MM:FI+) *m*/*z* calc'd for $C_6H_{18}O_2Si_2$ $[M]^+$ 178.08453, found 178.08526.

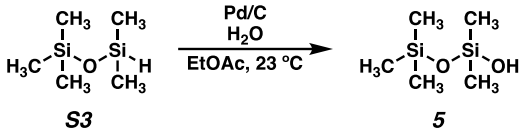

S3 *5*

Silanol **5**

To a 100-mL round-bottom flask equipped with a Teflon-coated magnetic stirring bar were added EtOAc (15 mL), deionized water (810 μL, 45.0 mmol, 3.0 equiv), and Pd/C (8.0 mg, 10 wt%, 7.5 μmol, 0.0005 equiv). The resulting black suspension was stirred rapidly at 23 ºC, and pentamethyldisiloxane (2.93 mL, 15.0 mmol, 1.0 equiv) was added dropwise over 5 min. *Caution: addition of siloxane **S3** results in rapid evolution of hydrogen gas*. After the complete addition of siloxane **S3**, the flask was equipped with a rubber septum which was pierced by an 18-G needle. After 1 h, gas evolution ceased, and consumption of siloxane **S3** was observed by GC/MS analysis. The reaction mixture was filtered directly through a 6 x 4 cm pad of neutral alumina and washed with an additional 50 mL of EtOAc. The crude product was concentrated via rotary evaporation (60 mmHg) while cooled in an ice bath. The crude, colorless oil was purified by column chromatography (0 to 25% Et_2O/Hexanes) to yield silanol **5** as a colorless oil (1.98 g, 12.1 mmol, 80% yield); ^{1}H NMR (500 MHz, C_6D_6) δ 2.91 (s, 1H), 0.17 (s, 9H), 0.14 (s, 6H); ^{13}C NMR (100 MHz, C_6D_6) δ 2.0, 0.7; ^{29}Si (via ^{1}H–^{29}Si HMBC, 79 MHz, C_6D_6) δ 7.4, –11.8; HRMS (MM:FI+) *m*/*z* calc'd for $C_5H_{17}O_2Si_2$ $[M+H]^+$ 165.07671, found 165.07618.

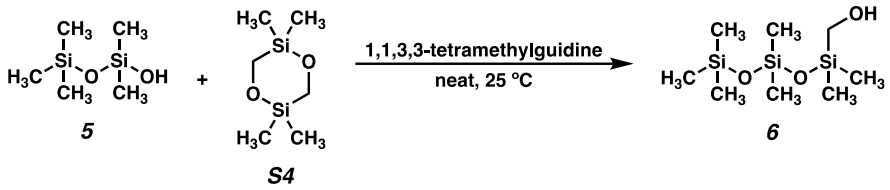

5 *S4* *6*

Carbinol **9**

To a ½-dram, septum-capped vial equipped with a Teflon-coated magnetic stirring bar were added silanol **5** (197.2 mg, 1.2 mmol, 1.2 equiv), 2,2,5,5-tetramethyl-1,4-dioxa-2,5-disilacyclohexane (**S4**) (176.4 mg, 1.00 mmol, 1.0 equiv) (*50*), and 1,1,3,3-tetramethylguanidine (12.5 μL, 0.10 mmol, 0.1 equiv). The vial was quickly evacuated and placed under an Ar atmosphere. After stirring for 1 h, full conversion of 2,2,5,5-tetramethyl-1,4-dioxa-2,5-disilacyclohexane was observed by GC/MS analysis. The reaction mixture was purified by flash column chromatography (0 to 25% Et_2O/hexanes) to yield carbinol **6** as a clear, colorless oil (223.8 mg, 0.886 mmol, 89% yield); ^{1}H NMR (500 MHz, C_6D_6) δ 3.21 (s, 2H), 0.20 (s, 6H), 0.17 (s, 9H), 0.16 (s, 6H); ^{13}C NMR (100 MHz, C_6D_6) δ 55.9, 1.9, 1.4, –1.3; ^{29}Si (via ^{1}H–^{29}Si HMBC, 79 MHz, C_6D_6) δ 7.4, 3.1, –19.6; HRMS (MM:FI+) *m*/*z* calc'd for $C_8H_{25}O_3Si_3$ $[M+H]^+$ 253.11115, found 253.11216.

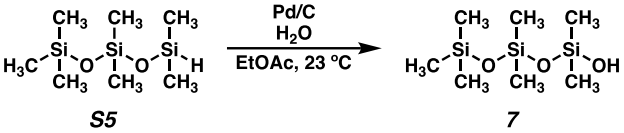

S5 *7*

Silanol **7**

To a 100-mL round-bottom flask equipped with a Teflon-coated magnetic stirring bar were added EtOAc (15 mL), deionized water (810 μL, 45.0 mmol, 3.0 equiv), and Pd/C (16.0 mg, 10 wt%, 0.015 mmol, 0.001 equiv). The resulting black suspension was stirred rapidly at 23 ºC, and 1,1,1,3,3,5,5-heptamethyltrisiloxane (4.03 mL, 15.0 mmol, 1.0 equiv) was added dropwise over 5 min. *Caution: Addition of siloxane **S5** results in rapid evolution of hydrogen gas*. After the complete addition of siloxane **S5**, the flask was equipped with a rubber septum which was pierced by an 18-G needle. After 1 h, gas evolution ceased, and consumption of siloxane **S3** was observed by GC/MS analysis. The reaction mixture was filtered directly through a 6 x 4 cm pad of neutral alumina and washed with an additional 50 mL of EtOAc to yield siloxane **7** as a clear, colorless oil (3.08 g, 12.9 mmol, 86% yield) which was used without further purification; (3.08 g, 12.9 mmol, 86% yield); ^{1}H NMR (400 MHz, C_6D_6) δ 0.17 (s, 6H), 0.17 (s, 9H), 0.13 (s, 6H); ^{13}C NMR (100 MHz, C_6D_6) δ 2.0, 1.4, 0.7; ^{29}Si (via ^{1}H–^{29}Si HMBC, 79 MHz, C_6D_6) 7.4, –12.1, –20.8; HRMS (MM:FI+) *m*/*z* calc'd for $C_7H_{23}O_3Si_3$ $[M+H]^+$ 239.09550, found 239.09478.

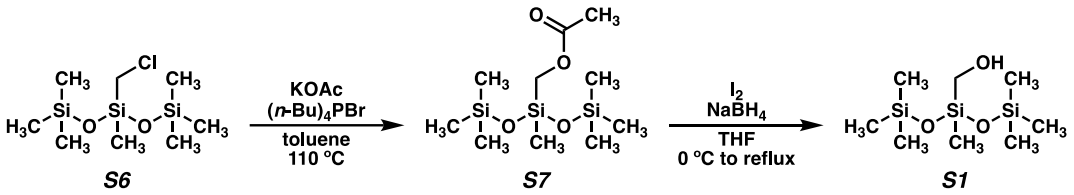

An oven-dried 25-mL round bottom flask equipped with a Teflon-coated magnetic stirring bar was charged with KOAc (3.68 g, 37.5 mmol, 1.25 equiv). The flask was then evacuated and immersed in a 130 ºC oil bath for 4 h to dry the KOAc. The flask was then cooled to 23 ºC affixed with an oven-dried Liebig condenser under Ar. The flask was then charged with (*n*-Bu)$_4$PBr (203.6 mg, 0.60 mmol, 0.02 equiv), toluene (6.0 mL), and 3-(chloromethyl)-1,1,1,3,5,5,5- heptamethyltrisiloxane (**S6**) (8.78 mL, 30.0 mmol, 1.0 equiv). The resulting white suspension was stirred rapidly and immersed in a 110 ºC oil bath for 24 h, after which time GC/MS analysis showed full conversion of 3-(chloromethyl)-1,1,1,3,5,5,5-heptamethyltrisiloxane (**S6**). The reaction mixture was then cooled to 23 ºC and transferred to a separatory funnel with deionized water (40 mL) and EtOAc (30 mL). The layers were separated, and the aqueous phase was extracted twice with EtOAc (2 x 15 mL). The combined organics were dried over Na_2SO_4, filtered, and concentrated to a clear, colorless oil. The crude product was purified by flash column chromatography (0 to 30% Et_2O/hexanes) to yield acetate **S7** as a clear, colorless oil with minor impurities (2.02 g, 6.86 mmol, 23% yield); ^{1}H NMR (400 MHz, C_6D_6) δ 3.80 (s, 2H), 1.73 (s, 3H), 0.19 (s, 3H), 0.14 (s, 18H); ^{13}C NMR (100 MHz, C_6D_6) δ 168.9, 55.0, 18.8, 0.2, –2.7; ^{29}Si (via ^{1}H–^{29}Si HMBC, 79 MHz, C_6D_6) 9.0, –30.1; HRMS (MM:FI+) *m*/*z* calc'd for $C_{10}H_{26}O_4Si_3$ $[M]^+$ 294.11389, found 294.11534.

To a flame-dried 25-mL, two-necked round-bottom flask equipped with a Teflon-coated magnetic stirring bar, a central Liebig condenser, and a rubber septum were added acetate **S7** (589.1 mg, 2.00 mmol, 1.0 equiv) and THF (6.7 mL). The resulting clear, colorless solution was cooled in an ice bath for 5 min, after which time $NaBH_4$ (181.6 mg, 4.80 mmol, 2.4 equiv) was added through the side neck in a single portion to afford a white suspension. To a separate, flame-dried 5-mL flask were added I_2 (507.6 mg, 2.00 mmol, 1.0 equiv) and THF (3.3 mL). The I_2 solution was gently swirled to mix, and the solution was added to the rapidly

stirring white suspension via the side neck septum over 1 h using a syringe pump. As the I_2 solution is added, the reaction mixture becomes dark brown and gradually fades to white. After complete addition of the I_2 solution, the reaction mixture is colorless and a white precipitate forms. The reaction flask was removed from the cooling bath, and the side neck septum was replaced with an oven-dried glass stopper. The reaction mixture was then heated to reflux by immersion in a 72 ºC oil bath. After 2 h, acetate **S7** was consumed by GC/MS analysis. The reaction was cooled in an ice bath for 10 min, after which time MeOH (2 mL) was added dropwise over 20 min. *Caution: Addition of MeOH is highly exothermic and results in the rapid evolution of hydrogen gas and should be performed cautiously.* After gas evolution had ceased, the reaction mixture was transferred to a separatory funnel with EtOAc (15 mL) and deionized water (15 mL). The layers were separated, and the aqueous phase was extracted twice with EtOAc (2 x 5 mL). The combined organics were washed with brine (10 mL), dried over Na_2SO_4, filtered, and concentrated to a clear, colorless oil. The crude product was purified by flash column chromatography (0 to 12% EtOAc/hexanes) to yield carbinol **S1** as a clear, colorless oil (302.4 mg, 1.20 mmol, 60% yield); ^{1}H NMR (400 MHz, C_6D_6) δ 3.13 (s, 2H), 0.21 (s, 3H), 0.17 (s, 18H); ^{13}C NMR (100 MHz, C_6D_6) δ 55.1, 1.9, –1.6; ^{29}Si (via ^{1}H–^{29}Si HMBC, 79 MHz, C_6D_6) 8.6, –27.8; HRMS (MM:FI+) *m/z* calc'd for $C_8H_{24}O_3Si_3$ $[M]^+$ 252.10332, found 252.10486.

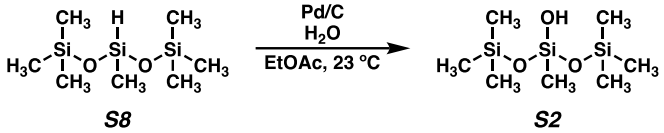

S8 ***S2***

Silanol **S2**

To a 100-mL round-bottom flask equipped with a Teflon-coated magnetic stirring bar were added EtOAc (15 mL), deionized water (810 μL, 45.0 mmol, 3.0 equiv), and Pd/C (16.0 mg, 10 wt%, 0.015 mmol, 0.001 equiv). The resulting black suspension was stirred rapidly at 23 ºC, and 1,1,1,3,3,5,5-heptamethyltrisiloxane (4.03 mL, 15.0 mmol, 1.0 equiv) was added dropwise over 5 min. *Caution: Addition of siloxane **S8** results in rapid evolution of hydrogen gas*. After the complete addition of siloxane **S8**, the flask was equipped with a rubber septum which was pierced by an 18-G needle. After 1 h, gas evolution ceased, and consumption of siloxane **S8** was observed by GC/MS analysis. The reaction mixture was filtered directly through a 6 x 4 cm pad of neutral alumina and washed with an additional 50 mL of EtOAc to yield siloxane **S2** as a clear, colorless oil (3.08 g, 12.9 mmol, 86% yield) which was used without further purification; (3.21 g, 13.5 mmol, 90% yield); ^{1}H NMR (400 MHz, C_6D_6) δ 0.18 (s, 18H), 0.13 (s, 3H); ^{13}C NMR (100 MHz, C_6D_6) δ 1.8, –2.5; ^{29}Si (via ^{1}H–^{29}Si HMBC, 79 MHz, C_6D_6) 8.2, –54.8; HRMS (MM:FI+) *m*/*z* calc'd for $C_7H_{23}O_3Si_3$ $[M+H]^+$ 239.09550, found 239.09455.

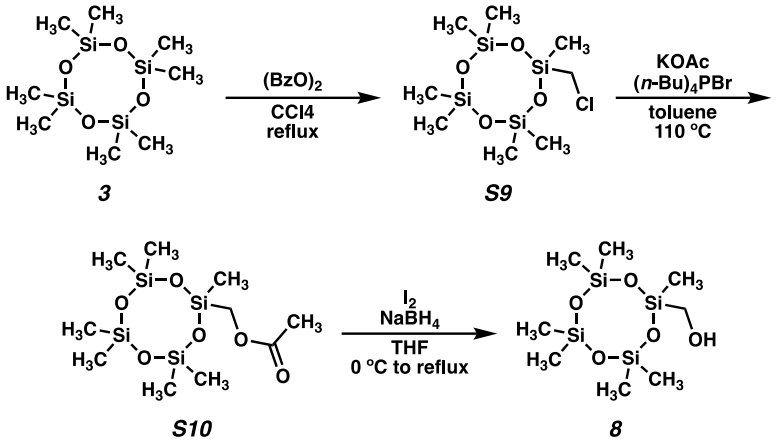

3 *S9* *S10* *8*

Carbinol **8**

To a flame-dried, 250-mL round bottom flask equipped with a Teflon-coated magnetic stirring bar and a Liebig condenser were added octamethylcyclotetrasiloxane (**3**) (24.8 mL, 80.0 mmol, 2.0 equiv), CCl_4 (28 mL), and SO_2Cl_2 (3.2 mL, 40 mmol, 1.0 equiv). The resulting clear, colorless solution was stirred rapidly, and $(BzO)_2$ (484.5 mg, 2.00 mmol, 0.05 equiv) was added in a single portion. The clear, colorless reaction was then heated to reflux by immersion in an 80 ºC oil bath. After 6 h, the clear, colorless reaction mixture was cooled to 23 ºC. The reaction mixture was concentrated via rotary evaporation, and the resulting clear, colorless oil was transferred to a separatory funnel with 100 mL EtOAc and washed twice with saturated aqueous $NaHCO_3$ (2 x 20 mL) and once with brine (20 mL). The organic layer was then dried over Na_2SO_4, filtered, and concentrated to a clear, colorless oil. The resulting crude mixture containing octamethylcyclotetrasiloxane, chloride **S9** was used directly without purification.

An oven-dried 100-mL round bottom flask equipped with a Teflon-coated magnetic stirring bar was charged with KOAc (9.81 g, 100 mmol, 1.25 equiv). The flask was then evacuated and immersed in a 130 ºC oil bath for 4 h to dry the KOAc. The flask was then cooled to 23 ºC affixed with an oven-dried Liebig condenser under Ar. The flask was then charged with $(n\text{-}Bu)_4PBr$ (542.9 mg, 1.60 mmol, 0.02 equiv), toluene (16.0 mL), and the crude mixture containing chloride **S9** as prepared above. The resulting white suspension was stirred rapidly and immersed in a 110 ºC oil bath for 24 h, after which time GC/MS analysis showed full conversion of chloride **S9**. The reaction mixture was then cooled to 23 ºC and transferred to a separatory funnel with deionized water (50 mL) and EtOAc (50 mL). The layers were separated, and the aqueous phase was

extracted twice with EtOAc (2 x 30 mL). The combined organics were dried over Na_2SO_4, filtered, and concentrated to a clear, colorless oil. Octamethylcyclotetrasiloxane was removed from the crude product under high vacuum (600 mTorr), and the remaining crude product was purified by flash column chromatography (0 to 30% Et_2O/hexanes) to yield acetate **S10** as a clear, colorless oil with minor impurities (1.54 g, 4.34 mmol, 11% yield); ^{1}H NMR (400 MHz, C_6D_6) δ 3.87 (s, 2H), 1.73 (s, 3H), 0.27 (s, 3H), 0.19 (s, 9H), 0.18 (s, 9H); ^{13}C NMR (100 MHz, C_6D_6) δ 170.6, 56.3, 20.4, 0.9, 0.9, 0.8, –1.5; ^{29}Si (via ^{1}H–^{29}Si HMBC, 79 MHz, C_6D_6) –18.0, –28.6; HRMS (MM:FI+) *m*/*z* calc'd for C10H26O6Si4 $[M]^+$ 354.08064, found 354.08203.

To a flame-dried, 50-mL two-necked round bottom flask equipped with a Teflon-coated magnetic stirring bar, a central Liebig condenser, and a rubber septum were added acetate **22** (886.6 mg, 2.50 mmol, 1.0 equiv) and THF (8.3 mL). The resulting clear, colorless solution was cooled in an ice bath for 10 min, and $NaBH_4$ (227.0 mg, 6.00 mmol, 2.4 equiv) was added in a single portion. To a separate, flame-dried 10-mL round bottom flask were added I_2 (634.5 mg, 2.50 mmol, 1.0 equiv) and THF (4.2 mL). The I_2 solution was mixed by swirling before being transferred to the rapidly stirring $NaBH_4$ suspension over 1 h via syringe pump addition. After complete addition, the flask was removed from the cooling bath, and the reaction was warmed to reflux (75 ºC oil bath temperature). After 2 h, GC/MS analysis indicated consumption of acetate **22**. The reaction was cooled to 23 ºC and immersed in an ice bath. The reaction was then carefully quenched with the dropwise addition of methanol (2 mL) over 15 min. The quenched reaction mixture was then transferred to a separatory funnel containing deionized water (15 mL) with EtOAc (15 mL). The layers were partitioned, and the aqueous layer was extracted twice with EtOAc (5 mL). The combined organics were dried over Na_2SO_4, filtered through a cotton plug, and concentrated to yield a clear, colorless oil. The crude product was purified by flash column chromatography (2 to 12% EtOAc/hexanes gradient) to yield carbinol **8** as a white, semi-crystalline solid (239.6 mg, 0.949 mmol, 38 % yield); ^{1}H NMR (400 MHz, C_6D_6) δ 3.22 (s, 2H), 0.26 (s, 3H), 0.22 (s, 6H), 0.21 (s, 3H), 0.19 (s, 9H); ^{13}C NMR (100 MHz, C_6D_6) δ 54.7, 1.0, 0.9, 0.9, –2.1; ^{29}Si (via ^{1}H–^{29}Si HMBC, 79 MHz, C_6D_6) –18.0, –26.2; HRMS (MM:FI+) *m*/*z* calc'd for $C_8H_{25}O_5Si_4$ $[M+H]^+$ 313.07791, found 313.07854

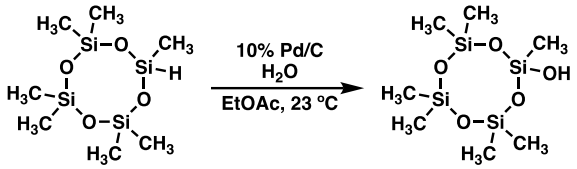

S11 *9*

Silanol **9**

To a 40-mL scintillation vial equipped with a Teflon-coated stirring bar were added Pd/C (2.7 mg, 2.5 μmol, 0.05 mol%), EtOAc (5.0 mL), and deionized water (270 μL, 15.0 mmol, 3.0 equiv). The vial was then capped with a septum cap which was vented to the atmosphere with an 18- G needle. The black suspension was stirred rapidly at 23 ºC, and silane **S11** (1.47 mL, 5.00 mmol, 1.0 equiv) was added dropwise over 15 min. *Caution: addition of silane **S11** results in rapid evolution of hydrogen gas*. The black suspension was vigorously stirred at 23 ºC for 1 h, after which time gas evolution had ceased and GC/MS analysis indicated consumption of the silane. The reaction mixture was filtered through a 6 x 4 cm pad of neutral alumina using EtOAc (50 mL). The filtrate was concentrated to a clear, colorless oil which was purified by flash column chromatography (hexanes to 30% EtOAc/hexanes) to yield silanol **14** as a clear, colorless oil (868.6 mg, 2.91 mmol, 58% yield); ^{1}H NMR (500 MHz, C_6D_6) δ 1.93 (s, 1H), 0.25 (s, 6H), 0.23 (s, 3H), 0.21 (s, 3H), 0.20 (d, J = 1.1 Hz, 9H); ^{13}C NMR (100 MHz, C_6D_6) δ 1.0, 0.9, 0.8, –3.0; ^{29}Si (via ^{1}H–^{29}Si HMBC, 79 MHz, C_6D_6) –18.8, –54.8; HMRS (MM:FI+) *m*/*z* calc'd for $C_7H_{23}O_5Si_4$ $[M+H]^+$ 299.06225, found 299.06337.

21. NMR Spectra

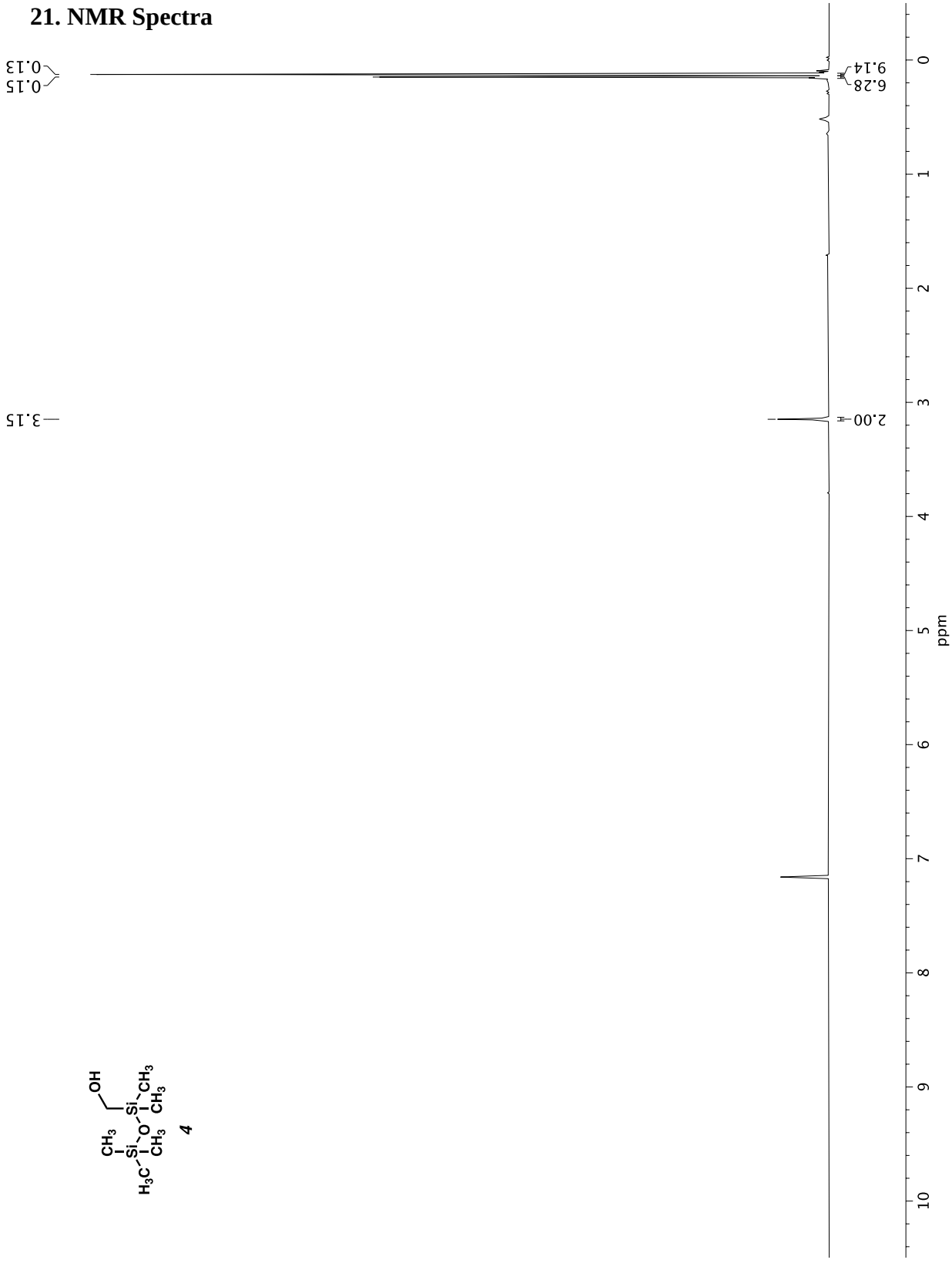

4

*^{1}H NMR (400 MHz, C_6D_6) of compound **4**.*

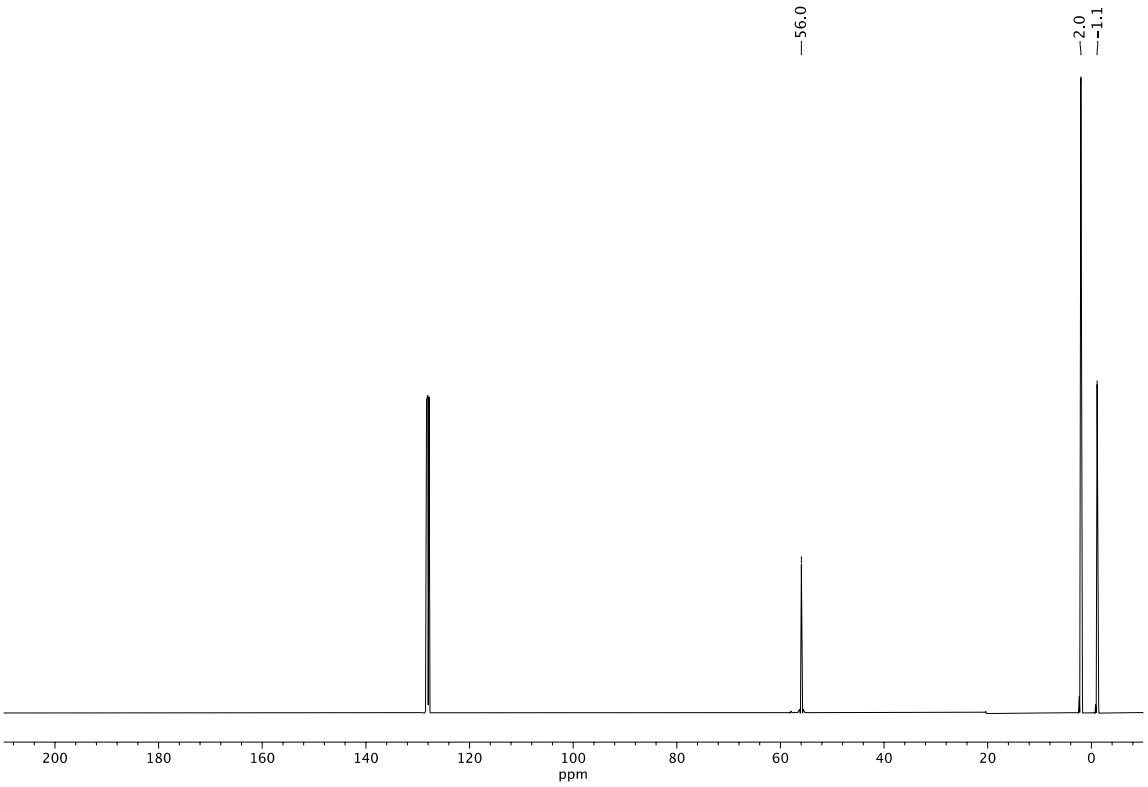

*^{13}C NMR (100 MHz, C_6D_6) of compound **4**.*

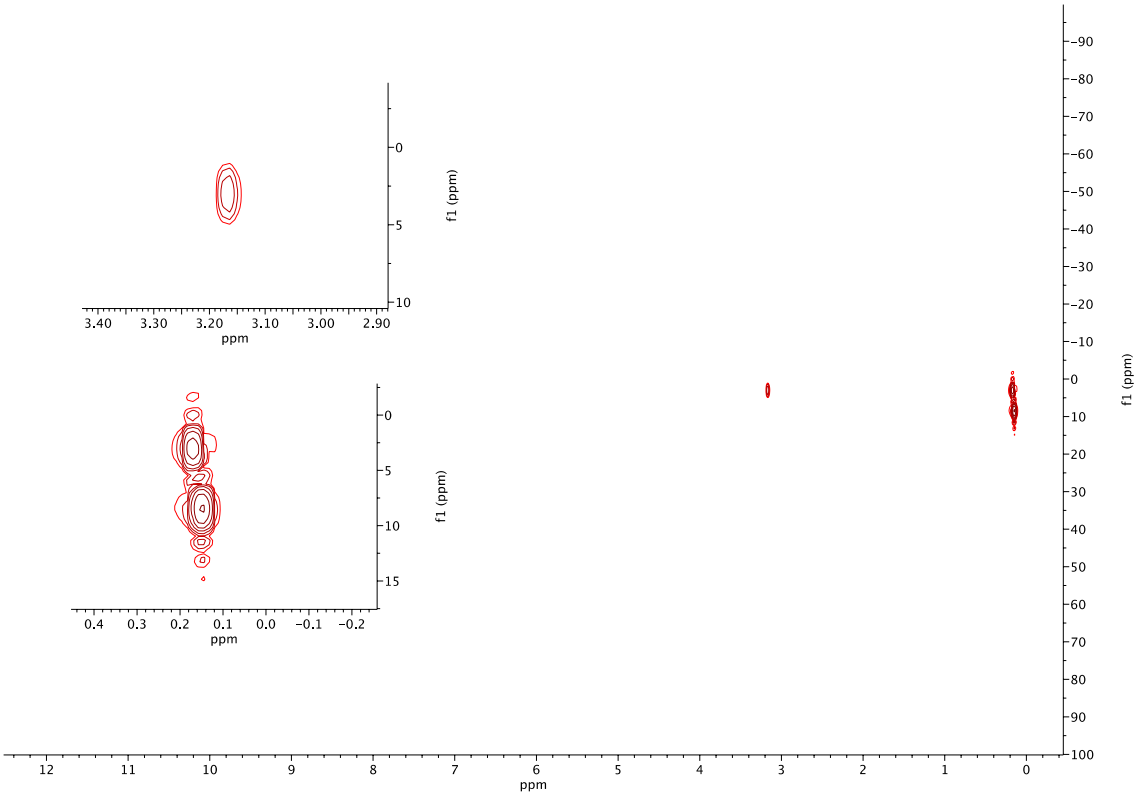

*^{1}H–^{29}Si HMBC (400 MHz, C_6D_6) of compound **4**.*

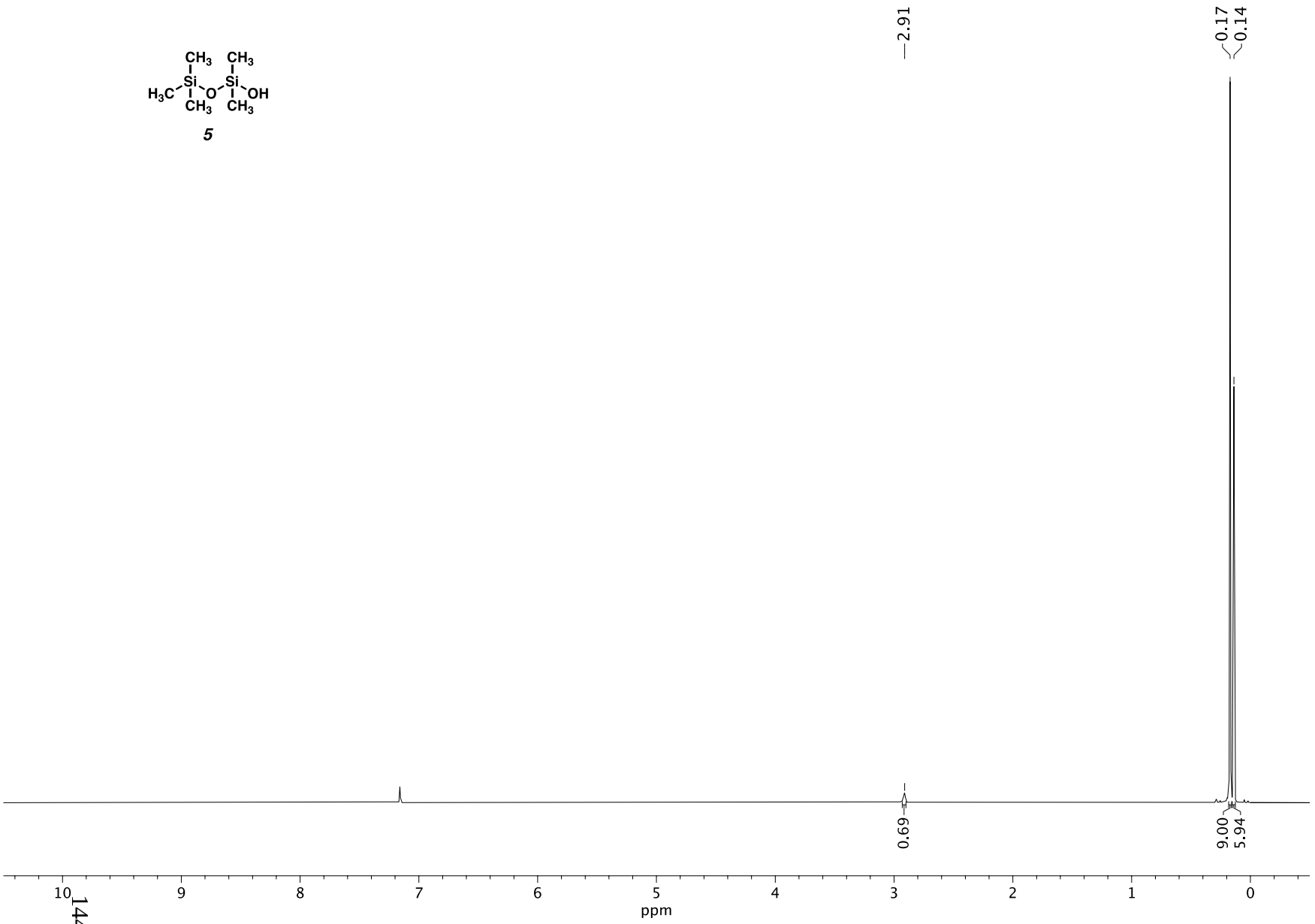

*[1]H NMR (400 MHz, C_6D_6) of compound **5**.*

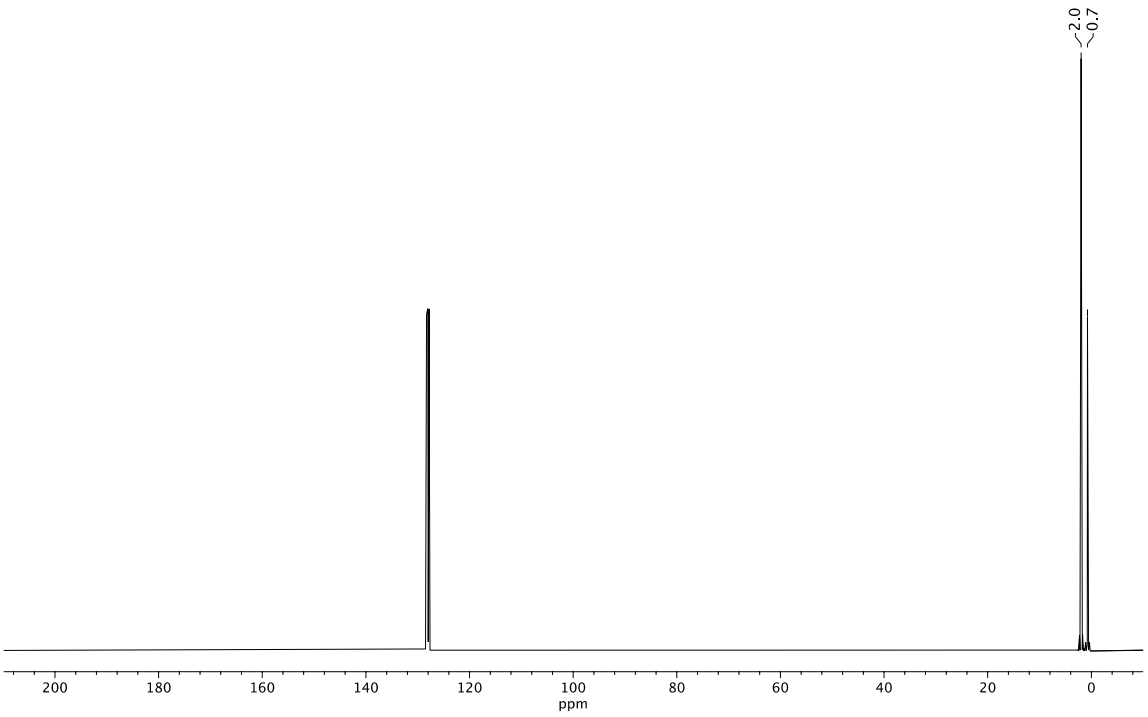

*^{13}C NMR (100 MHz, C_6D_6) of compound **5**.*

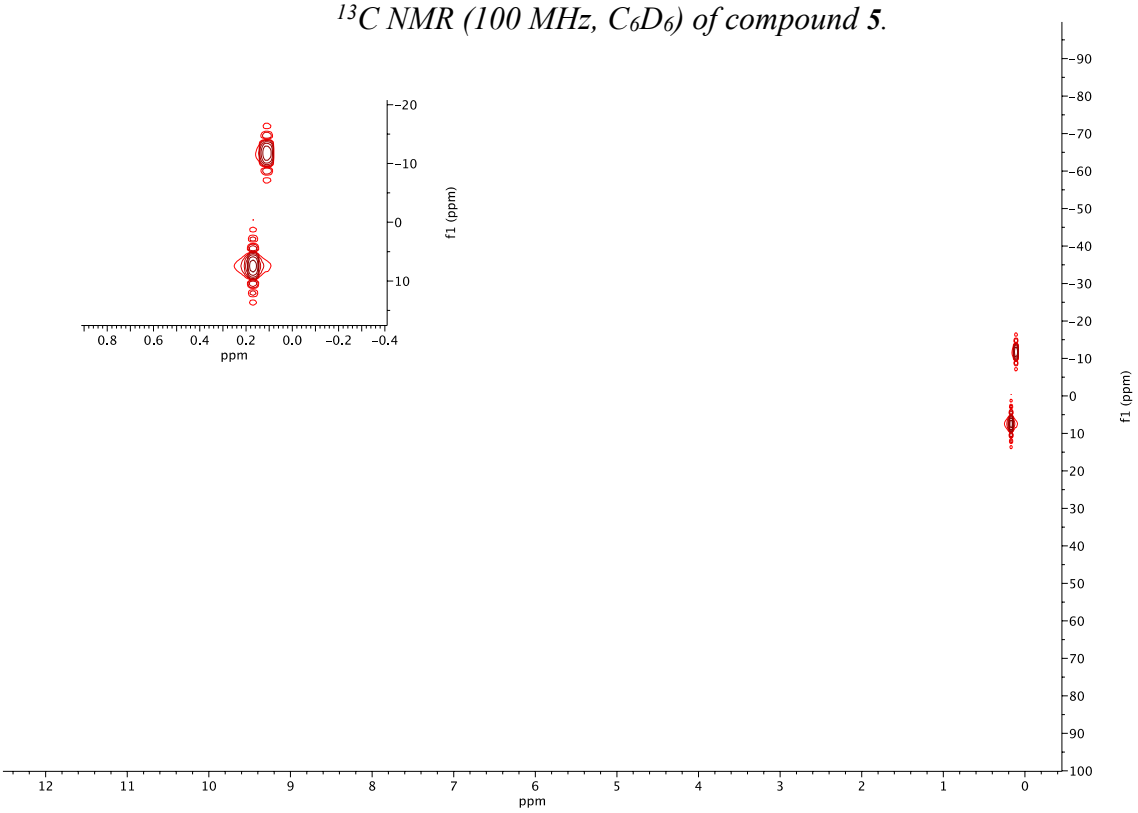

*^{1}H–^{29}Si HMBC (400 MHz, C_6D_6) of compound **5**.*

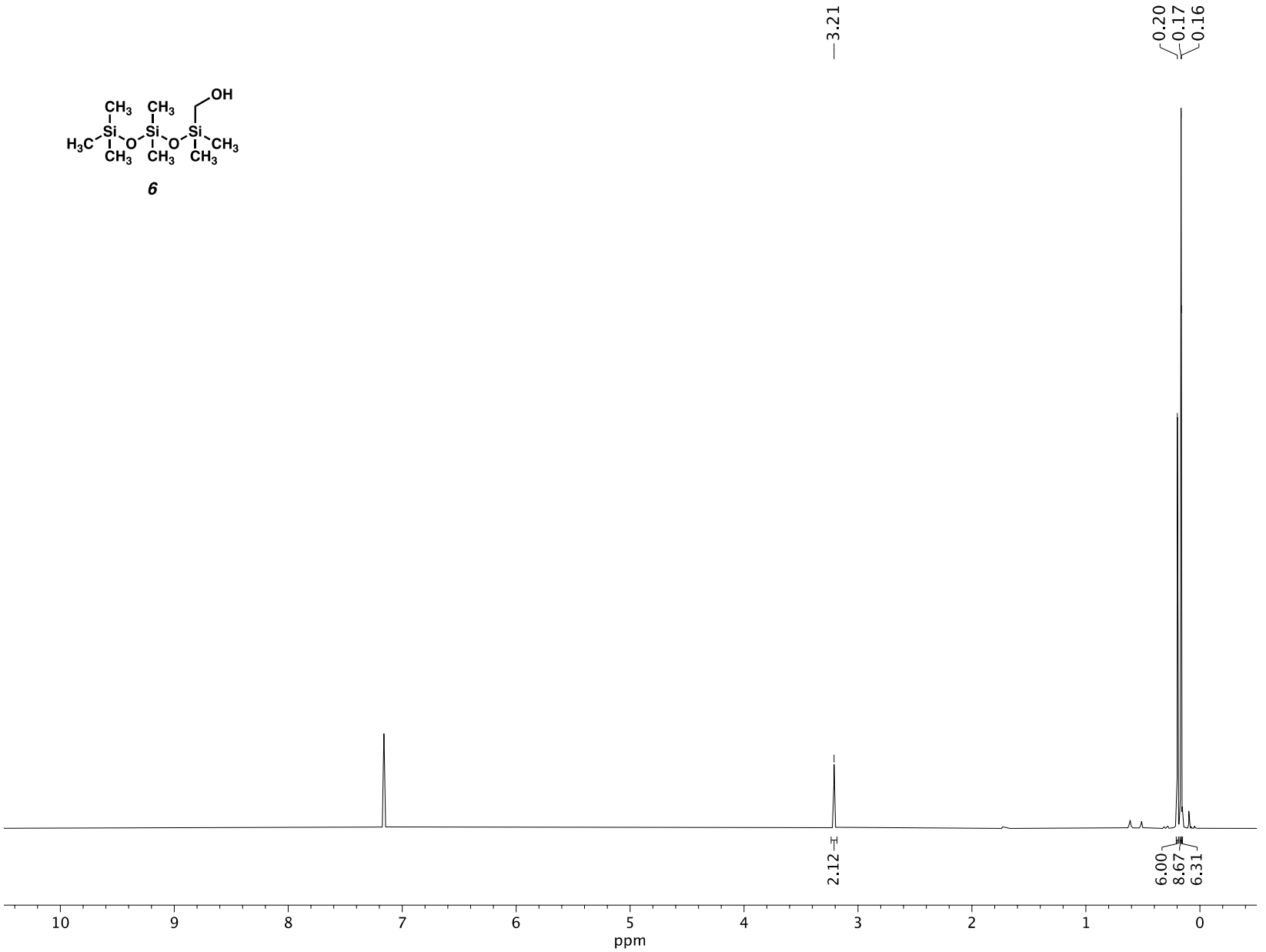

6

*^{1}H NMR (500 MHz, C_6D_6) of compound **6**.*

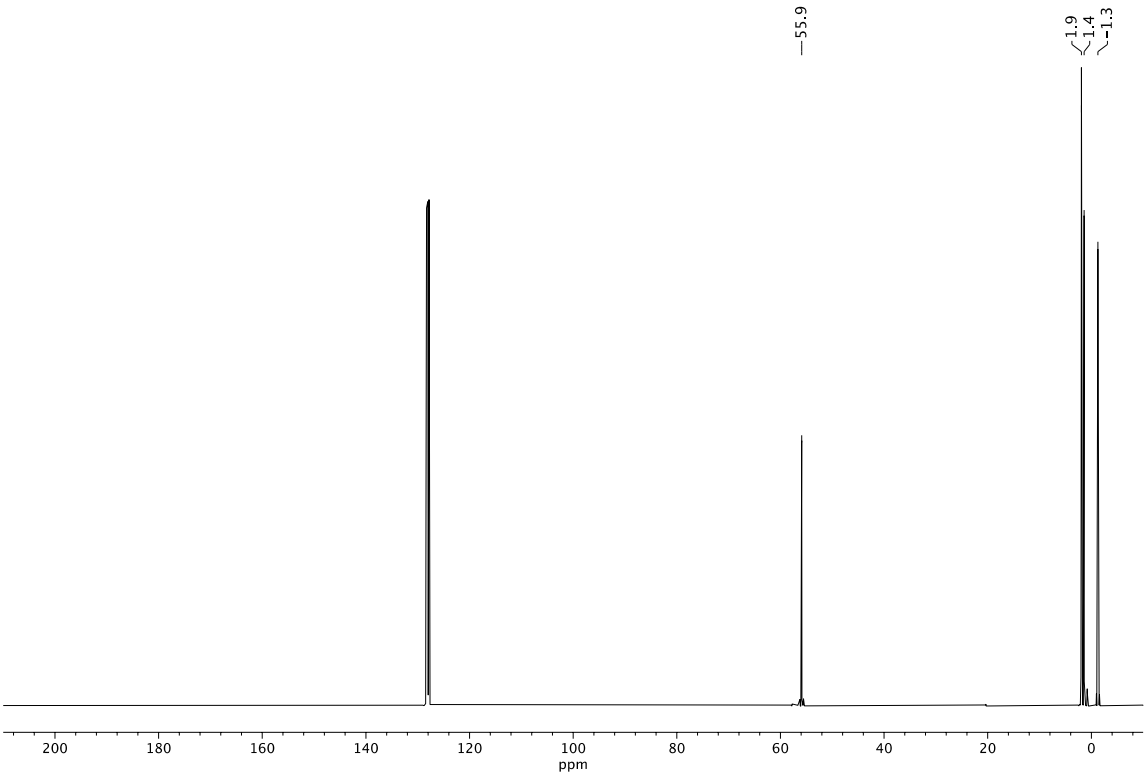

*^{13}C NMR (100 MHz, C_6D_6) of compound **6**.*

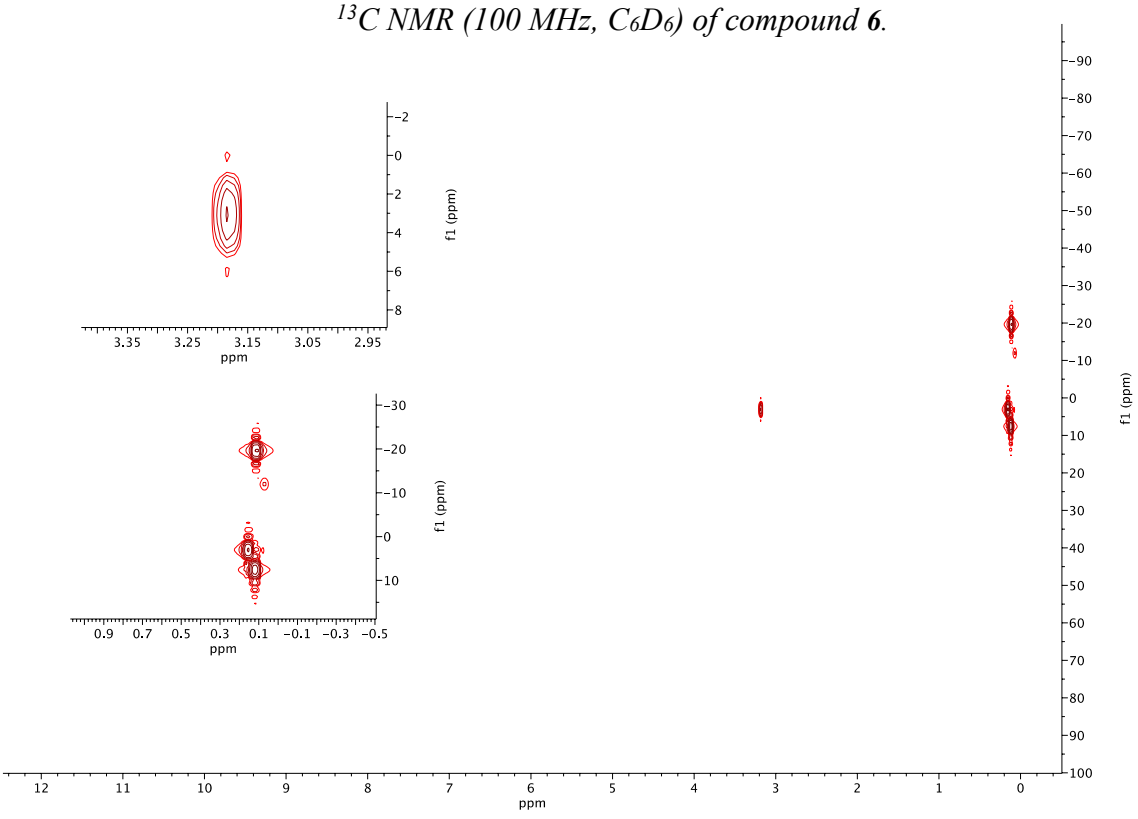

*^{1}H–^{29}Si HMBC (400 MHz, C_6D_6) of compound **6**.*

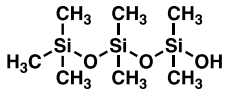

7

[1]H NMR (400 MHz, C_6D_6) of compound 7.

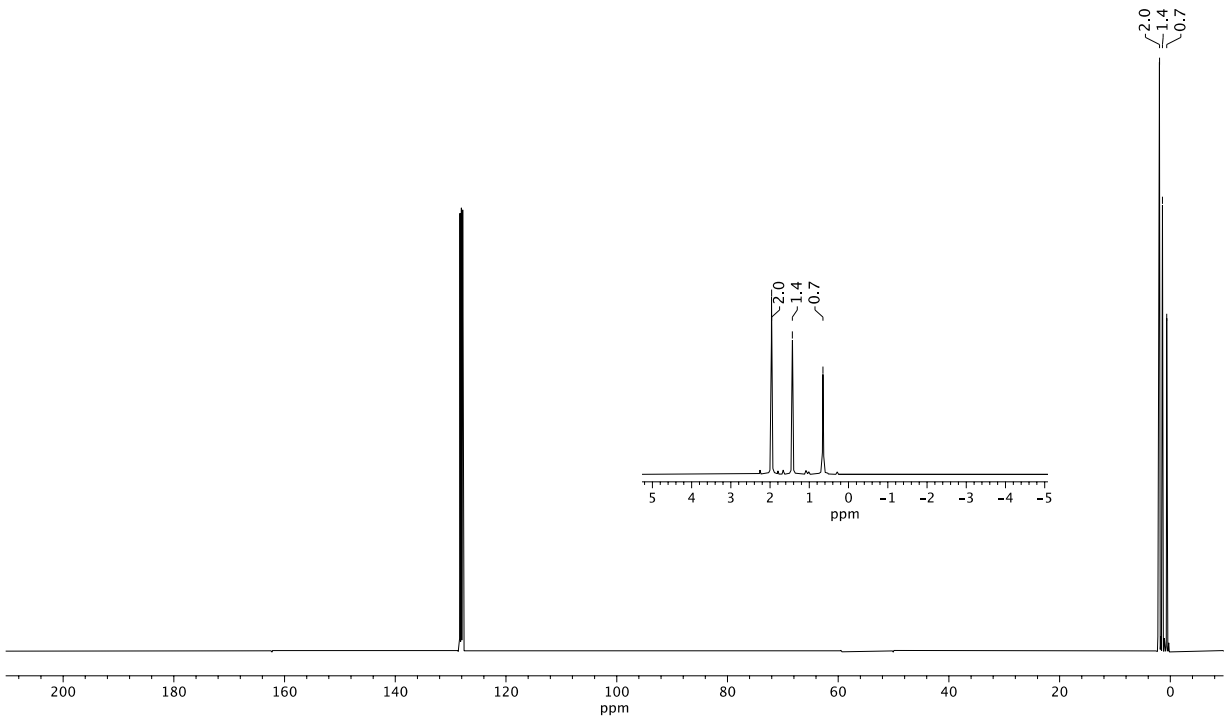

^{13}C NMR (100 MHz, C_6D_6) of compound 7.

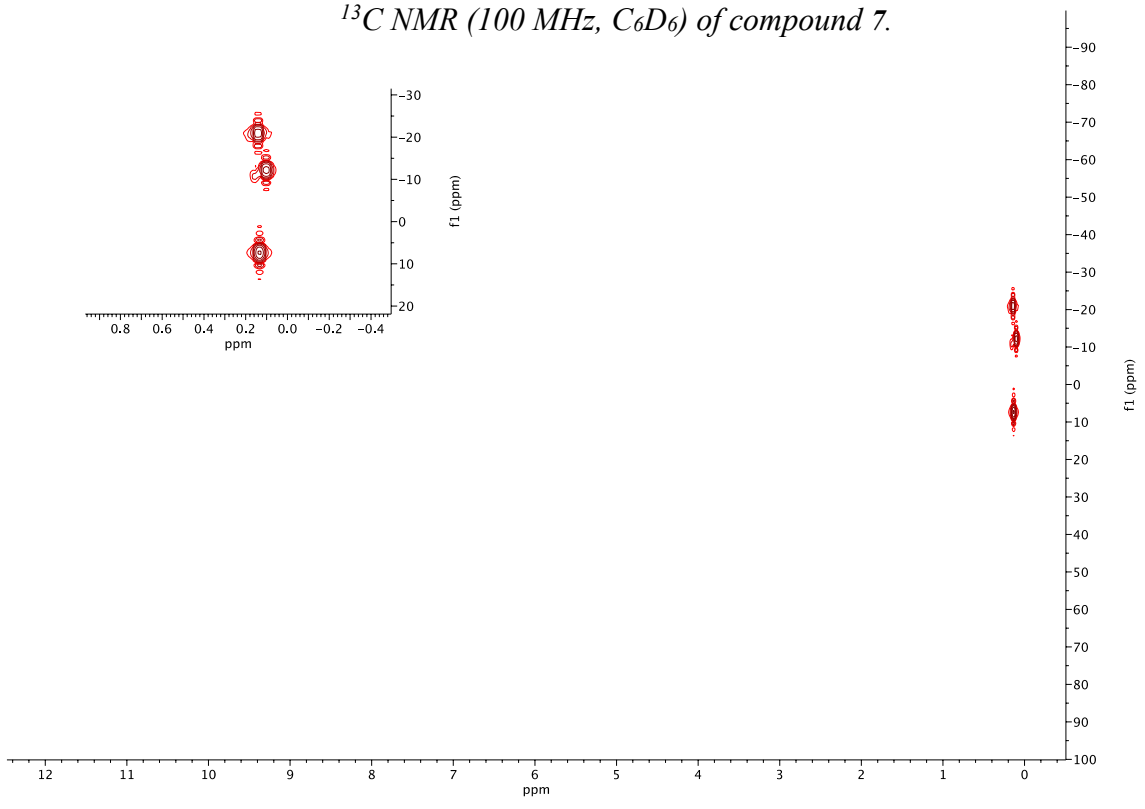

^{1}H–^{29}Si HMBC (400 MHz, C_6D_6) of compound 7.

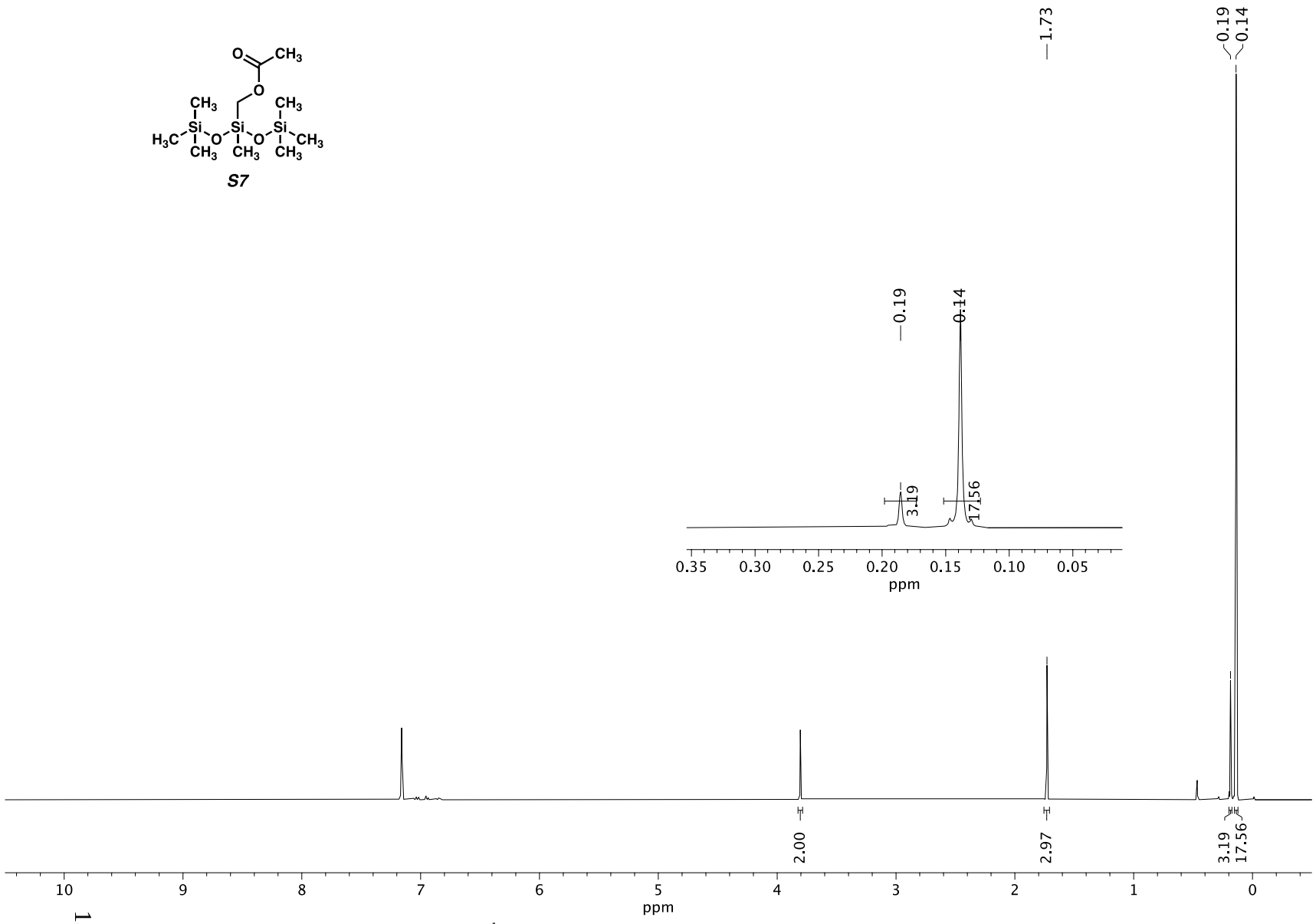

*^{1}H NMR (400 MHz, C_6D_6) of compound **S7**.*

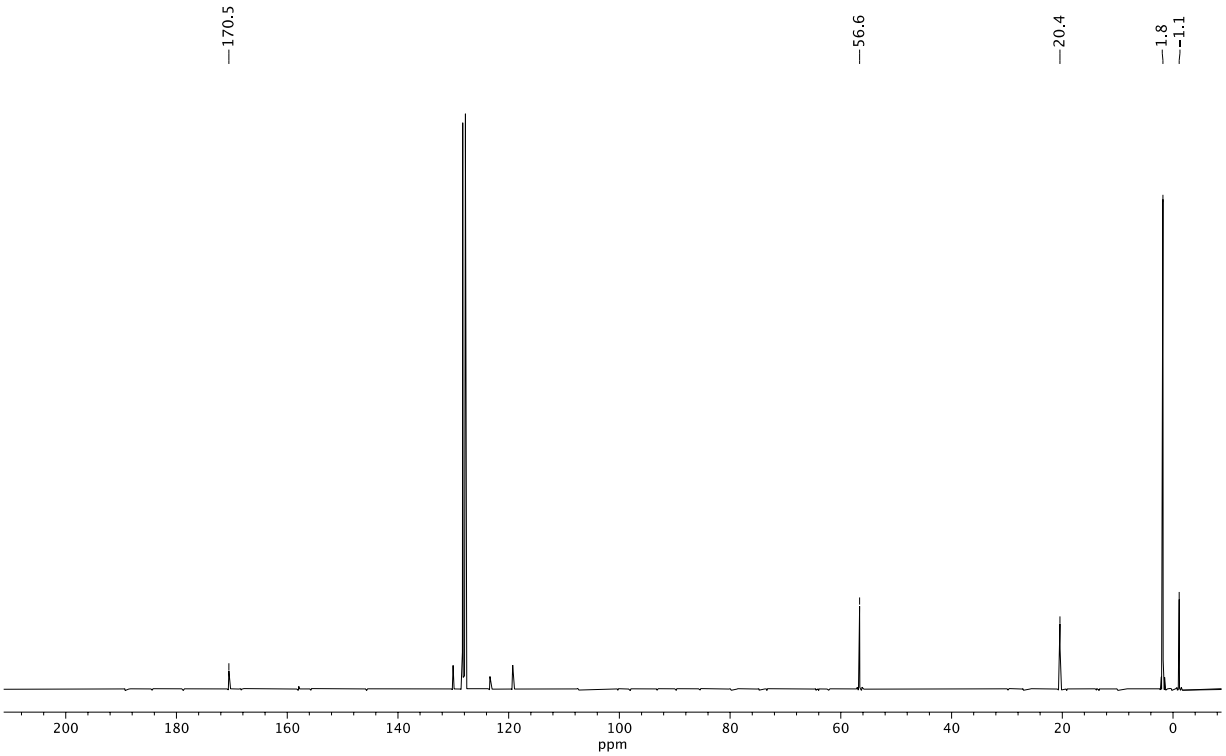

*^{13}C NMR (100 MHz, C_6D_6) of compound **S7**.*

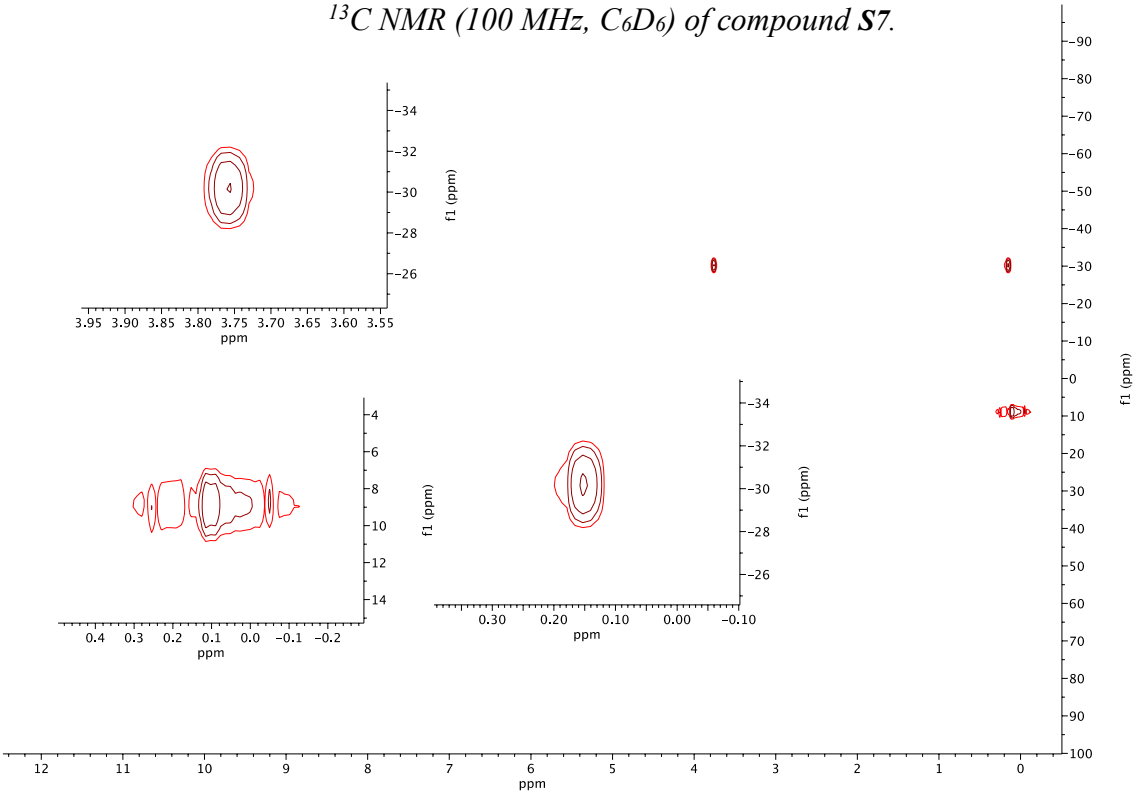

^{1}H–^{29}Si HMBC (400 MHz, C_6D_6) of compound S7.

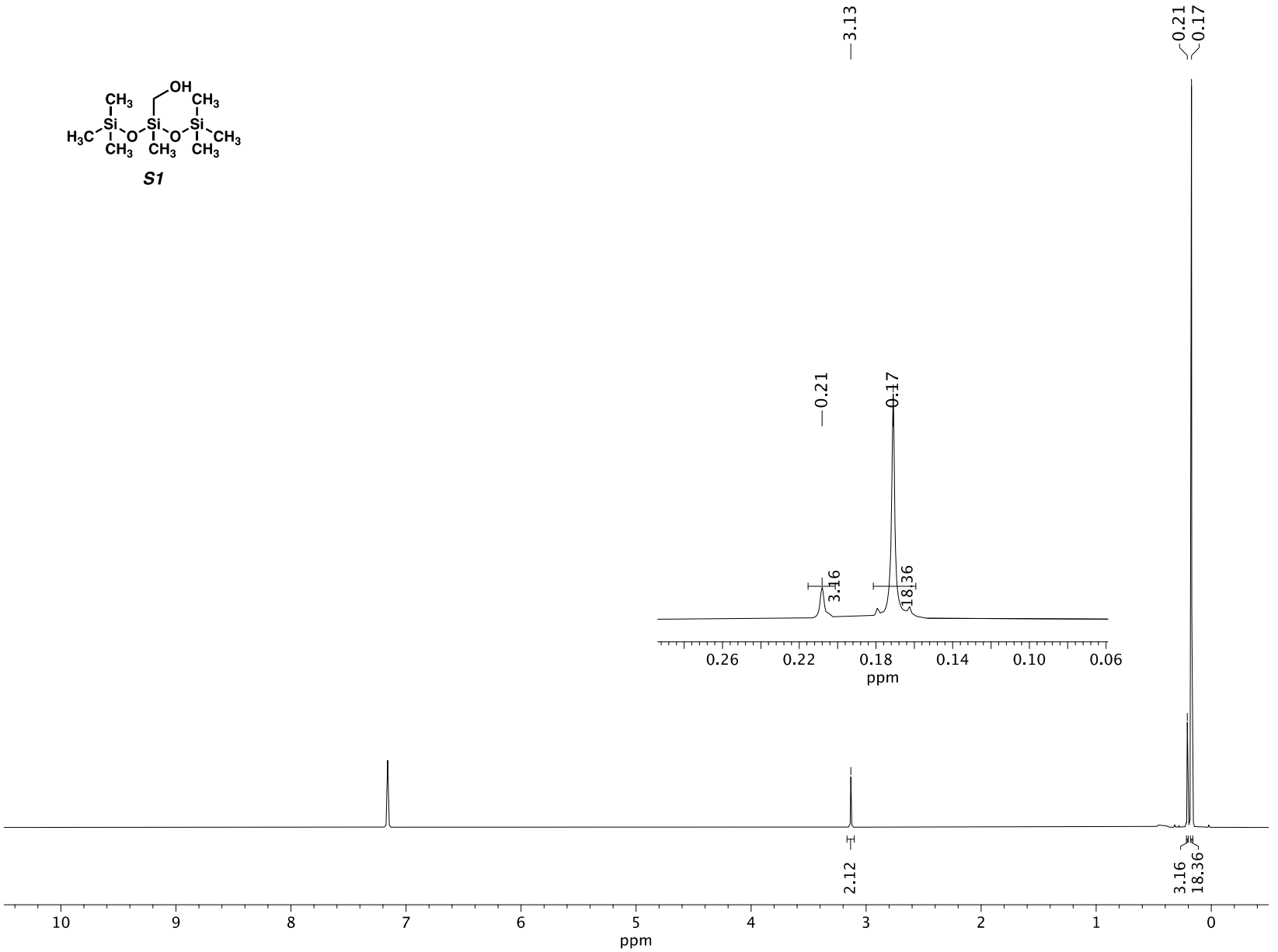

*^{1}H NMR (400 MHz, C_6D_6) of compound **S1**.*

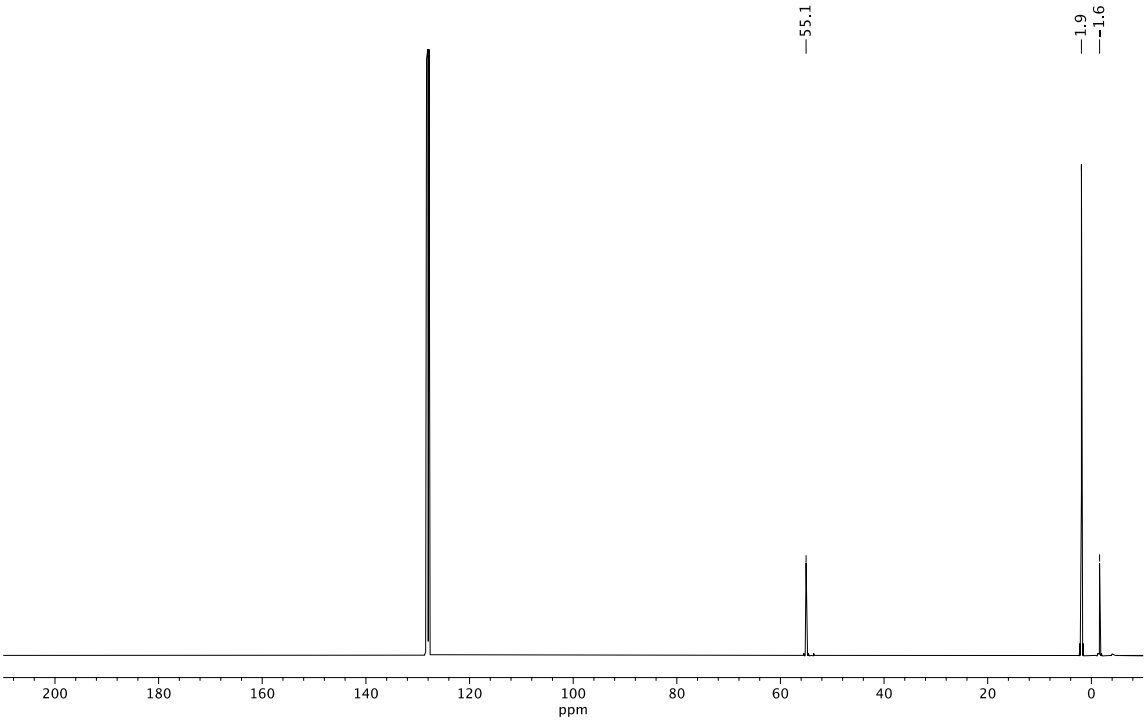

*^{13}C NMR (100 MHz, C_6D_6) of compound **S1**.*

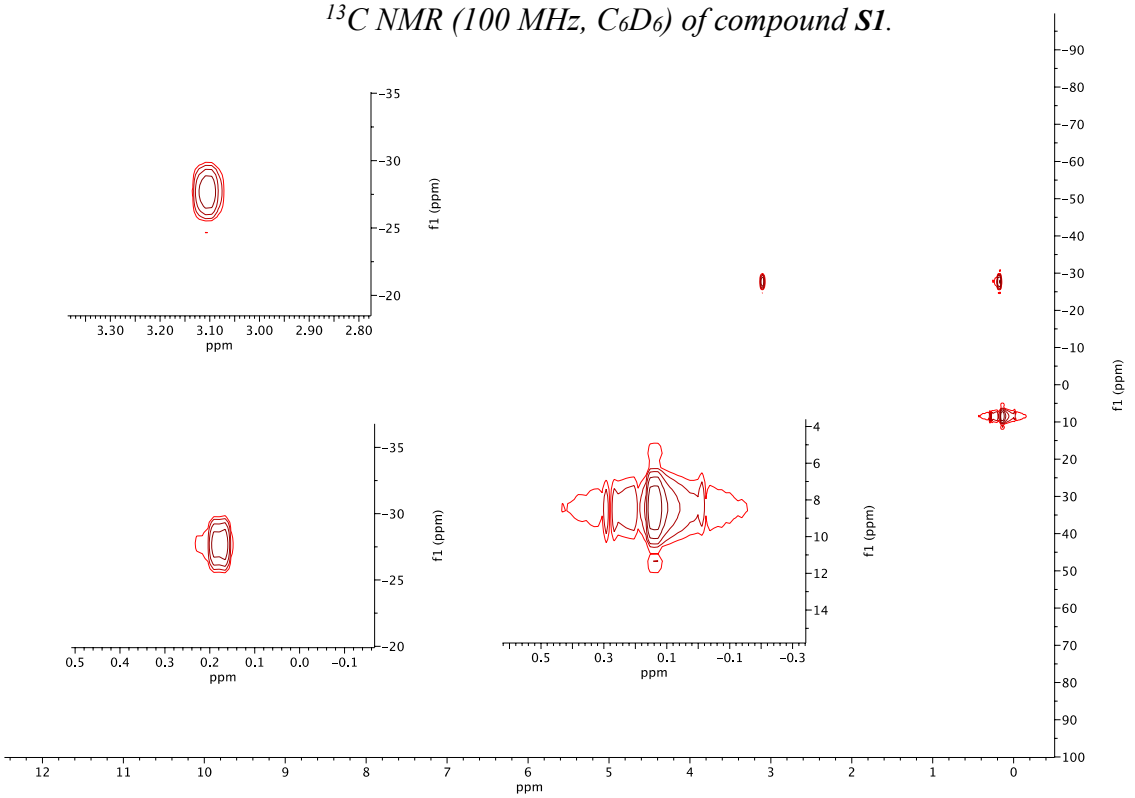

*^{1}H–^{29}Si HMBC (400 MHz, C_6D_6) of compound **S1**.*

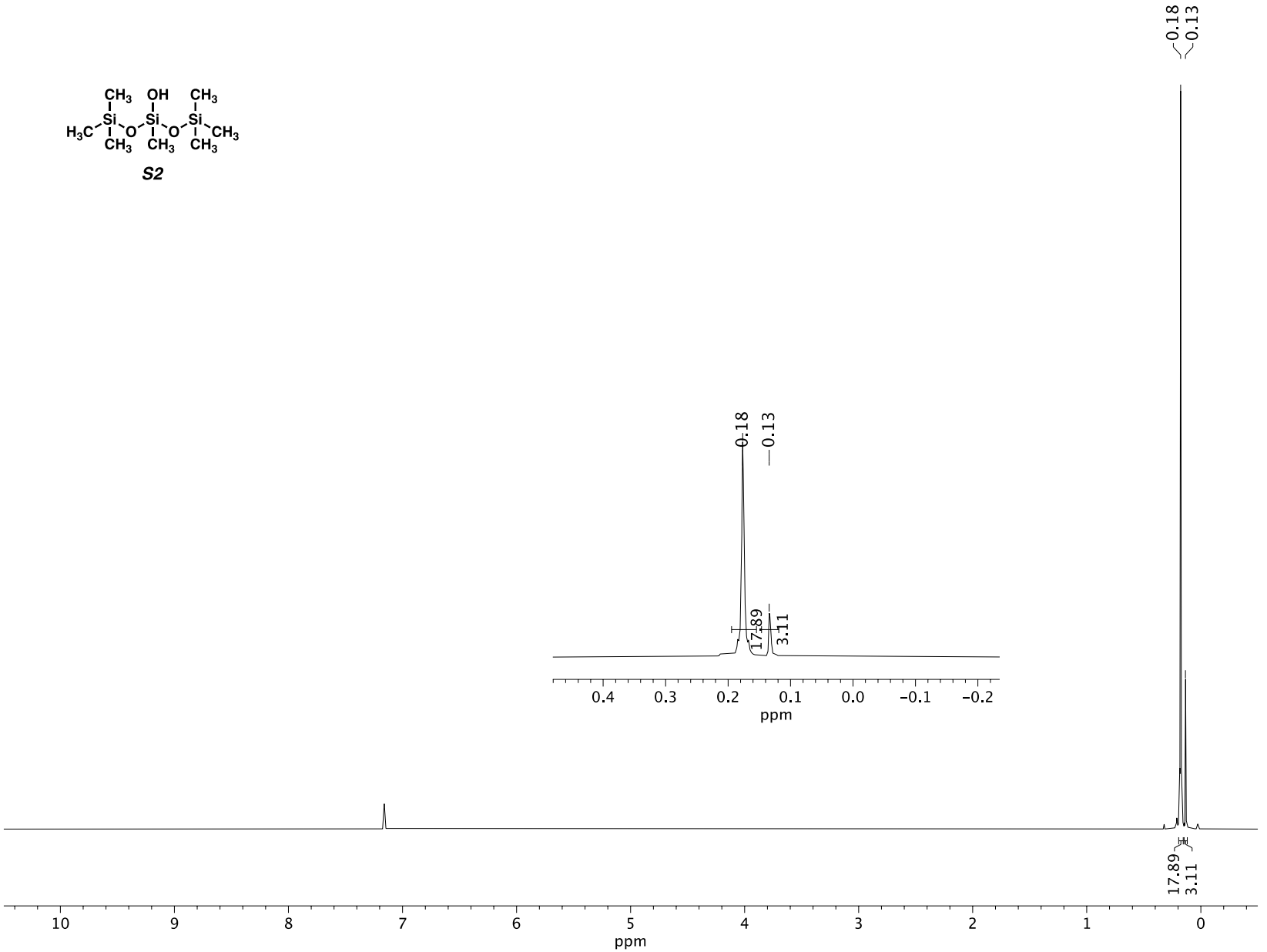

*^{1}H NMR (400 MHz, C_6D_6) of compound **S2**.*

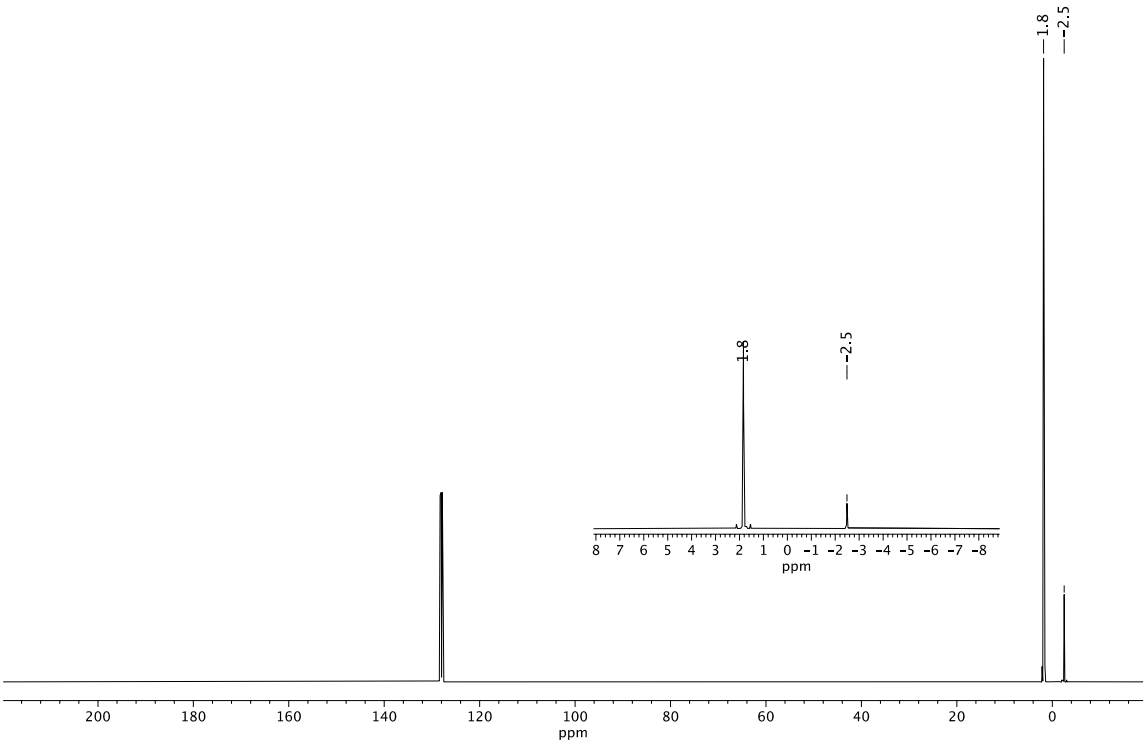

*^{13}C NMR (100 MHz, C_6D_6) of compound **S2**.*

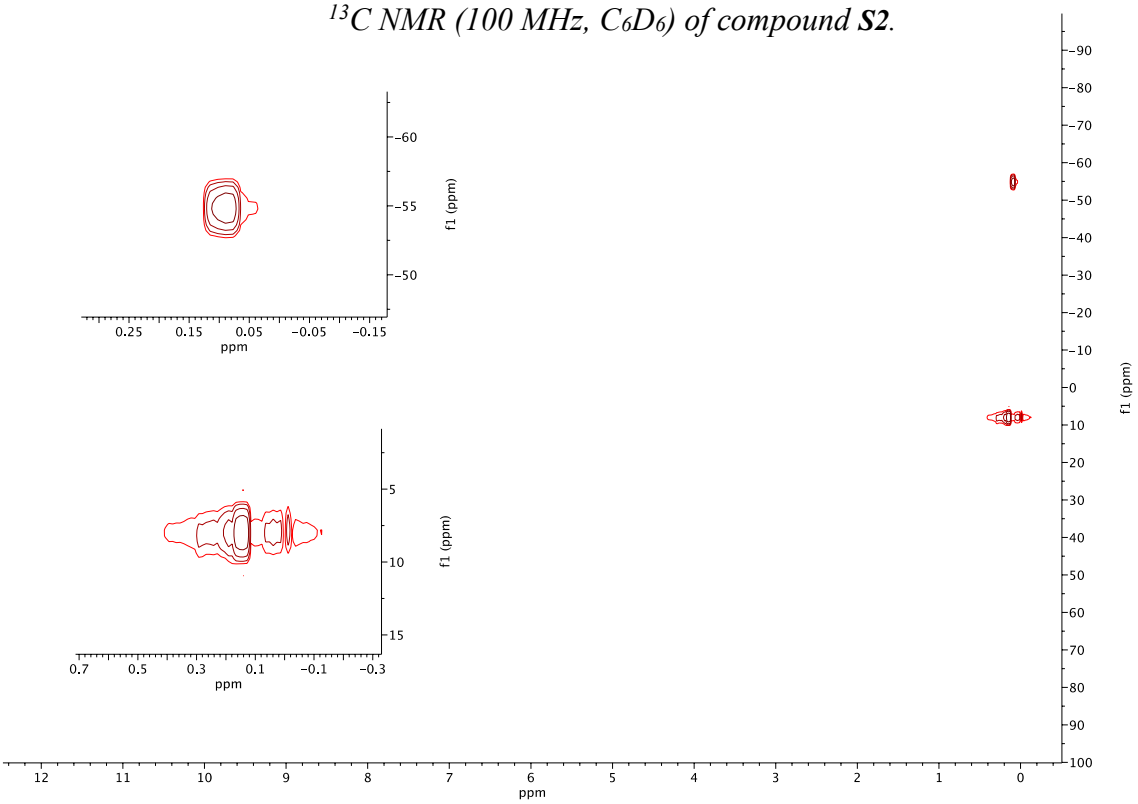

*^{1}H–^{29}Si HMBC (400 MHz, C_6D_6) of compound **S2**.*

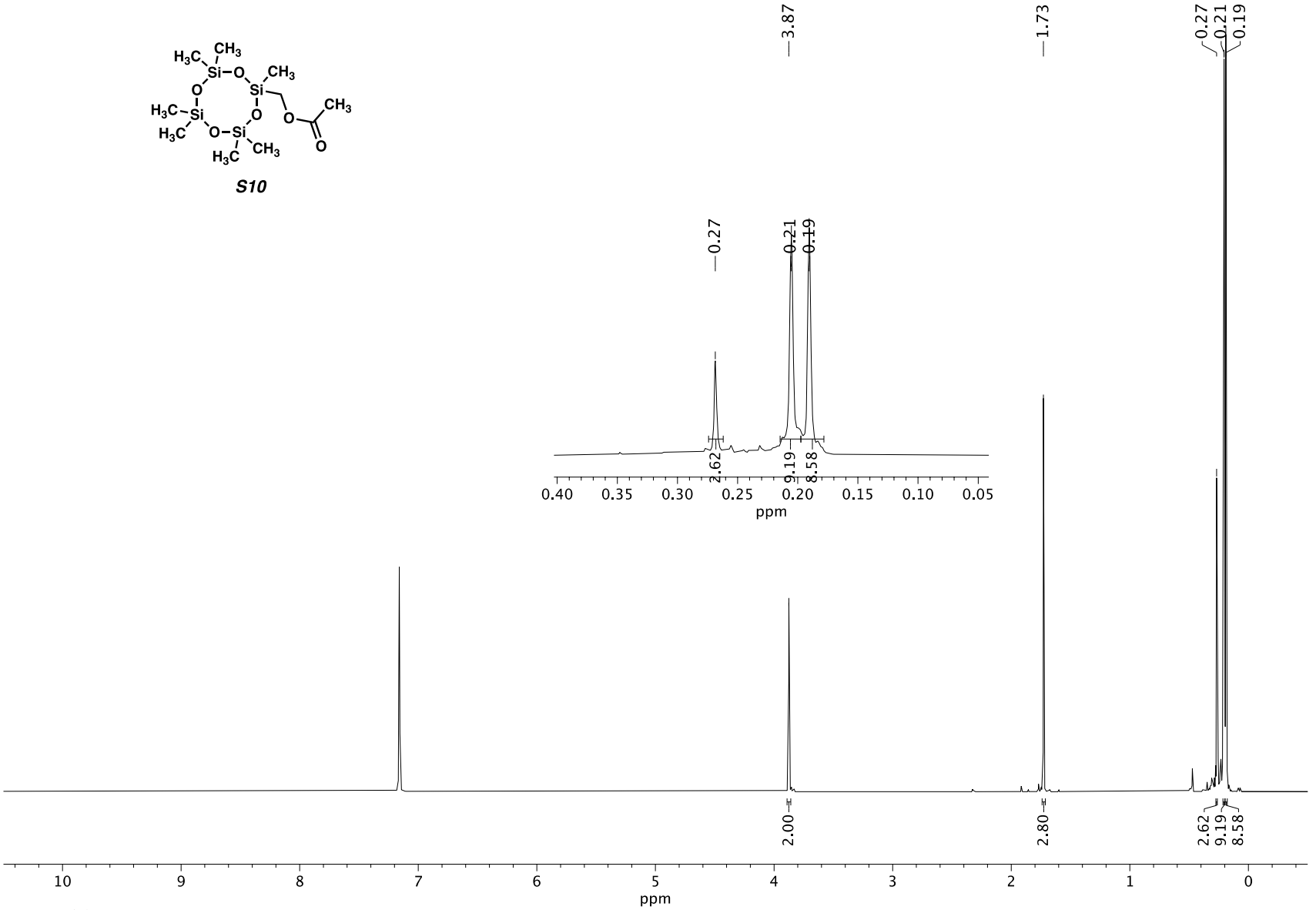

*^{1}H NMR (500 MHz, C_6D_6) of compound **S10**.*

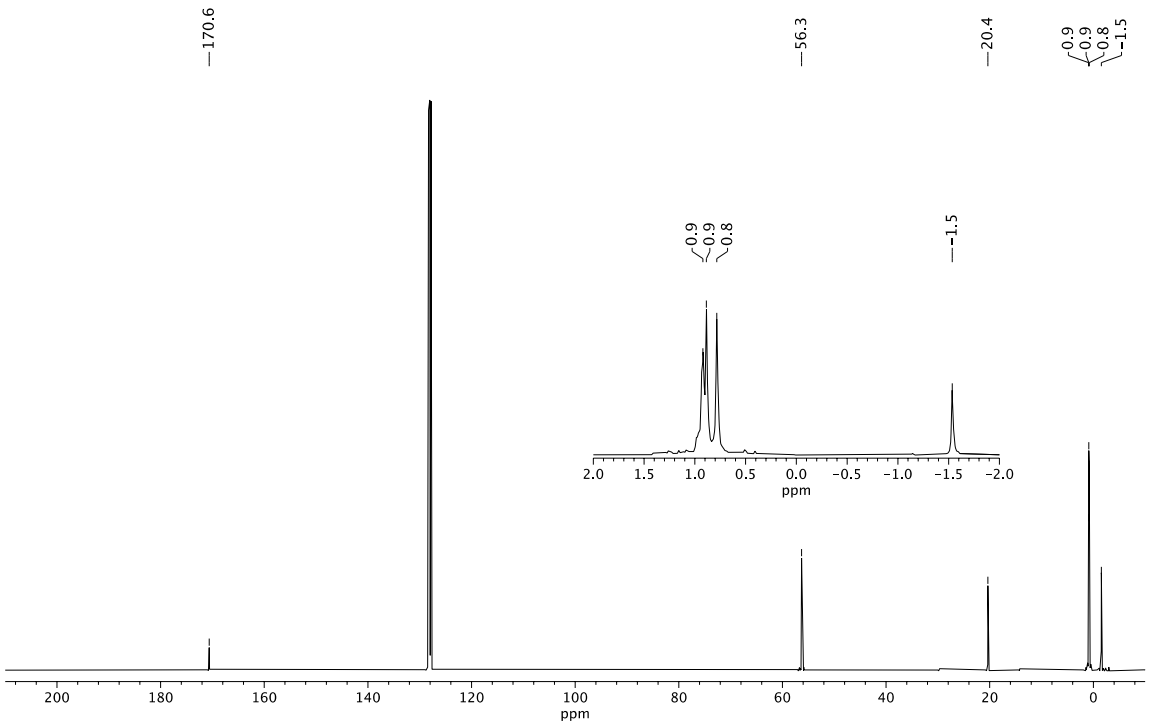

*^{13}C NMR (100 MHz, C_6D_6) of compound **S10**.*

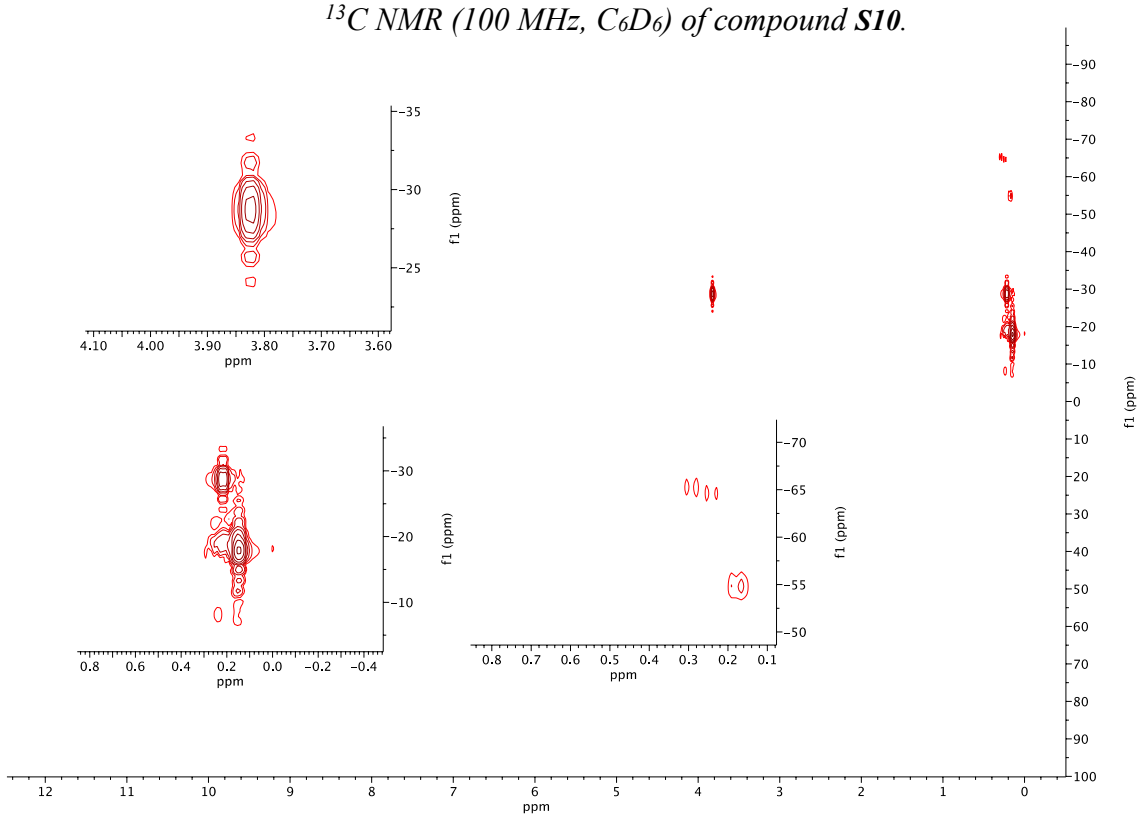

*^{1}H–^{29}Si HMBC (400 MHz, C_6D_6) of compound S**10**.*

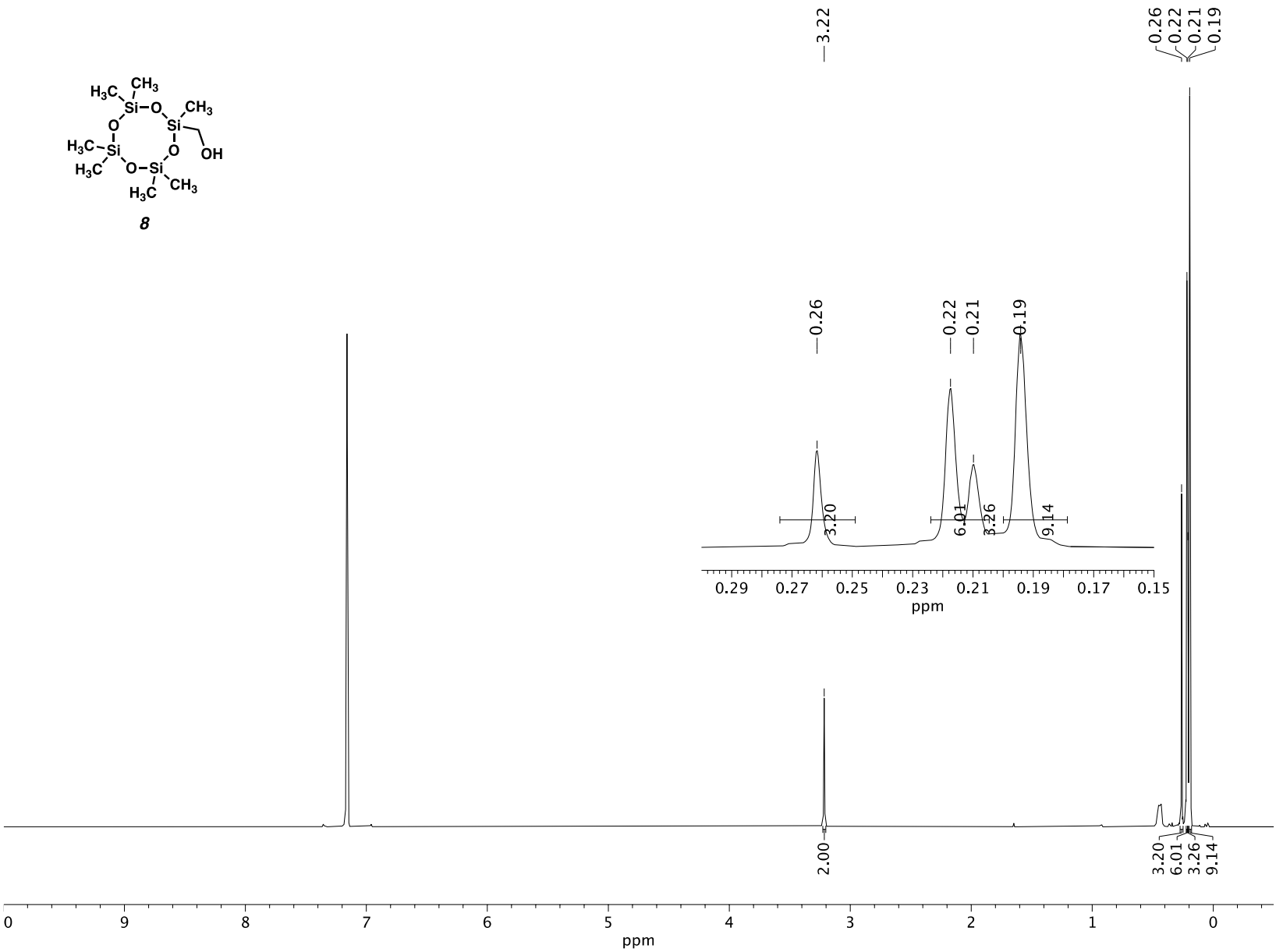

*^{1}H NMR (400 MHz, C_6D_6) of compound **8**.*

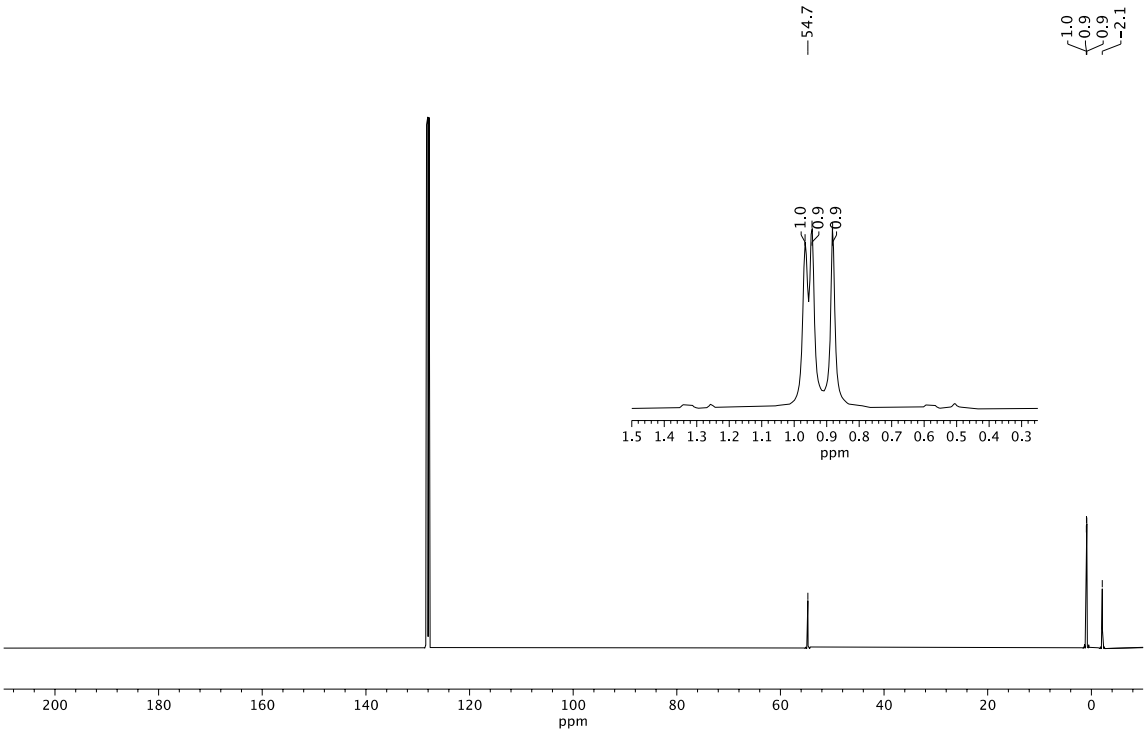

*^{13}C NMR (100 MHz, C_6D_6) of compound **8**.*

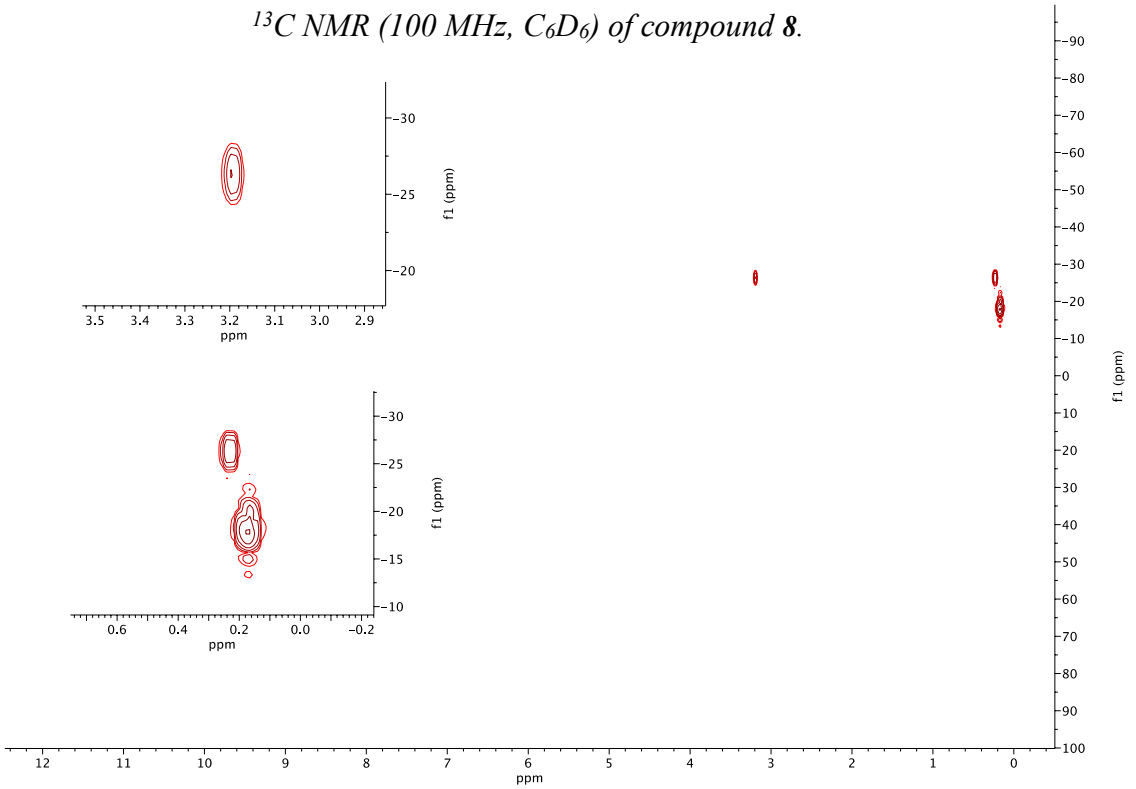

*^{1}H–^{29}Si HMBC (400 MHz, C_6D_6) of compound **8**.*

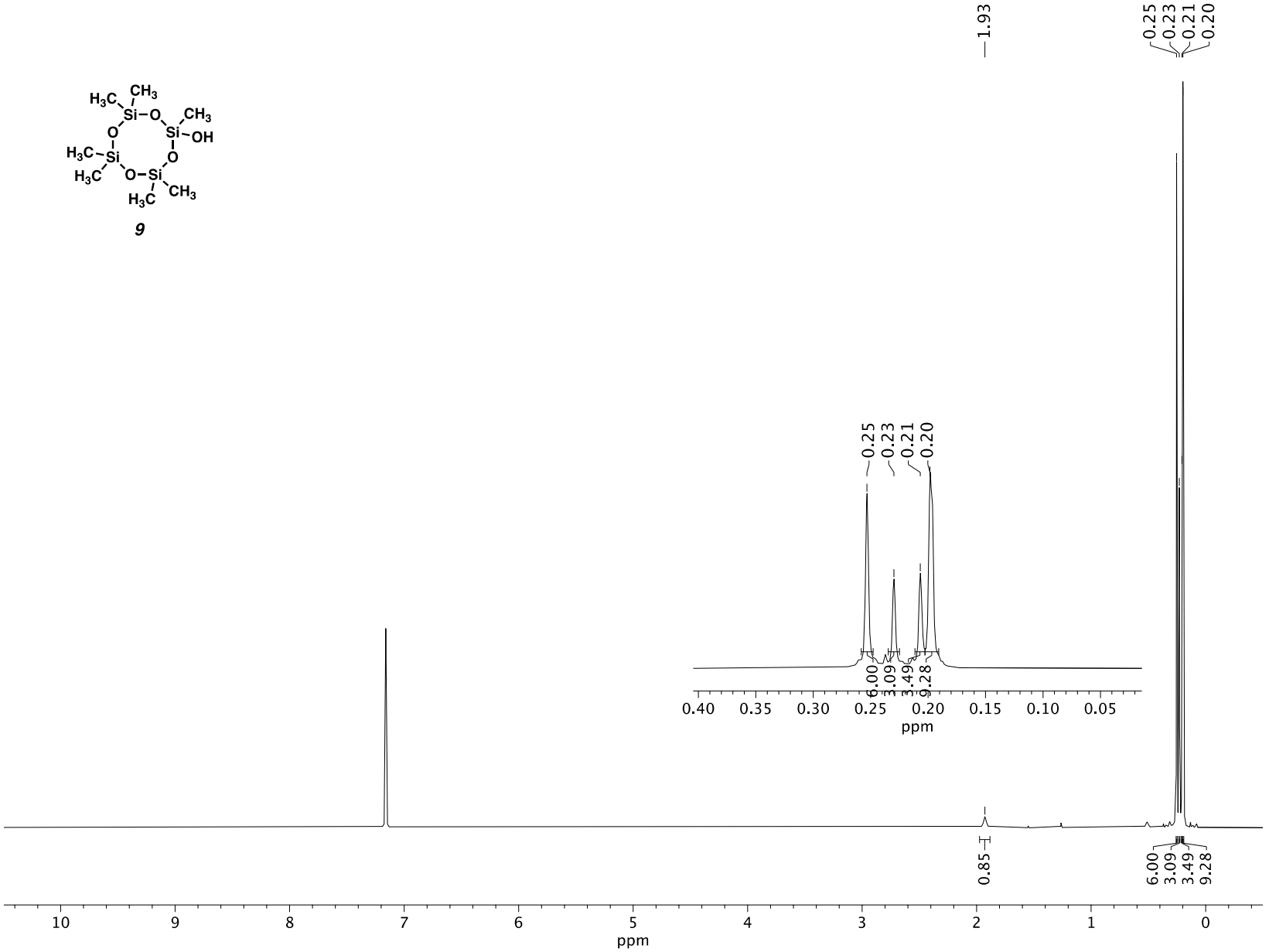

9

*^{1}H NMR (400 MHz, C_6D_6) of compound **9**.*

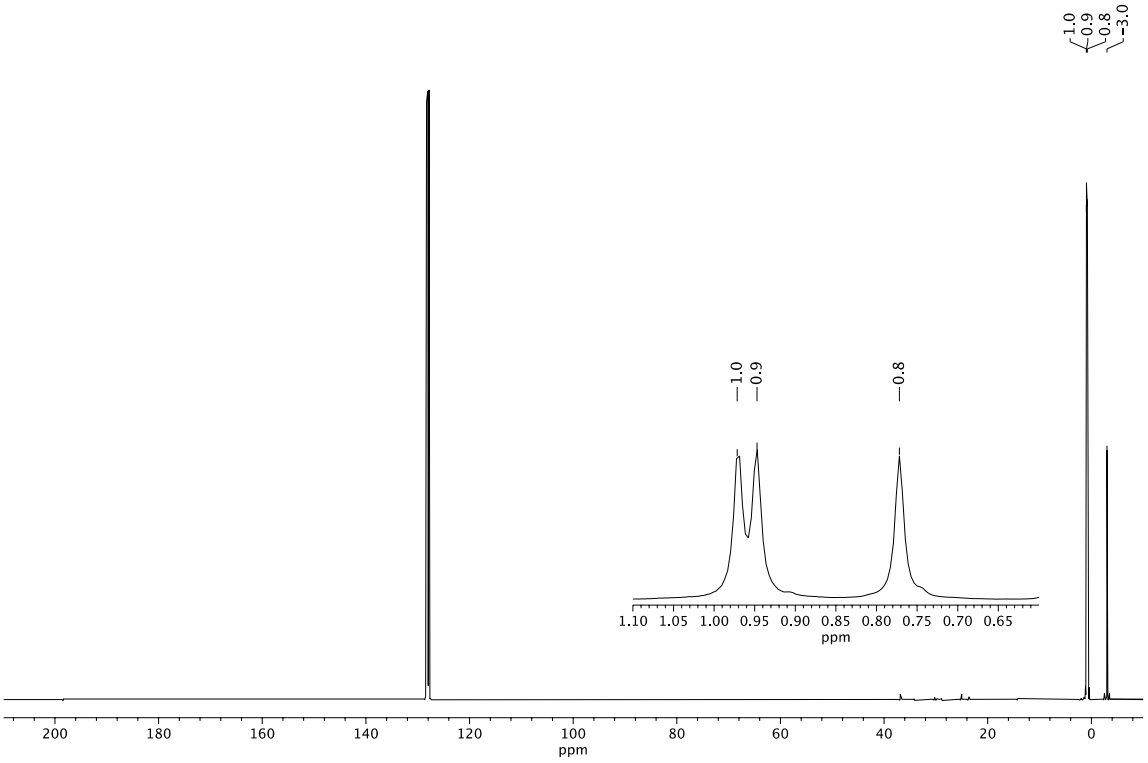

*^{13}C NMR (100 MHz, C_6D_6) of compound **9**.*

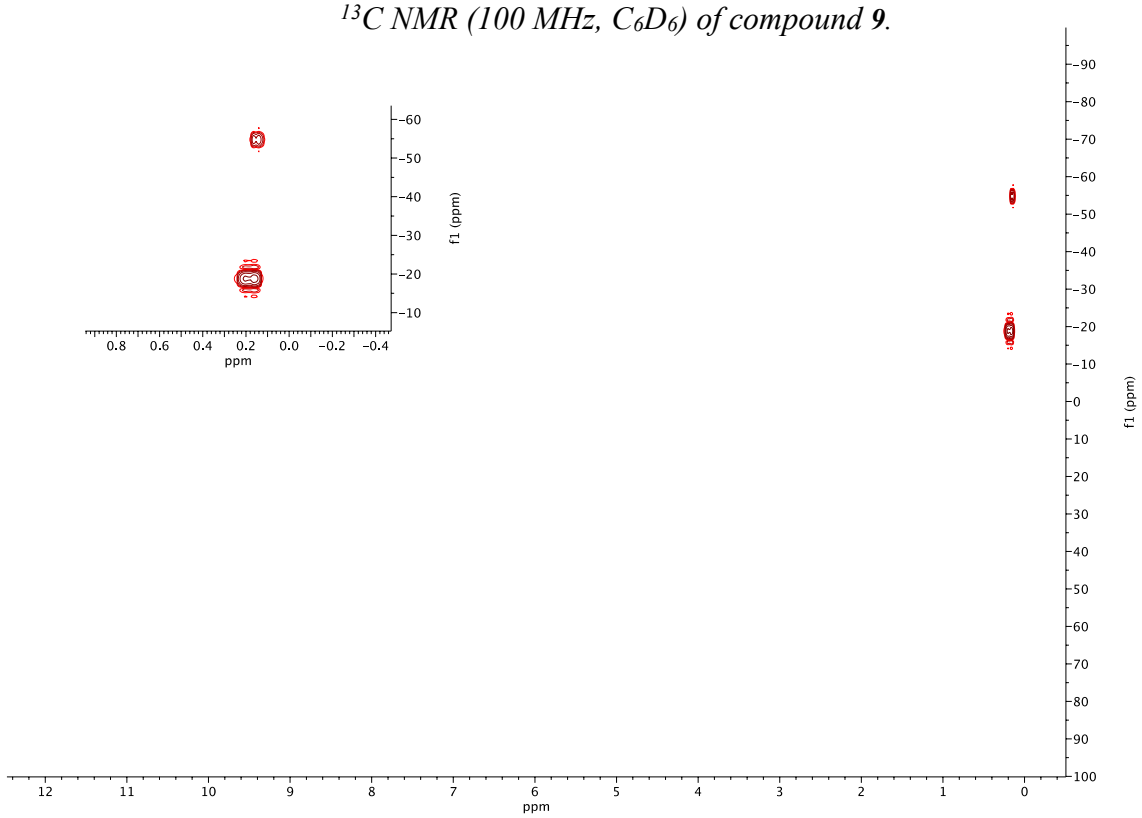

*^{1}H–^{29}Si HMBC (400 MHz, C_6D_6) of compound **9**.*

References and Notes

1. J. Chelikowsky, in *Silicon: Evolution and Future of a Technology*, P. Siffert, E. F. Krimmel, Eds. (Springer, 2004), pp. 1–22.

2. W. Noll, Ed., "Applications of Technical Silicone Products in Various Branches of Industry" in *Chemistry and Technology of Silicones* (Academic Press, 1968), pp. 531–638.

3. A. J. O'Lenick, *Silicones for Personal Care* (Allured Publishing, ed. 2, 2008).

4. C. Rücker, K. Kümmerer, Environmental chemistry of organosiloxanes. *Chem. Rev.* **115**, 466–524 (2015). doi:10.1021/cr500319v Medline

5. W. Noll, Ed., "Preparation of Polyorganosiloxanes" in *Chemistry and Technology of Silicones* (Academic Press, 1968), pp. 190–245.

6. K. Mojsiewicz-Pieńkowska, D. Krenczkowska, Evolution of consciousness of exposure to siloxanes-review of publications. *Chemosphere* **191**, 204–217 (2018). doi:10.1016/j.chemosphere.2017.10.045 Medline

7. S. Genualdi, T. Harner, Y. Cheng, M. Macleod, K. M. Hansen, R. van Egmond, M. Shoeib, S. C. Lee, Global distribution of linear and cyclic volatile methyl siloxanes in air. *Environ. Sci. Technol.* **45**, 3349–3354 (2011). doi:10.1021/es200301j Medline

8. D.-G. Wang, W. Norwood, M. Alaee, J. D. Byer, S. Brimble, Review of recent advances in research on the toxicity, detection, occurrence and fate of cyclic volatile methyl siloxanes in the environment. *Chemosphere* **93**, 711–725 (2013). doi:10.1016/j.chemosphere.2012.10.041 Medline

9. X. Xiang, N. Liu, L. Xu, Y. Cai, Review of recent findings on occurrence and fates of siloxanes in environmental compartments. *Ecotoxicol. Environ. Saf.* **224**, 112631 (2021). doi:10.1016/j.ecoenv.2021.112631 Medline

10. N. A. Warner, A. Evenset, G. Christensen, G. W. Gabrielsen, K. Borgå, H. Leknes, Volatile siloxanes in the European arctic: Assessment of sources and spatial distribution. *Environ. Sci. Technol.* **44**, 7705–7710 (2010). doi:10.1021/es101617k Medline

11. O. L. Flaningam, Vapor pressures of poly(dimethylsiloxane) oligomers. *J. Chem. Eng. Data* **31**, 266–272 (1986). doi:10.1021/je00045a002

12. Y. D. Lei, F. Wania, D. Mathers, Temperature-Dependent Vapor Pressure of Selected Cyclic and Linear Polydimethylsiloxane Oligomers. *J. Chem. Eng. Data* **55**, 5868–5873 (2010). doi:10.1021/je100835n

13. Global Silicones Council, "Regulatory Information"; https://globalsilicones.org/regulation/.

14. ECHA (European Chemicals Agency), "Inclusion of substances of very high concern in the Candidate List for eventual inclusion in Annex XIV" (2018); https://echa.europa.eu/documents/10162/2be7bcbf-f797-c28c-2c67-939664155c7c.

15. ECHA, "Support Document for Identification of Octamethylcyclotetrasiloxane (D_4) as a Substance of Very High Concern because of its PBT and vPvB properties" (2018); https://echa.europa.eu/documents/10162/115f70a9-a387-1525-d49f-b715e84996e4.

16. E. C. Tuazon, S. M. Aschmann, R. Atkinson, Atmospheric Degradation of Volatile Methyl-Silicon Compounds. *Environ. Sci. Technol.* **34**, 1970–1976 (2000). doi:10.1021/es9910053

17. M. W. Alton, E. C. Browne, Atmospheric Degradation of Cyclic Volatile Methyl Siloxanes: Radical Chemistry and Oxidation Products. *ACS Environ. Au* **2**, 263–274 (2022). doi:10.1021/acsenvironau.1c00043 Medline

18. S. Varaprath, J. M. McMahon, K. P. Plotzke, Metabolites of hexamethyldisiloxane and decamethylcyclopentasiloxane in Fischer 344 rat urine—A comparison of a linear and a cyclic siloxane. *Drug Metab. Dispos.* **31**, 206–214 (2003). doi:10.1124/dmd.31.2.206 Medline

19. S. Varaprath, K. L. Salyers, K. P. Plotzke, S. Nanavati, Identification of metabolites of octamethylcyclotetrasiloxane ($D(_4)$) in rat urine. *Drug Metab. Dispos.* **27**, 1267–1273 (1999). Medline

20. M. B. Reddy, M. E. Andersen, P. E. Morrow, I. D. Dobrev, S. Varaprath, K. P. Plotzke, M. J. Utell, Physiological modeling of inhalation kinetics of octamethylcyclotetrasiloxane in humans during rest and exercise. *Toxicol. Sci.* **72**, 3–18 (2003). doi:10.1093/toxsci/kfg001 Medline

21. F. H. Arnold, Directed Evolution: Bringing New Chemistry to Life. *Angew. Chem. Int. Ed.* **57**, 4143–4148 (2018). doi:10.1002/anie.201708408 Medline

22. R. A. Sheldon, J. M. Woodley, Role of Biocatalysis in Sustainable Chemistry. *Chem. Rev.* **118**, 801–838 (2018). doi:10.1021/acs.chemrev.7b00203 Medline

23. T. D. Sutherland, I. Horne, K. M. Weir, C. W. Coppin, M. R. Williams, M. Selleck, R. J. Russell, J. G. Oakeshott, Enzymatic bioremediation: From enzyme discovery to applications. *Clin. Exp. Pharmacol. Physiol.* **31**, 817–821 (2004). doi:10.1111/j.1440-1681.2004.04088.x Medline

24. N. S. Sarai, B. J. Levin, J. M. Roberts, D. E. Katsoulis, F. H. Arnold, Biocatalytic Transformations of Silicon—The Other Group 14 Element. *ACS Cent. Sci.* **7**, 944–953 (2021). doi:10.1021/acscentsci.1c00182 Medline

25. C. Rücker, E. Grabitz, K. Kümmerer, Are Si–C bonds cleaved by microorganisms? A critical review on biodegradation of methylsiloxanes. *Chemosphere* **321**, 137858 (2023). doi:10.1016/j.chemosphere.2023.137858 Medline

26. N. P. Dunham, F. H. Arnold, Nature's Machinery, Repurposed: Expanding the Repertoire of Iron-Dependent Oxygenases. *ACS Catal.* **10**, 12239–12255 (2020). doi:10.1021/acscatal.0c03606 Medline

27. K. Mittra, M. T. Green, Reduction Potentials of P450 Compounds I and II: Insight into the Thermodynamics of C–H Bond Activation. *J. Am. Chem. Soc.* **141**, 5504–5510 (2019). doi:10.1021/jacs.9b00242 Medline

28. J. Münch, P. Püllmann, W. Zhang, M. J. Weissenborn, Enzymatic Hydroxylations of sp^3-Carbons. *ACS Catal.* **11**, 9168–9203 (2021). doi:10.1021/acscatal.1c00759

29. C. J. C. Whitehouse, S. G. Bell, L.-L. Wong, $P450_{BM3}$ (CYP102A1): Connecting the dots. *Chem. Soc. Rev.* **41**, 1218–1260 (2012). doi:10.1039/C1CS15192D Medline

30. A. M. Doncaster, R. Walsh, Gas phase reaction between iodine and tetramethylsilane. Part 2.—Kinetics and the bond dissociation energy $D(Me_3SiCH_2—H)$. *J. Chem. Soc., Faraday Trans. I* **72**, 2908–2916 (1976). doi:10.1039/f19767202908

31. S. T. Jung, R. Lauchli, F. H. Arnold, Cytochrome P450: Taming a wild type enzyme. *Curr. Opin. Biotechnol.* **22**, 809–817 (2011). doi:10.1016/j.copbio.2011.02.008 Medline

32. S. Bähr, S. Brinkmann-Chen, M. Garcia-Borràs, J. M. Roberts, D. E. Katsoulis, K. N. Houk, F. H. Arnold, Selective Enzymatic Oxidation of Silanes to Silanols. *Angew. Chem. Int. Ed.* **59**, 15507–15511 (2020). doi:10.1002/anie.202002861 Medline

33. H. M. Girvan, H. E. Seward, H. S. Toogood, M. R. Cheesman, D. Leys, A. W. Munro, Structural and spectroscopic characterization of P450 BM3 mutants with unprecedented P450 heme iron ligand sets. *J. Biol. Chem.* **282**, 564–572 (2007). doi:10.1074/jbc.M607949200 Medline

34. R. E. Childs, W. G. Bardsley, The steady-state kinetics of peroxidase with 2,2′-azino-di-(3-ethyl-benzthiazoline-6-sulphonic acid) as chromogen. *Biochem. J.* **145**, 93–103 (1975). doi:10.1042/bj1450093 Medline

35. M. S. Quesenberry, Y. C. Lee, A rapid formaldehyde assay using purpald reagent: Application under periodation conditions. *Anal. Biochem.* **234**, 50–55 (1996). doi:10.1006/abio.1996.0048 Medline

36. R. E. Ireland, D. W. Norbeck, Application of the Swern oxidation to the manipulation of highly reactive carbonyl compounds. *J. Org. Chem.* **50**, 2198–2200 (1985). doi:10.1021/jo00212a041

37. K. Chen, F. H. Arnold, Engineering new catalytic activities in enzymes. *Nat. Catal.* **3**, 203–213 (2020). doi:10.1038/s41929-019-0385-5

38. S. B. J. Kan, R. D. Lewis, K. Chen, F. H. Arnold, Directed evolution of cytochrome c for carbon-silicon bond formation: Bringing silicon to life. *Science* **354**, 1048–1051 (2016). doi:10.1126/science.aah6219 Medline

39. I. Taniguchi, S. Yoshida, K. Hiraga, K. Miyamoto, Y. Kimura, K. Oda, Biodegradation of PET: Current Status and Application Aspects. *ACS Catal.* **9**, 4089–4105 (2019). doi:10.1021/acscatal.8b05171

40. S. Yoshida, K. Hiraga, T. Takehana, I. Taniguchi, H. Yamaji, Y. Maeda, K. Toyohara, K. Miyamoto, Y. Kimura, K. Oda, A bacterium that degrades and assimilates poly(ethylene terephthalate). *Science* **351**, 1196–1199 (2016). doi:10.1126/science.aad6359 Medline

41. S. Miri, R. Saini, S. M. Davoodi, R. Pulicharla, S. K. Brar, S. Magdouli, Biodegradation of microplastics: Better late than never. *Chemosphere* **286**, 131670 (2022). doi:10.1016/j.chemosphere.2021.131670 Medline

42. D. G. Gibson, L. Young, R.-Y. Chuang, J. C. Venter, C. A. Hutchison 3rd, H. O. Smith, Enzymatic assembly of DNA molecules up to several hundred kilobases. *Nat. Methods* **6**, 343–345 (2009). doi:10.1038/nmeth.1318 Medline

43. S. Kille, C. G. Acevedo-Rocha, L. P. Parra, Z.-G. Zhang, D. J. Opperman, M. T. Reetz, J. P. Acevedo, Reducing codon redundancy and screening effort of combinatorial protein

libraries created by saturation mutagenesis. *ACS Synth. Biol.* **2**, 83–92 (2013). doi:10.1021/sb300037w Medline

44. H. Zhao, W. Zha, *In vitro* 'sexual' evolution through the PCR-based staggered extension process (StEP). *Nat. Protoc.* **1**, 1865–1871 (2006). doi:10.1038/nprot.2006.309 Medline

45. C. E. Boville, D. K. Romney, P. J. Almhjell, M. Sieben, F. H. Arnold, Improved Synthesis of 4-Cyanotryptophan and Other Tryptophan Analogues in Aqueous Solvent Using Variants of TrpB from *Thermotoga maritima*. *J. Org. Chem.* **83**, 7447–7452 (2018). doi:10.1021/acs.joc.8b00517 Medline

46. F. W. Studier, Protein production by auto-induction in high density shaking cultures. *Protein Expr. Purif.* **41**, 207–234 (2005). doi:10.1016/j.pep.2005.01.016 Medline

47. F. P. Guengerich, M. V. Martin, C. D. Sohl, Q. Cheng, Measurement of cytochrome P450 and NADPH-cytochrome P450 reductase. *Nat. Protoc.* **4**, 1245–1251 (2009). doi:10.1038/nprot.2009.121 Medline

48. C. R. Otey, in *Directed Enzyme Evolution: Screening and Selection Methods*, F. H. Arnold, G. Georgiou, Eds. (Humana Press, 2003), pp. 137–139.

49. M. Reiter, A. Kronast, S. Kissling, B. Rieger, In Situ Generated ABA Block Copolymers from CO_2, Cyclohexene Oxide, and Poly(dimethylsiloxane)s. *ACS Macro Lett.* **5**, 419–423 (2016). doi:10.1021/acsmacrolett.6b00133 Medline

50. S. A. Erhardt, F. Hoffmann, J. O. Daiss, J. Stohrer, E. Herdtweck, B. Rieger, Synthesis of 2,2,5,5-tetrasubstituted 1,4-dioxa-2,5-disilacyclohexanes via organotin(IV)-catalyzed transesterification of (acetoxymethyl)alkoxysilanes. *Chemistry* **19**, 4818–4825 (2013). doi:10.1002/chem.201202124 Medline